From Department of Medicine, Huddinge
Karolinska Institutet, Stockholm, Sweden

REDOX AND EPIGENETIC MODULATORS REGULATE CARDIAC FUNCTION AND REMODELING IN HEALTH AND DISEASE

Zaher Elbeck

Karolinska Institutet

Stockholm 2023

All previously published papers were reproduced with permission from the publisher.
Published by Karolinska Institutet.
Printed by Universitetsservice US-AB, 2023
© Zaher ElBeck, 2023
ISBN 978-91-8017-149-6
Cover illustration: The Krebs cycle in mitochondria produces metabolites that regulate gene expression by modulating DNA methylation, thus influencing heart function.

Redox and epigenetic modulators regulate cardiac function and remodeling in health and disease.

THESIS FOR DOCTORAL DEGREE (Ph.D.)

By

Zaher ElBeck

The thesis will be defended in public at Huddinge, Karolinska Institutet, Blickagången 16, NEO Building, Erna Möllersalen (5th floor).

Monday, the 16th of October 2023, at 14:00

Principal Supervisor:
Professor Christer Betsholtz
Karolinska Institutet
Department of Medicine, Huddinge
Integrated Cardio Metabolic Centre

Co-supervisor(s):
Associated professor Ákos Végvári
Karolinska Institutet
Department of Medical Biochemistry and Biophysics
Proteomics Biomedicum

Professor Lars Lund
Karolinska Institutet
Department of Medicine, Solna
Karolinska University Hospital

Opponent:
Professor Claes Gustafsson
University of Gothenburg
Institute of Biomedicine
Department of Medical Biochemistry and Cell biology

Examination Board:
Professor Anders Virtanen
University of Uppsala
Department of Cell and Molecular Biology
Division of Microbiology and immunology

Associated professor Andreas Lennartsson
Karolinska Institutet
Department of Biosciences and Nutrition

Assistant professor Hong Qian
Karolinska Institutet
Department of Medicine, Huddinge

To everyone who was told, you would never succeed ….

To my mother, to the soul of my father, who both did everything possible for me …

To all my family and friends ….

POPULAR SCIENCE SUMMARY OF THE THESIS

¨Do you know that there is an ongoing fight in your body? Attackers are continuously trying to destroy your cells, but there are guarders that are defending them ... These attackers are called free radicals, while the guarders are called antioxidants…. ¨

How many times have you spotted such text or heard it in a TV program or from a natural therapist or influencer?

Antioxidants is a highly popular topic in society, with the recommendations of health or social influencers to maintain a daily intake of antioxidants as supplements, or to rely on a diet that is rich in antioxidants. The reason for this is the common misconception of depicting oxidants (or free radicals) as bad and dangerous elements that damage our cells, while featuring the antioxidants as life-guarders against them. However, extensive research during the past decades could not bring compelling supportive evidence about the benefits of antioxidative supplements or treatments. Moreover, antioxidants were extensively tried as therapy in multiple diseases, including heart failure and cardiovascular diseases, trials that have all ultimately failed.

This does not imply that antioxidants are not good or do not have beneficial effects, but rather that we still do not know the precise mechanisms regulating antioxidants and oxidants in our cells. Therefore, random and excessive uptake of antioxidants might have adverse effects, outweighing any anticipated benefits.

In my thesis, I explore and clarify the nature of oxidants and antioxidants and reveal novel mechanisms that regulate our cellular defense against oxidants. I highlight that all oxidants and antioxidants are (bio)chemical compounds, meaning that each of them has also its unique biological function in our cells due to its chemical structure, besides being oxidants or antioxidants. Oxidation or reduction determines whether two compounds can react together to mediate a biological function in our cells. I show that heart failure is not necessarily associated with reduced capacity of defense against antioxidants, and therefore that our intake of antioxidants is not always useful and may instead have adverse effects. By using experimental models for heart failure, I show that an antioxidative treatment improves cardiac function in those subjects that have reduced antioxidative capacity but worsens heart function in subjects with sufficient antioxidative capacity. Therefore, in order to harness antioxidative therapy for theraputic use, a personalized approach is likely essential. This would involve assessing an individual's antioxidative capacity before initiating treatment.

POPULAR SCIENCE SUMMARY (SVENSKA)

"*Visste du att det pågår en kamp i din kropp? Angripare försöker ständigt förstöra dina celler, men det finns försvarare som skyddar dem... Dessa angripare kallas fria radikaler, medan försvararna kallas antioxidanter...*¨

Hur många gånger har du sett en sådan text eller hört den i ett TV-program eller från en naturläkare eller influenser?

Antioxidanter är ett extremt populärt ämne i samhället, med rekommendationer från hälso- eller sociala influenser att dagligen inta antioxidanter som kosttillskott eller äta en kost rik på antioxidanter. Anledningen till detta är att oxidanter (eller fria radikaler) anses vara dåliga och farliga element som skadar våra celler, samtidigt som antioxidanterna framställs som räddare i nöden. Omfattande forskning under de senaste decennierna har inte kunnat ge konkreta bevis för nyttan med antioxidativa kosttillskott eller behandlingar. Omfattande försök med antioxidanter för att behandla olika sjukdomar, inklusive hjärtsvikt och hjärt-kärlsjukdomar, har misslyckats.

Detta innebär inte att antioxidanter inte är bra eller saknar fördelaktiga effekter, utan snarare att vi fortfarande inte känner till de exakta mekanismerna som reglerar antioxidanter och oxidanter i våra celler. Därför kan slumpmässig och överdriven konsumtion av antioxidanter ha skadliga effekter som överväga eventuella fördelar.

I min avhandling undersöker jag oxidanters och antioxidanters natur och avslöjar nya mekanismer i vårt cellulära försvar mot oxidanter. Jag betonar att alla oxidanter och antioxidanter också är (bio)kemiska föreningar med andra viktiga funktioner i våra celler utöver att de är oxidanter eller antioxidanter. Oxidation eller reduktion avgör om två föreningar kan reagera tillsammans för att mediera en biologisk funktion i våra celler. Jag visar att hjärtsvikt inte nödvändigtvis är förknippad med nedsatt förmåga hos cellen att försvara sig mot antioxidanter, och därför är behandling med antioxidanter inte alltid av nytta. Tvärtom det kan i vissa fall i stället leda till skadliga effekter. Genom att använda experimentella modeller för hjärtsvikt visar jag att en antioxidativ behandling förbättrar hjärtfunktionen hos individer med nedsatt antioxidativ kapacitet. Hos individer med god antioxidativ kapacitet försämra istället hjärtfunktionen. Därför är det avgörande med ett individualiserat tillvägagångssätt för att förbättra den kliniska effektiviteten av potentiell antioxidativ terapi. Detta skulle innebära att bedöma en individs antioxidativa kapacitet innan behandlingen påbörjas.

ABSTRACT

Oxidative species are a divergent group of cellular metabolites with a wide variety of functions. Together with reductants, they regulate almost all cellular functions, from mediating cellular communications to catalyzing a variety of biochemical reactions, and further to post-translationally modifying proteins. The past decades' focus on oxidative species as injurious byproducts associated with diseases have not yielded any clinical success. For example, attempts to improve heart function by antioxidative treatments have rather, in some cases, had adverse effects on heart failure. Therefore, there is unmet need for a change in the way we perceive redox biology, namely, to replace the traditional view on oxidants as unambiguous foes with more openminded perspective on the broad functions of the redox system and the novel mechanisms that regulate the endogenous antioxidative capacity. An urge for unbiased approaches is further supported by the recent technical advances in multi omics, which have enabled the exploration of complex mechanisms beyond traditional boundaries.

In our recent manuscript on BioRxiv (Elbeck *et al.*, 2022), on which this thesis is largely based, we present evidence using multipronged omics that mitochondrial isocitrate dehydrogenase 2 (IDH2) governs an extensive redox-regulatory mechanism in cardiac mitochondria. We found that IDH2 together with nuclear factor erythroid 2-related factor 2 (NRF2) coordinates a novel antioxidative mechanism through a feedforward cycle involving 2-oxoglutarate (2OG) and L2-hydroxyglutarate (L2HG). We further found that this redox cycle regulates gene expression through an unconventional mechanism involving intronic DNA hydroxymethylation. We explored the possible implications of these findings for the treatment of heart failure, taking into consideration the previously failed clinical trials. We obtained evidence for sexual dimorphism in mice in which females showed a more robust antioxidative defense reflecting on their heart failure phenotype: a less severe dilated cardiomyopathy (DCM) compared to males. We tested our hypothesis using a novel pharmacological compound AZ925, which activated the NRF2 pathway. Our conclusion is that enhancing the antioxidative capacity has a positive impact on cardiac function only when endogenous antioxidative capacity is limited, highlighting new possibilities for precision medicine.

In the **literature review** part of this thesis, I aimed to explore literature beyond the protective role of the redox system. Here, I dig deeply into the multifaceted essential—but overlooked—functions of this system. I also aimed to explain my reasoning behind the design and interpretation of some of the data presented in Elbeck *et al*., 2022. Moreover, I further explored if data from cases of patients with DCM were potentially supportive of my hypothesis (**Project I**).

In Project II, I have investigated the importance of miR-208b-3p, which is a highly induced micro-RNA (miR) in the myocardia of patients with DCM. I propose that miR208b-3p plays a role in the cardiac reverse remodeling observed in some patients with heart failure as a potential *redoxmiR*, which represents one of the arms of the redox system discussed in this monograph.

Project III does not deal directly with redox biology, but it is rather related to the concept of translatable genetic information beyond the canonical protein coding and translational reading frames via alternative splicing. We propose the existence of multiple isoforms of muscle lim protein (MLP) translated at extremely low levels from same *Mlp* pre-mRNA as the full length MPL protein, even in $Mlp^{-/-}$ animals that have a deletion in *Mlp* exon2. These isoforms retain some of the functional domains of their full-length protein, and therefore may mediate distinct functions.

The overall goal of my work has been to use recent technical advances to explore biological mechanisms beyond some of its preconceived boundaries, and thereby to unveil novel molecular mechanisms that could ultimately lead to improved personalized and precise treatments of several diseases, including redox therapies for heart failure.

LIST OF SCIENTIFIC PAPERS

This thesis includes only a manuscript published on BioRxiv

Elbeck, Z., Hossain, M.B., Siga, H., Oskolkov, N., Karlsson, F., Lindgren, J., Walentinsson, A., Remedios, C.D., Koppenhöfer, D., Jarvis, R., Bürli R., Jamier T., Franssen E., Firth M., Degasperi A., Bendtsen C., Dudek J., Kohlhaas M., Nickel A. G., Lund L. H., Maack C., Végvári A. & Betsholtz C. (2022). Epigenetic modulators link mitochondrial redox homeostasis to cardiac function. *BioRxiv*.

LIST OF OTHER PAPERS NOT INCLUDED IN THE THESIS

1- Grote Beverborg, N., Später, D., Knöll, R., Hidalgo, A., Yeh, S. T., **Elbeck, Z**., Silljé H.H. W., Eijgenraam T. R, Siga H., Zurek M., Palmér M., Pehrsson S., Albery T., Bomer N., Hoes M. F., Boogerd C. J., Frisk M., van Rooij E., Damle S., Louch W. E., Wang Q-D., Fritsche-Danielson R, Chien K.R., Hansson K. M., Mullick A. E., de Boer R.A. & van der Meer, P. (2021). Phospholamban antisense oligonucleotides improve cardiac function in murine cardiomyopathy. *Nature Communications,* 12(1), 5180.

2- Lostal, W., Roudaut, C., Faivre, M., Charton, K., Suel, L., Bourg, N., Best H., Smith J. E., Gohlke J., Corre G., Li X., **Elbeck Z.**, Knöll R., ves Deschamps J-Y., Granzier H. & Richard, I. (2019). Titin splicing regulates cardiotoxicity associated with calpain 3 gene therapy for limb-girdle muscular dystrophy type 2A. *Science translational medicine,* 11(520), eaat6072.

CONTENTS

LIST OF ABBREVIATIONS

AP-1	Activator protein 1
BS seq	Bisulfite sequencing
DEGs	Differentially expressed genes
DCM	Dilated cardiomyopathy
DUOX1 and 2	Dual oxidase 1 and 2
EC coupling	Excitation-contraction coupling
ETC	Electron transport chain
ER	Endoplasmic reticulum
$FADH_2$	Reduced flavin adenine dinucleotide
GPx	GSH peroxidase
GR	GSSG reductase
GRX	Glutaredoxins
GSH	Reduced glutathione
GSSG	Oxidized glutathione
GST	Glutathione S transferase
HCM	Hypertrophic cardiomyopathy
HF	Heart failure
HFrEF	Heart failure with reduced ejection fraction
HFpEF	Heart failure with preserved ejection fraction
HMOX1	Heme oxygenase
IDH2	Mitochondrial isocitrate dehydrogenase 2
iNOS/nNOS/eNOS	Inducible, neuronal, endothelial Nitric oxide synthase
IPA	Ingenuity pathway analysis
L/D2-HG	L/D2-hydroxyglutarate
LMNA	Lamin A/C
MHC	Myosin heavy chain
miRNA	Micro RNA
Mlp	muscle lim protein; also known as cysteine and glycine rich protein 3 (Csrp3)
NADH	Reduced nicotinamide adenine dinucleotide

NADPH	Reduced nicotinamide adenine dinucleotide phosphate
NF-κB	nuclear factor kappa-light-chain-enhancer of activated B cells
NNT	Mitochondrial nicotinamide nucleotide transhydrogenase
NRF2	Nuclear factor erythroid 2-related factor 2
•NO	Nitric oxide
NOXs	NADPH oxidases
NQO1	NAD(P)H quinone dehydrogenase 1
OGDHc	2-oxoglutarate dehydrogenase complex
OGDHL	Oxoglutarate dehydrogenase like
OSGIN1	Oxidative stress induced growth inhibitor 1
OxBS seq	Oxidative bisulfite sequencing
OXPHOS	Mitochondrial oxidative phosphorylation
RBM20	RNA binding motif protein 20
RedoximiRs	miRNAs that regulate redox responses
ROS/mtROS	Reactive oxygen species/mitochondrial ROS
RyR2	Ryanodine receptor 2
SOD	superoxide dismutase enzymes
SR	Sarcoplasmic reticlum
TCA cycle	Tricarboxylic acid cycle, also called Krebs cycle
TEM	Transmission electron microscopy
TET1-3	Tet methylcytosine dioxygenase 1
Trx	Thioredoxins
TrxR	Thioredoxin reductases
TTN	Titin
XOR	Xanthine oxidoreductase
XDH	Xanthine dehydrogenase
XO	Xanthine oxidase
2OG	2-oxoglutarate; also known as α-ketoglutarate (α-KG)

1 INTRODUCTION AND LITERATURE REVIEW

Despite improvements in medical and devise-based therapy, patients diagnosed with heart failure (HF) have a poor prognosis. HF remains the most common cause of morbidity and mortality worldwide (World Health Organization (WHO, 2019)). HF is a complex clinical syndrome with high etiological and clinical heterogeneity associated with a variety of comorbidities. Oxidative stress and imbalance of myocardial substrate metabolism are common features of HF (Bertero and Maack, 2018). However, approaches aiming to ameliorate oxidative stress in HF have so far not had positive clinical effects despite promising results from pre-clinical studies (van der Pol et al., 2019; Zhou and Tian, 2018). Adverse effects associated with excessive quenching of physiological levels of reactive oxygen species (ROS) could be one explanation underlying this failure, as ROS act as cellular signaling molecules in many normal physiological processes (Santos et al., 2011; Song et al., 2014).

In our recent study (Elbeck et al., 2022), on which this thesis is largely based, we employed a multipronged approach, involving a comprehensive approach that combines metabolic, transcriptional, and epigenetic analyses, to study the regulation of endogenous antioxidant defenses in the heart and their associated cellular signal transduction pathways. Our results challenge current concepts about general defects in the antioxidative capacity in heart failure and instead support an alternative view in which the antioxidative capacity in the failing heart is not always compromised. We show that IDH2, which was recently suggested to be a primary source of cardiac mitochondrial NADPH (Nickel et al., 2015), governs an antioxidative feedforward loop involving 2-oxoglutarate and L2-hydroxyglutarate in mitochondria and mutually coordinates these with other key defensive pathways, such as NRF2 (Elbeck et al., 2022).

The results of my thesis work highlight a different perspective on redox biology than the common view. Rather than perceiving oxidants as dangerous compounds, I consider them important cellular metabolites that, together with reductants, controls numerous biological functions. Below, I start by giving an overview of major sources of oxidative stress, with a focus placed on the heart, as well as of major antioxidative mechanisms. I next discuss in more detail the function of redox metabolites as cellular signaling molecules, regulators of redox-dependent reactions and modulators of protein structure and function. Finally, I discuss redox-associated crosstalk between mitochondria and the nucleus and the ensuing DNA methylation.

I also highlight some common misconceptions in the field using basic chemical and biological knowledge together with own observations supported by published literature. I mark some

commonly used terms that I however consider misnomers or misleading with quotation marks " ", which I will then further explain in more detail in subsequent sections.

1.1 CHEMISTRY AND BIOCHEMISTRY OF OXIDANTS

Redox reactions involve transfer of one or more electrons between two compounds. The compound that loses electrons is oxidized, and the compound that takes up electrons is reduced. Redox is the abbreviation for a pair of *red*uctant and *ox*idant, the reductant being the compound that donates electrons and, thus, reduces other compounds, and the oxidant being the compound that takes up the electrons and, hence, oxidizes other compounds.

> "Life is nothing but an electron looking for a place to rest."
>
> Nobel Prize-winning physiologist Albert Szent-Györgyi

The chemical tendency of a compound to either donate or take up electrons is reflected by its *redox potential* (E_h), which is a measure of the affinity of a compound for electrons. The value of the redox potential is usually set in comparison to that of hydrogen (E_0), with compounds having $E_h > E_0$ are considered oxidizing agents, and compounds having $E_h < E_0$ are considered reducing agents (Milo and Phillips, 2015). In biology, reductants are commonly called antioxidants or nucleophiles, while oxidants are sometimes called pro-oxidant, oxidative species or electrophiles.

Redox pairs are not only formed when an electron moves completely from one molecule to another, but also when there is a shift in electron density *within* molecules, such as in all organic compounds that contain more than one periodic element. Periodic elements, such as H, C, N, O and S, differ in their electronegativity (H<C≲S<N<O), and therefore they induce a shift in electron densities of covalent bonds toward one of the atoms. This concept forms the basis for the reactivity of all *bio*- compounds and for the principle that is utilized by all enzymes to facilitate reactions in their active centers.

Some oxidants may—wrongly but commonly—be called antioxidants because they have an extraordinary ability to elicit expression of enzymes involved in antioxidative responses, such as sulforaphane (SF). SF has an isothiocyanate group (−N=**C**=S), in which, both nitrogen and sulfur atoms have higher electronegativity than carbon, which leaves the carbon with a micro-positive charge. This electrophilic carbon will be susceptible to nucleophilic attack (Brown and Hampton, 2011), and therefore it is an oxidant (or pro-oxidant), not a reductant (or antioxidant).

1.1.1 Intracellular oxidants

Based on the active atom, oxidants have been categorized in different groups, including reactive *oxygen* species, reactive *nitrogen* species, and others.

Reactive oxygen species (ROS) are biochemical compounds that have an active oxygen atom in their chemical structure. ROS represents the largest subset of oxidants in cells. ROS are not a homogenous family of compounds, as commonly thought, but rather a widely divergent group of compounds with very distinct chemical properties and biological functions.

Singlet oxygen ($^1O_2$, an excited state of molecular oxygen O_2 with rearrangements in surface electrons) can capture an electron and form a superoxide free radical ($O_2^{\bullet -}$). However, superoxide is not a highly reactive radical (due to the low reduction potential of the O_2/ $O_2^{\bullet -}$ couple) and lacks the possibility to penetrate through biological membranes, and therefore it stays in the compartment where it is generated. Nevertheless, stepwise reduction of superoxide via 1-electron transfers can produce multiple highly reactive oxygen species (**Figure 1**) (Nordberg and Arnér, 2001).

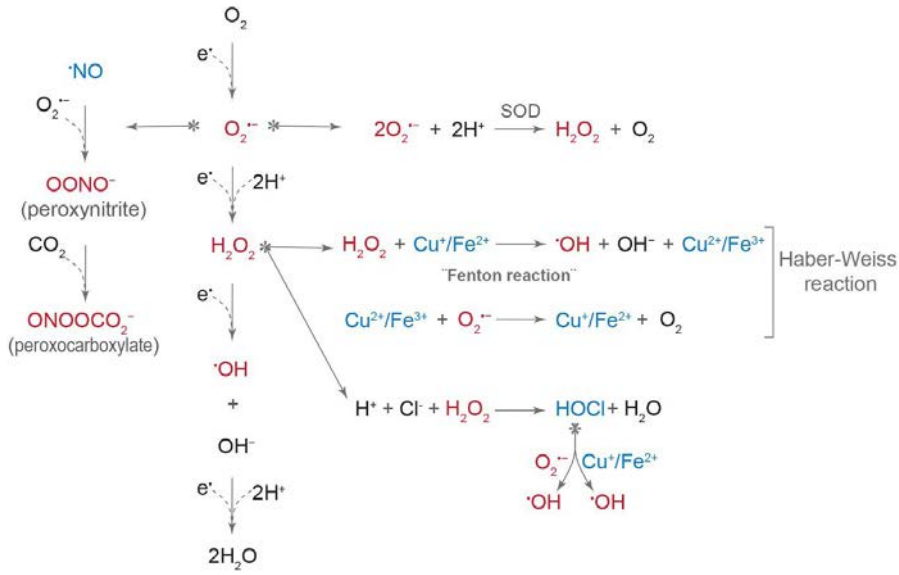

Figure 1: Stepwise reduction of molecular oxygen via 1-electron transfers and ensuing ROS

Information in the figure is adapted from Nordberg et al., 2001 (Nordberg and Arnér, 2001)

Two superoxide molecules are dismutated to hydrogen peroxide (H_2O_2) by superoxide dismutase enzymes (SOD). H_2O_2 is not a free radical, but it is a highly important intermediate that can diffuse through biological membranes and induce the formation of highly reactive radicals such as hydroxyl radical ($^{\bullet}OH$) and hypochlorous acid (HOCl). Hydroxyl radical has

strong reactivity with biomolecules and can be produced via the Fenton reaction of H_2O_2 with transient metals (Fe^{2+} or Cu^{+}) or via other reactions (reviewed in (Nordberg and Arnér, 2001)) (**Figure 1**).

Nitric oxide ($^{\bullet}NO$ or NO for simplicity, the dot denotes unpaired electron, which makes NO a radical) is a **reactive nitrogen species** (RNS) that represents another important radical produced in the cell. $^{\bullet}NO$ does not readily react with biomolecules, but it easily reacts with other radicals, such as ROS, producing either less reactive molecules, or ¨highly cytotoxic¨ radicals, depending on their surrounding milieu. Peroxynitrite ($OONO^{-}$) and peroxocarboxylate ($ONOOCO_2^{-}$) are examples of ¨cytotoxic¨ ensuing radicals. Peroxynitrite results from the reaction of $^{\bullet}NO$ with $O_2^{\bullet-}$, while peroxocarboxylate results from the further reaction of peroxynitrite with CO_2 (**Figure 1**) (Nordberg and Arnér, 2001). As indicated earlier, I marked the terms *highly cytotoxic* and *cytotoxic* property with quotation marks because I question its validity, as I will discuss in more detail in subsequent sections.

1.2 CELLULAR SOURCES OF OXIDANTS

Oxidants are produced by numerous enzymes in multiple organelles or compartments within the cell, either as main products, or as a by-product for a variety of biochemical reactions and activities (Balaban et al., 2005). It is commonly accepted that the mitochondrial electron transport chain is the main source of oxidants produced in the cell, but there are also other relevant mitochondrial and cellular sources (discussed in the subsequent sections 1.2.1.2-1.2.5) that may become particularly important in certain physiological or pathological contexts or in certain cell types.

1.2.1 Mitochondria

Mitochondria play a seminal role in cardiac metabolism. Alterations in mitochondrial function have deleterious effects on most cellular processes, and mitochondrial health is continuously sensed by the cell, leading to remodeling of their structure and function according to the physiological state and environmental stimuli. To enable quick and continuous supply of ATP to their contractile machinery, cardiomyocytes have densely packed mitochondria adjacent to the sarcomeres (**Figure 2**). Mitochondria constitute almost one quarter of the total volume of a cardiomyocyte (Sack et al., 2017). This makes the heart the most vulnerable organ for functional abnormalities upon alterations of oxidative phosphorylation or mitochondrial metabolic pathways.

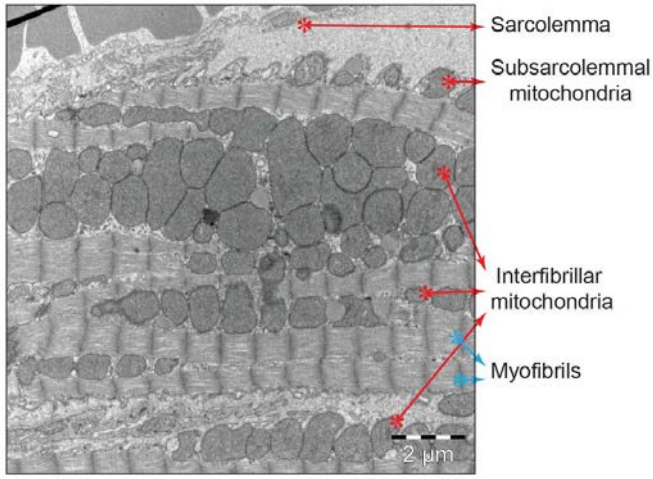

Figure 2: Images of LV myocardium of WT mice, captured with transmission electron microscopy
The source of the image is our work in collaboration with Kjell Hultenby.

Before going into the main sources of mitochondrial ROS, I will give a brief introduction to mitochondrial ATP production, as many steps in this process are considered major sources of oxidants in the cell.

1.2.1.1 Mitochondrial energetics

Mitochondria convert energy emanating from glucose and fatty acids into electron carriers, *e.g.*, nicotinamide adenine dinucleotide (NADH) and flavin adenine dinucleotide ($FADH_2$) through the citric acid cycle. Subsequently, by oxidizing electron carriers, energy is gained to phosphorylate ADP to ATP in the mitochondrial electron transport chain, i.e., oxidative phosphorylation.

Acetyl-coenzyme A (acetyl-CoA) represents the carbon source of the citric acid cycle. Acetyl-CoA is produced in the mitochondria from acetylating coenzyme A (CoA) through breaking down carbohydrates by glycolysis, β-oxidizing of fatty acids, or catabolizing multiple amino acids. Acetyl-CoA is then oxidized in the citric acid cycle (also known as Krebs cycle) through a series of biochemical reactions to harness its chemical energy into reducing power in NADH or $FADH_2$ (**Figure 3**).

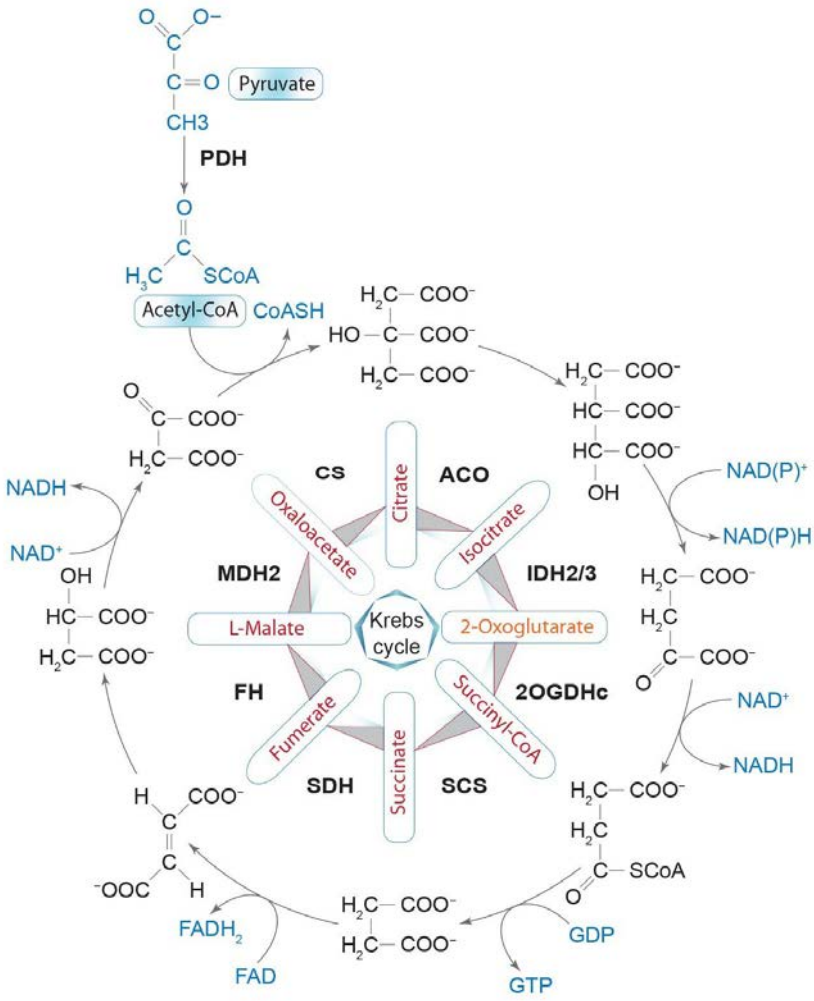

Figure 3: A cartoon over Kerbs cycle and electron transport system of the mitochondria

PDH: Pyruvate dehydrogenase. CS: Citrate synthase, ACO: Aconitase, IDH2/3: Mitochondrial isocitrate dehydrogenase 2 and 3, 2OGDHc: 2-Oxoglutarate dehydrogenase complex, SCS: Succinyl-CoA synthetase, SDH: Succinate dehydrogenase, FH: Fumarate hydratase (also known as fumarase), MDH2: Mitochondrial malate dehydrogenase. The figure is adapted from Wikipedia.

In addition to recharging electron carriers, the Krebs cycle also produces numerous intermediate metabolites that are essential for the biosynthesis of several biomolecules such as amino acids, for signal transduction, and for enzymatic activities (the last two will be discussed in section 1.5).

Reduced electron carriers, *e.g.*, NADH and $FADH_2$ deliver the electron to the electron transport chain (ETC) to regenerate ADP into ATP. ETC consists of four complexes of multi-subunit enzymes embedded in the inner mitochondrial membrane (**Figure 4**). An electron that

originates from the oxidation of NADH or FADH2 enters the ETC through complex I or complex II, respectively, where it mediates sequential redox reactions along the ETC complexes and mobile electron carriers (ubiquinone and cytochrome c). The electron finally reaches complex 4, where it reduces oxygen to water. The passage of the electron through each of the ETC complexes I, III and IV is coupled with a movement of proton(s) (H^+) from the mitochondrial matrix side to the intermembrane space, which creates a protonmotive force (the force is the potential result of the disequilibrium between proton concentrations across the membrane). This electrochemical gradient created by the ETC is then utilized by complex V (F_1F_0 ATPase) to regenerate ATP from ADP via channeling the proton back to the matrix side through ATP synthase (Munro and Treberg, 2017).

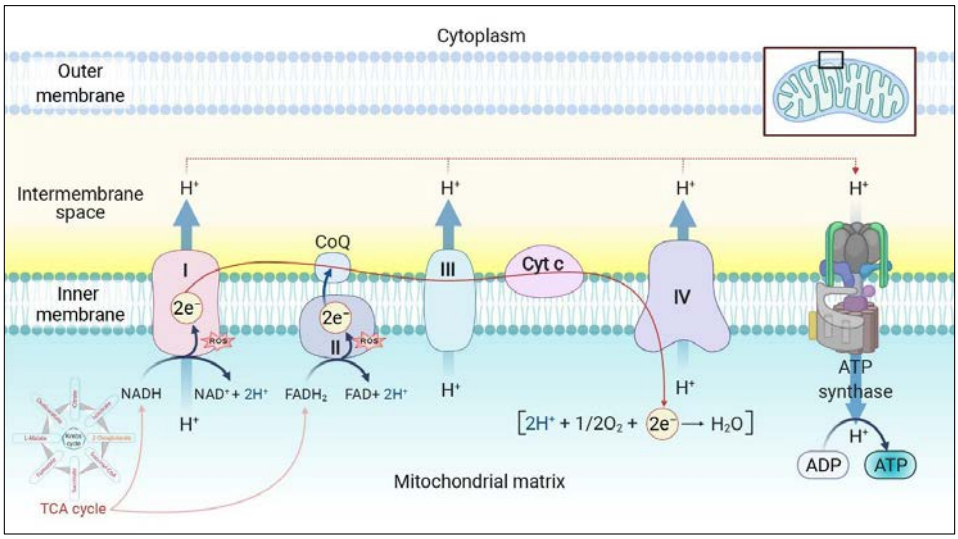

Figure 4: A cartoon over electron transport system of the mitochondria

Part of the figure is adapted from "Electron Transport Chain" template in BioRender.com (2022).

1.2.1.2 Mitochondrial sources of oxidative species:

As stated above, the mitochondrion is considered a major source of cellular ROS, *i.e.*, ~90% of the total ROS produced within the cell (Balaban et al., 2005).

A small amount of the electrons ¨leaks¨ from the electron transfer chain complexes to reduce O_2 to $O_2^{\bullet-}$ and further to H_2O_2. Complex I and III were found to be the major sites for $O_2^{\bullet-}$, where an electron can be transferred from the flavin group in complex I or ubiquinol in complex III to the molecular oxygen (**Figure 4**) (Murphy, 2009). (The misconception regarding the term ¨leak¨ is discussed in further details in section 1.4).

The rate of H_2O_2 production from ETS is correlated with the protonmotive force, but inversely related to the rate of ATP regeneration. As the flow of electrons through the ETS is coupled

with the translocation of proton, the increase in protonmotive force will delay the flow of electrons through ETS. As a consequence, electrons will build up in the redox centers of the enzymes of the ETC complexes and the electron carriers NADH and $FADH_2$, putting them in a more reduced state, *i.e.*, richer in electrons (*i.e.*, higher $NADH/NAD^+$ ratio). This increases $O_2^{\bullet-}$ production, as impeded electrons will reduce O_2 more readily (Munro and Treberg, 2017). Post-translational modifications of proteins in the ETC might also hamper electron flux through the ETC, and therefore increases $O_2^{\bullet-}$ production (Weissman and Maack, 2021).

Although the electron transfer chain complexes I and III are often viewed as the major sites of mitochondrial ROS (mtROS) production, multiple other mitochondrial enzymes may also significantly contribute to mtROS production. However, the contribution of these sites to total mtROS varies enormously according to the substrates being oxidized and to the physiological condition (Quinlan et al., 2013; Shadel and Horvath, 2015; Starkov et al., 2004). In this context, the dihydrolipoamide dehydrogenase (DLD) component of the 2-oxoglutarate dehydrogenase complex (OGDHc)) was found to be a significant contributor to mtROS production in the brain, an effect further enhanced under pathological conditions that altered $NADH/NAD^+$ ratio (Jordan et al., 2019; Starkov et al., 2004).

However, OGDHc has been recently found *not* to be a significant contributor to mtROS production in the heart, but on the contrary to play a major role in the elimination of mtROS. NADH produced by OGDHc is preferentially shuttled to nicotinamide nucleotide transhydrogenase (NNT) to regenerate NADPH, and therefore enhances the antioxidant capacity of the heart (Wagner et al., 2020).

1.2.2 NADPH oxidase

NADPH oxidase (NOXs) are a family of enzymes that utilize NADPH as an electron donor to generate $O_2^{\bullet-}$ from O_2. The family is composed of seven isoforms (NOX1-5, and dual oxidase 1 and 2 (DUOX1,2)), which localize to the membrane of cells or organelles. The primary role for NOXs family is either to produce $O_2^{\bullet-}$ that is subsequently dismutated to H_2O_2 by associated SOD enzymes, or to produce H_2O_2 directly (by NOX4 and DOX1,2).

ROS generated by some NOXs comprise an important host defense mechanism in some cells (*e.g.*, ROS produced by NOX2 in phagocytes, or by DUOXs in some epithelial cells). However, the fact that there are no other anabolic or catabolic known functions for NOXs beyond ROS production may point toward other important roles. Indeed, NOXs constitute an important controlled redox signaling mechanism in all cells, through directly generating low levels of

ROS localized to the microenvironment of certain proteins. These target proteins are involved in pathways related to multiple cellular processes, such as survival, migration, differentiation and proliferation (Santos et al., 2011).

NOX2 and NOX4 are among the most studied and abundant members of NOX family in the heart. These two isoforms have several major differences in their activation, localization and the species of ROS produced, suggesting that they may play different roles in the heart. NOX2 is considered ¨maladaptive¨, whereas NOX4 is considered protective (Santos et al., 2011; Weissman and Maack, 2021). However, in a subsequent section (1.4.1) of this monograph, I discuss in further detail the beneficial physiological roles of ROS generated by both NOX2 and NOX4, and why I consider the term ¨maladaptive¨ misleading.

1.2.3 Nitric oxide synthase

The free radical •NO is produced by nitric oxide synthases (NOS) through catalytic conversion of L-arginine to L-citrulline utilizing O_2 and NADPH (**Figure 5**) (Knowles and Moncada, 1994). The NOS family is comprised of three isoforms (inducible (iNOS), neuronal (nNOS) and endothelial NOS (eNOS)). Both eNOS and nNOS are constitutively expressed in the cardiovascular system, including cardiomyocytes, whereas the expression of iNOS is induced upon certain pathological conditions, such as septic cardiomyopathy, as a response to endotoxin or mediators of inflammation (Thoenes et al., 1996; Weissman and Maack, 2021). The potency of iNOS in producing •NO is ~5 times higher than that of eNOS or nNOS (Sun et al., 2010).

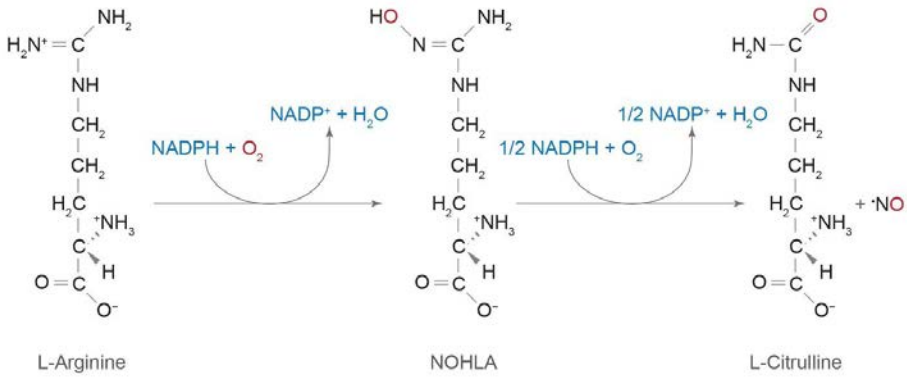

Figure 5: Production of NO by NOSs

NOHLA: N^{ω}-hydroxy-L-arginine, the figure was adapted from Wikipedia.

The primarily localization of nNOS is the sarcoplasmic reticulum in the cardiomyocytes, where it regulates calcium homeostasis and contractility through •NO-dependent nitrosylation of

cysteine residues of key proteins involved in these processes (Weissman and Maack, 2021). Cardiomyocytes express also eNOS, but less than endothelial cells (Balligand et al., 1995). iNOS is expressed in a wide variety of other cell types (Balligand et al., 1994).

The physiological signaling of NOS is considered protective in general. However, NOSs become uncoupled in the absence of tetrahydrobiopterin (BH4), which is an essential cofactor for their canonical production of $^{\bullet}NO$. Subsequently, electron flux through uncoupled NOSs induces the reduction of oxygen to $O_2^{\bullet-}$ instead of $^{\bullet}NO$. In turn, $O_2^{\bullet-}$ could react with $^{\bullet}NO$ to form $OONO^-$, which induces protein nitration and nitroxidative ¨stress¨ (Santos et al., 2011; Weissman and Maack, 2021). Nevertheless, the negative impact and ¨stress¨ induced by $OONO^-$ are debatable, as will be discussed later in this monograph.

1.2.4 Xanthine oxidoreductase

Xanthine oxidoreductase (XOR) is a multifunctional enzyme complex that may exist in two interconvertible isoforms through posttranslational modifications, *e.g.*, xanthine dehydrogenase (XDH) and xanthine oxidase (XO). XOR catalyses the final two steps in purine catabolism by oxidizing hypoxanthine to uric acid, which is a proinflammatory agent and a fundamental antioxidant. In addition to uric acid, two ROS, *e.g.*, $O_2^{\bullet-}$ and H_2O_2, are also produced by XOR, through utilizing O_2 as an electron acceptor by the XO isoform, or NAD^+ by the XDH isoform, and thus acting as a NADH oxidase. Moreover, XOR can act as nitrate and nitrite reductase producing $^{\bullet}NO$ that has vasodilatory effects and thus can regulate blood pressure and flow (**Figure 6**) (Bortolotti et al., 2021).

Elevated and aberrant XOR activities have been observed in multiple cardiovascular diseases, and inhibition of XOR could have beneficial effects *in vivo*. Therefore, XORs have been targeted for inhibition in numerous clinical studies, which aimed to ameliorate pathological consequences associated with elevated XOR activities, but without any clinical success (Weissman and Maack, 2021).

The lack of clinical benefits from targeting XOR would emphasis again the importance of considering physiological (not only pathological) roles of oxidants and their regulating enzymes. This topic will be the focus of a subsequent sections of this monograph, as a general concept relating to all oxidants, not only XORs-associated oxidants. XORs and their fundamental physiological functions were recently comprehensively reviewed by Bortolotti and colleagues (Bortolotti et al., 2021).

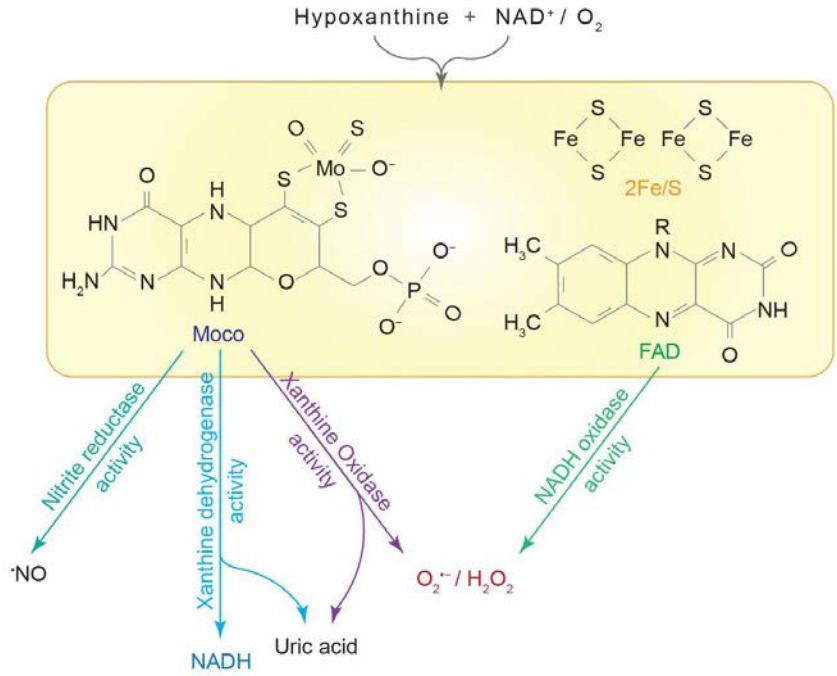

Figure 6: XOR structure and function

Mcoc: molybdopterin cofactor containing a molybdenum atom, the figure was adapted from Bortolotti *et al.,* (Bortolotti et al., 2021).

1.2.5 Other sources of cellular oxidants

Redox reactions are all about electron movements, and therefore the majority of, if not all, cellular biochemical reactions are in fact redox reactions that involve oxidants and reductants. In principle, any of these reactions could be a potential source of oxidative species under particular circumstances or in pathological conditions.

All above-described sources of oxidative species in sections (1.2.1-4) are ubiquitous enzymes involved in multiple mechanisms and in multiple cell types. Other potential enzymatic sources of oxidative species might only be relevant for a specific mechanism; those will not be discussed here. However, certain other potential sources that are involved in the excitation-contractions coupling of cardiomyocytes will be briefly mentioned below (1.4).

1.3 REDUCTIVE SYSTEMS

The production of oxidants is not the sole determinant of their cellular levels; scavenging systems are another major factor controlling oxidant levels. The intracellular milieu is generally

reductive, but we live in an oxidizing environment. This would therefore imply that our cells are equipped with powerful reductive systems that can maintain such disequilibrium.

The word *antioxidative* would give the immediate impression that the main role for the reductive system is to neutralize oxidants, but this is misleading. Many posttranslational modifications of proteins are functional chemical moieties originating from oxidants or reductants. Redox is even essential for fundamental biochemical modifications of proteins, such as disulfide bond formation and correct protein folding. Therefore, the role of the reductive system extends far beyond neutralizing ROS; it controls numerous essential biological processes. Thus, it might be more accurate to call it a *reductive* rather than *antioxidative* system, as the latter only implicates one of its many roles.

Cellular redox homeostasis is maintained by the reductive system, which is comprised of multiple components, such as reductants (nucleophiles), regulatory transcriptional factors, and a variety of enzymes (**Figure 7**). In this section, I will discuss several of these components, but with the focus on those elements that are more relevant to cardiomyocytes, and to our recent study on these cells (Elbeck et al., 2022).

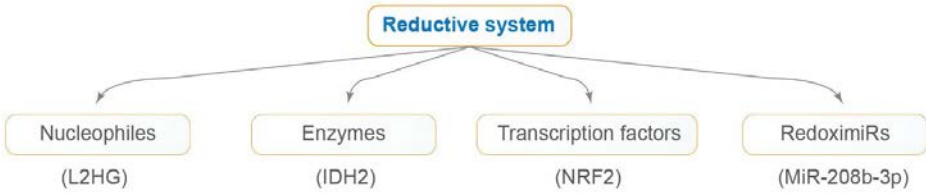

Figure 7: The components of the reductive system

The item mentioned below each box in parentheses is an example for a component of the reductive system that has been a subject for the experimental work of this monograph and our recent published paper (Elbeck et al., 2022).

1.3.1 Endogenous nucleophiles and their related enzymes

Nucleophiles (or reductants) are compounds rich in electrons that donate electrons to oxidants, either directly or by being substrates or cofactors for redox reactions. Glutathione is considered the main reductant in cells, but there are also multiple other reductants that collectively maintain adequate redox homeostasis.

Glutathione (GSH) is a tripeptide composed of three amino-acids (γ-L-glutamyl-L-cysteinyl glycine). GSH is a highly abundant reductant in all cells, prevalent at high intracellular concentrations (0.1-10 mM) (Meister, 1988). Two GSH are oxidized to form GSSG by donating their electrons to reduce other oxidized compounds. The majority of the cellular GSH

(98%) exists in its reduced form, and localizes predominantly to the cytoplasm, and to some extent (10-15%) to the mitochondria (Lu, 2013).

GSH plays an important role in antioxidative defense, as well as in cellular signaling. GSH acts as a substrate in a variety of redox reactions catalyzed by enzymes involved in antioxidative defense, detoxification, and modification of protein structure and function through posttranslational modification. Therefore, GSH is directly or indirectly involved in numerous cellular functions (Lu, 2013). GSH was controversially reported to have the ability to reduce superoxide directly, but this reaction, if it ever happens, would be slow and may results in the formation of other types of ROS (Winterbourn, 2016).

The levels of cellular GSH do not only depend on its direct synthesis from its constitutive amino acids, but also on its utilization and regeneration. GSH synthesis is allosterically regulated through high levels of GSH inhibiting its first step of synthesis, which is catalyzed by the γ-glutamyl-cysteine ligase (GCL). At the utilization and regeneration level, consumed GSH during the reduction of H_2O_2 to water by **GSH peroxidase (GPx)**, is regenerated by **GSSG reductase (GR)** that reduces GSSG back to GSH utilizing NADPH as an electron donor.

GSH can also be conjugated to the thiol (-SH) moiety of a cysteine residue in proteins through a process called glutathionylation, which modulates the structure or function of proteins or protects them from further oxidation. Glutathionylation is catalyzed by **glutathione S transferase (GST)**, whereas deglutathionylation is catalyzed by **glutaredoxins (GRX)** using GSH as a reductant (**Figure 8**) (Lu, 2013).

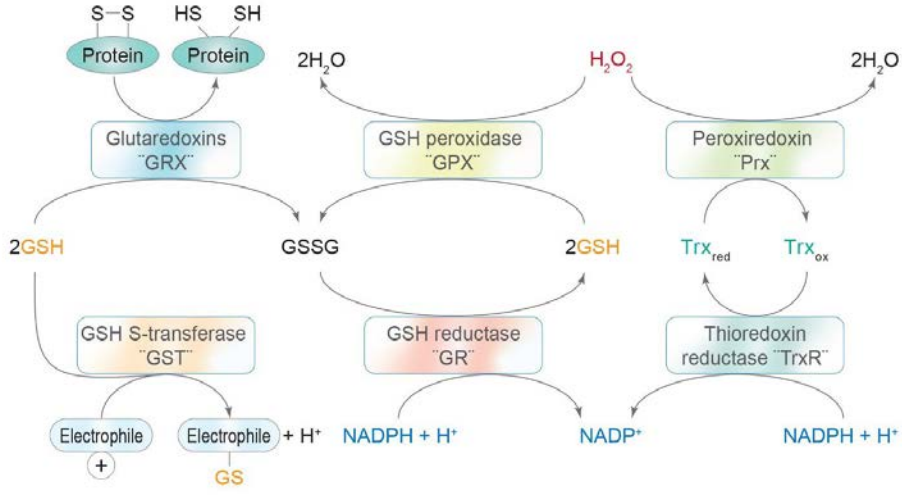

Figure 8: Prominent cellular nucleophiles and some of their dependent enzymes and reactions

GSH: Glutathione, Trx: Thioredoxin, the figure was adapted from Espinosa-Diez et al.,(Espinosa-Diez et al., 2015).

Thioredoxins (Trx) are other important cellular reducing peptides with oxidoreductase activity. Three distinct variants have been identified in humans, among which are Trx1 (12 kDa), which is the most studied variant, and Trx2 that localizes to the mitochondria. All thioredoxins have a conserved -Cys-Gly-Pro-Cys- domain in their active site (Nordberg and Arnér, 2001).

Thioredoxin expression is induced under oxidative stress, where they play a seminal role in the reduction of peroxides. Thioredoxins also play a regulatory role by translocating to the nucleus and regulating the DNA binding of the transcription factors AP-1 and NF-κB. The disulfide bond formed in the active site of oxidized thioredoxins is reduced by **thioredoxin reductases (TrxR)** (**Figure 8**). TrxR are NADPH-dependent isoenzymes that contain selenium in the form of selenocysteine at their C-terminal active site. The selenocysteine residue is essential for the activity of TrxR, and it enables TrxR to reduce a wide variety of substrates, and not only the disulfide bond in oxidized Trx. In fact, TrxR can reduce disulfides in certain other proteins, as well as in certain oxidized disulfide, or non-disulfide low molecular weight compounds (Nordberg and Arnér, 2001).

Ascorbic acid (Vitamin C), a water-soluble vitamin, is a major reductant in the plasma, which prevents the formation of lipid hydroperoxide. Low density lipoprotein (LDL) can readily be oxidized by free radicals forming lipid peroxides, which in turn break down to form reactive lipid aldehyde products that modify LDL apolipoproteins. Subsequent uncontrolled scavenging of aldehyde-modified apolipoproteins by macrophages forms foam cells, which ultimately initiate the atherosclerotic lesion (Esterbauer et al., 1993). Moreover, ascorbate, together with GSH and α-tocopherol, also plays a role in protecting lipids in membranes from oxidative damage (Nordberg and Arnér, 2001).

Whereas ascorbate is a water-soluble vitamin, **α-tocopherol** (vitamin E) is lipid soluble, and therefore it protects biological membranes from oxidative damage. It can react with unpaired electrons of the peroxyl radicals through its hydroxyl group, and thus prevent subsequent lipid peroxidation, whereby the oxidized form of α-tocopherol is then reduced back by ascorbate (Nordberg and Arnér, 2001).

Another important cellular reductant is the reduced form of the R-α-Lipoic acid (*i.e.*, **dihydrolipoic acid (DHLA**), which is a component of the dihydrolipoyl transacetylase (E2) of the 2-oxoglutarate dehydrogenase complex (OGDC). DHLA has antioxidative properties that can directly scavenge ROS, or regenerate many other reductants (Moini et al., 2002).

Reduced ubiquinone (ubiquinol, coenzyme Q/Q10) is also considered as an antioxidant. Q10 is found in plasma membranes and represents a mobile component of the mitochondrial electron transport chain. It is a medical supplement that is widely given to patients with mitochondrial dysfunctions or as nutritional anti-aging supplement, despite the lack of proof of clinical benefit (Wang and Hekimi, 2016).

In addition to all reductants mentioned above, there is a wide variety of other cellular compounds that may act as essential reductants in certain contexts, such as L2-hydroxyglutarate (L2HG) and others (Elbeck et al., 2022). Other cellular reductants have been reviewed in (Espinosa-Diez et al., 2015; Nordberg and Arnér, 2001) and other review articles, and they will not be further discussed here. However, the redox role of L2HG will be illustrated in a subsequent section (1-5).

1.3.2 Reduced nicotinamide adenine dinucleotide phosphate (NADPH)

Enzymatic regeneration of glutathione and other reductants requires reduced nicotinamide adenine dinucleotide phosphate (NADPH). NADPH is a reductant itself, but it does not reduce oxidative species directly, it instead represents an essential electron donor for numerous biological reactions, including redox reactions. Thus, the redox couple $NADP^+$/NADPH represents the key element in the maintenance of redox homeostasis.

NADPH is produced by multiple enzymes in the cell (**Figure 9**). The contribution of each of these sources to the cellular NADPH pool varies according to the cellular compartment and to the cell type. In most cell types, glucose 6-phosphate dehydrogenase (**G6PD**) is considered a main contributor of cytosolic NADPH through the pentose phosphate pathway. $NADP^+$ dependent isocitrate dehydrogenases (**IDH1 & 2**) are also a relevant source for both cytosolic (*i.e.,* IDH1) and mitochondrial (*i.e.,* IDH2) NADPH through catalyzing oxidative decarboxylation of isocitrate (as an electron donor) to 2-oxoglutarate. In heart and liver, the contribution of IDHs to the pool of NADPH exceeds that of G6PD by severalfold (Koju et al., 2022), where particularly IDH2 followed by nicotinamide nucleotide transhydrogenase (NNT) represent the quantitively largest sources of cardiac mitochondrial NADPH (Nickel et al., 2015; Wagner et al., 2020).

Mitochondrial nicotinamide nucleotide transhydrogenase (**NNT**) regenerates NADPH from NADH in a reversible reaction, and therefore plays an important role in maintaining an appropriate ratio of NADPH/NADH. Moreover, both cytosolic and mitochondrial $NADP^+$ dependent malic enzymes (**NADP-ME**) contribute to the pool of NADPH through catalyzing the reversible oxidative decarboxylation of L-malate to pyruvate. Moreover, glutamate

dehydrogenase (**GDH**) produces NADPH through catalyzing the reversible oxidative deamination of glutamate to 2-oxoglutarate. In addition to what has been mentioned above, there are few other sources for NADPH, including folate metabolism as well as other sources (Koju et al., 2022).

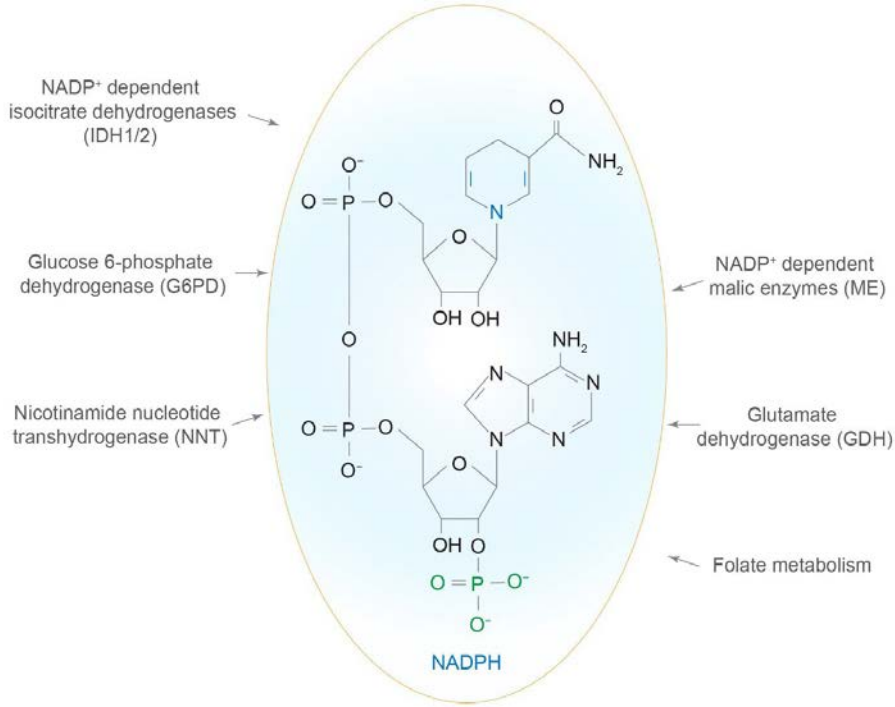

Figure 9: Cellular sources of NADPH

NADPH: Reduced nicotinamide adenine dinucleotide phosphate, it differs from NADH by having a phosphate group (PO_3^-) highlighted in green.

In a subsequent section of this monograph, IDH2 and NNT will be highlighted with more details, as they both are the most relevant sources of NADPH in cardiac mitochondria, and because IDH2 represents the main topic of our recent work about the regulation of the endogenous antioxidative capacity in cardiomyocytes (Elbeck et al., 2022).

1.3.3 Other redox-dependent enzymes

In addition to enzymes mentioned above, there are numerous other enzymes that catalyze the reduction of oxidative species or regulate the reductive system in general. **Superoxide dismutases** (SOD) represent a family of key enzymes that dismutate superoxide to water:

$$2O_2^{\bullet-} + 2H^+ \xrightarrow{SOD} H_2O_2 + O_2$$

SODs are metal-containing enzymes. Mn-SOD is an essential enzyme for survival, which localizes to mitochondria where it dismutates $O_2^{\bullet-}$ generated by the electron transport chain. The other two members of the SOD family, *i.e.*, Cu-SOD and Zn-SOD are localized to the cytoplasm and are not essential for survival (Nordberg and Arnér, 2001).

Generated H_2O_2 can also be dismutated to water by the glutathione- or thioredoxin-dependent systems, or by **catalase**. Catalase is a prominent enzyme located in peroxisomes and dismutates hydrogen peroxide to water. Although catalase function does not require NADPH, its binding to NADPH increases its efficiency and stability. Catalase also localizes to the mitochondria, especially in the liver, but it has minimal contribution to the dismutation of hydrogen peroxide in muscular mitochondria in comparison to the glutathione- or thioredoxin-dependent systems (Munro and Treberg, 2017; Nordberg and Arnér, 2001).

Also **aldehyde dehydrogenase 2** (ALDH2) represents an important mitochondrial antioxidative enzyme that detoxifies products of lipid peroxidation, such as malondialdehyde (MDA) and 4-hydroxynonenal (4-HNE) (Weissman and Maack, 2021).

1.3.4 Redox-dependent transcription factors

Redox homeostasis is regulated through numerous transcription factors. These factors sense and adjust redox homeostasis to meet cellular physiological needs through activating the transcription of genes involved in the detoxification of oxidative species or in redox signaling. NRF2 is considered the master regulator of redox homeostasis, but there are also many other redox-dependent transcription factors, such as AP-1, NF-κB, NRF1, HIF-1, TP53, and others (Espinosa-Diez et al., 2015; Lu, 2013). Here, I will only highlight NRF2, AP-1 and NF-κB with more details, as they are the most important transcriptional factors for the antioxidative defense. It also provides background for the mutual regulation between NRF2 and IDH2 described in our recent work (Elbeck et al., 2022).

I- NRF2: Nuclear factor-erythroid factor 2-related factor 2 (NFE2L2, or NRF2) is a key transcription factor that regulates the transcription of more than 1000 genes containing antioxidative-response-element (ARE) with the consensus sequence 5′-TGACnnnGC-3′ in their promoters. Under normal stress-free conditions, NRF2 has a very short half-life. The stability of NRF2 is controlled by its interaction with KEAP1, which is an adaptor subunit of Cullin3 (CUL3)-dependent E3 ubiquitin ligase complex that polyubiquitinylates NRF2 for targeting to proteasomal degradation (**Figure 10**).

Oxidative stress induces posttranslational modification of NRF2 or KEAP1, causing the dissociation of NRF2 from KEAP1. Dissociated NRF2 escapes proteasomal degradation and translocates to the nucleus, where it heterodimerizes with the Small MAF proteins. Subsequently, the NRF2-Small MAF heterodimer binds to the ARE regulatory element present in the promoters of numerous genes to activate their transcription (**Figure 10**) (Canning and Bullock, 2014; Lu, 2013; Suzuki and Yamamoto, 2015).

Several mechanisms have been described for the role of oxidants in regulating NRF2 signaling. Oxidants induce a conformational change of KEAP1 through oxidizing its cysteine residues located in a region between the BTB and Kelch repeat domains. This induces a change in the 3D structure of KEAP1, preventing it from binding to NRF2 (Dinkova-Kostova et al., 2002). Moreover, ROS activates both protein kinase RNA (PKR)-like ER kinase (PERK) and PKC-δ, which phosphorylate NRF2, causing its dissociation from KEAP1 (Cullinan et al., 2003; Huang et al., 2002).

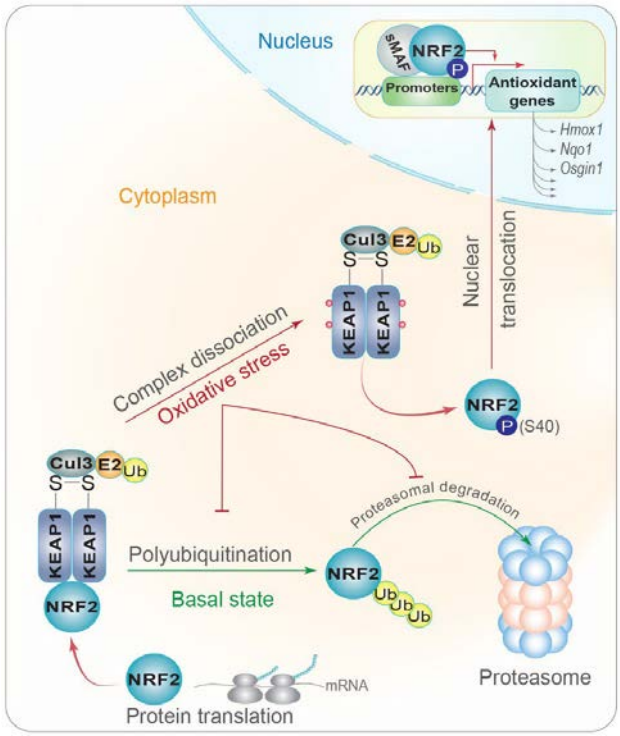

Figure 10: KEAP1 dependent regulation of NRF2

Under basal conditions, NRF2 is kept inactive by Keap1 with a very short turnover half-life (few min). Oxidative stimuli induce the dissociation of NRF2 from KEAP1 and its subsequent nuclear translocation to activate the transcription of antioxidative genes.

NRF2 downstream target genes encode many enzymes that regulate antioxidative responses. Among these downstream targets of NRF2 are genes encoding for the catalytic subunit of glutamate-cysteine ligase (GCLC) and glutathione S-transferase (GST).

Among downstream target genes of NRF2 are also the three HMOX1, NQO1 and OSGIN1 genes, which I have utilized in my work to monitor cardiomyocyte antioxidative responses to multiple redox stimuli (H2O2, sulforaphane, NAC, KEAP1-inhibitor, Tet1-3-knockdown) (Elbeck et al., 2022). The reason behind choosing these genes was that they represent temporal indicators of different phases of the cellular response to oxidative stimuli. HMOX1 and NOQ1 are induced during the initial phase of the response, while the induction of OSGIN1 would represent a late phase when cells have ultimately activated apoptotic pathways to eliminate damaged cells, after exhausting the possibilities to counteract and repair the damage.

- HMOX1 (heme oxygenase) degrades heme molecules into biliverdin/bilirubin, ferrous ion Fe^{2+}, and carbon monoxide (CO) (**Figure 11**). Both biliverdin and CO are believed to protect against oxidative damage. Patients with Gilbert syndrome, who have elevated serum levels of biliverdin, have lower incidence of cardiovascular diseases, believed to be the consequence of protection from oxidative damage (Schwertner and Vitek, 2008). CO, on the other hand, is extremely toxic at high concentrations, but at low concentration believed to induce protective pathways that inhibit apoptosis (Vieira et al., 2008). Fe^{2+} appears to be a toxic by-product, as it participates in the Fenton reaction to generate ROS. However, low levels of ROS could be beneficial in initiating cellular signaling for defensive mechanisms to prime cells for better antioxidative capacity.

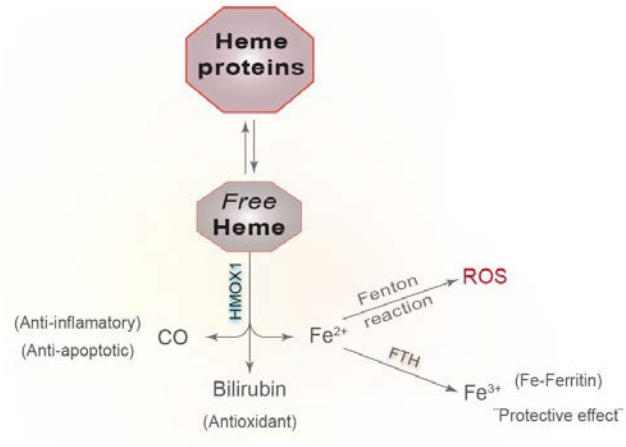

Figure 11: Antioxidative role of Hmox1

CO: Carbon monoxide, FTH: Ferritin heavy chain.

It is probably worth mentioning that these attractive effects of HMOX1 and CO have been used as basis for multiple preclinical and clinical studies, however without positive outcome in any large clinical trials thus far. Excessive inhibition of endogenous antioxidants could probably explain the failures of antioxidant clinical trials. However, for HMOX1 and CO, there might be more relevant explanations for the failure, as the scientific methodology and accuracy of several relevant publications on HMOX1 and CO have been questioned at the peer review site (PubPeer), raising concerns about the studies' validity. A protective effect of HMOX1 is likely, as the high induction of HMOX1 in response to oxidative stress, as well as the presence of multiple isoforms of HMOX1 in the cytoplasm, mitochondria, and nucleolus, point to versatile and context-dependent functions. Clearly, however, it will require more careful research to unveil any real beneficial mechanisms.

- NQO1(NAD(P)H quinone dehydrogenase 1) is a cytosolic reductase that catalyzes two-electron-reduction of quinones to hydroquinones, and hence prevents its one-electron-reduction to semiquinone free radicals. Moreover, NQO1 stabilizes the tumor suppressor factor P53, which either activates DNA repair, or eliminates damaged cells by activating apoptosis (Ross and Siegel, 2004).

- OSGIN1 (oxidative stress induced growth inhibitor 1) is an oxidative stress response protein that mediates apoptosis by inducing the release of cytochrome c from mitochondria (Brennan et al., 2017).

II- NF-κB: The nuclear factor kappa-light-chain-enhancer of activated B cells (NF-κB) is a homo- or heterodimer of 5 distinct proteins that share a Ref homology domain (RHD) in their N-terminus. Through RHD, NF-κB binds to DNA to regulate transcription of specific genes (*e.g.*, *FTH*, *SOD2*, *HIF-1α*) involved in the production of cytokines and in protecting cells against multiple noxious factors such as free radicals, heavy metals or viruses (Lingappan, 2018).

Similar to NRF2, NF-κB proteins are kept inactive by inhibitory κB (IκB) proteins. Upon stress, IκB is phosphorylated by IκB-kinase complex (IKK) and subsequently targeted for proteasomal degradation. The latter releases NF-κB so that it can bind to a consensus sequence 5′-GGGRNNYYCC-3′ present in the promoter or enhancer of target genes (Espinosa-Diez et al., 2015). Moreover, the regulation of NF-κB is mutually orchestrated by other reductive elements, such as KEAP1, which also inhibit the activation of NF-κB by mediating the degradation of IKKβ (Lee et al., 2009), in addition to its role in inhibiting NRF2.

III- AP-1: Activator protein 1 (AP-1) is a heterodimer of proteins of c-Fos, c-Jun, ATF and JDP families, which binds to the 12-O-**T**etradecanoyl**p**hobol-13-**a**cetate (TPA)-responsive element (5′-TGAG/CTCA-3′) or cAMP responsive element (5′-TGACGTCA-3′) in DNA. AP-1 regulates numerous cellular processes, including response to oxidants, proliferation, apoptosis, survival, and others. Moreover, AP-1 activity is regulated by oxidants, which induce the expression of *c-fos* and *c-jun* (Janssen et al., 1997), and modulate its DNA binding affinity by reducing specific cysteine residues in its structure (Abate et al., 1990).

In addition to the redox-dependent transcription factors, enzymes and molecules mentioned above, redox is also regulated by numerous miRs, termed "redoximiRs". However, one potential redoximiR (i.e., miR-208b-3p) will be discussed in a subsequent part of this monograph (Study II, section 2.2), and will therefore not be further discussed here.

In summary, this section has discussed how redox is regulated by a network of complex and interconnected mechanisms, involving multiple elements of small molecules, enzymes, transcription factors and noncoding RNAs. Some of these elements activate certain redox-depedent mechanisms and others may simultaneously inhibit them in a collective mechanism that will ultimately orchestrate and fine-tune the adequate redox response or signaling.

1.4 BIOLOGICAL ROLES OF REDOX, FRIENDS OR FOES?

Conceptually, the term ¨ROS¨ (or oxidants in generals) has been extensively associated with negative perceptions, such as ¨Oxidative ***damage***¨, ¨electron ***leakage***¨, ***apoptosis*** etc. However, the widespread and wide variety of oxidative species, as well as the highly complex and interconnected mechanisms involved in generating, regulating, and neutralizing oxidants refute these concepts.

The unanimously negative views on ROS have probably historical roots in many studies linking excessive production of ROS with disease. Even though this correlation might be true, I question the view that ROS are always injurious by-products in the situations where they are observed or even elevated.

I also question the view that electrons ¨*leak*¨ from a healthy system to form ¨*dangerous*¨ superoxide $O2^{\bullet-}$. If so, why wouldn't nature have evolved a tighter system that prevents ¨*leakage*¨ of electrons, which could save massive ¨dissipated energies¨ required for the generation of ROS and their subsequent scavenging.

The answers that would ultimately refute these negative concepts lay in the vital roles of ROS and other oxidants in physiological functions. Oxidants and reductants are not only produced

to neutralize each other's negative consequences, but probably in most cases instead to participate in numerous normal biological functions, from being utilized as defensive weapons against infections (in phagocytes), to being utilized in signal transduction and post translational modifications of proteins (Munro and Treberg, 2017; Nordberg and Arnér, 2001).

Before providing examples about the crucial roles for redox in regulating essential cellular functions, I will briefly discuss an essential mechanism for cardiomyocytes contraction called **EC coupling**, as it is highly regulated by redox modifications, and as the heart is the focus of this monograph.

In cardiomyocytes, the mechanism that transmits electrochemical signal of the action potential (excitation) into mechanical response (contraction) is called excitation-contraction coupling (**EC coupling**). In this process, the polarization of cardiomyocyte's membrane (sarcolemma) is established by both *active* (powered by ATP) and *passive* (driven by electrochemical gradient) selective-transport of ions (mainly K^+, Na^+ and Ca^{2+}) across membrane through gated ion-selective-channels. This selective gating generates an electrical voltage across the membrane known as the **action potential (AP)** (**Figure 12**).

During this process, the resting potential is generated by a constitutive active inward flux of 3 K^+ ions for every 2 outward pumped Na^+ ions through an ATP-fueled Na^+/K^+ATPase1/2 channel. This creates a higher inner concentration of K^+ (I_{K1}). K^+ ions then flow outward driven by their electrochemical gradient, until an equilibrium is reached, causing the polarization of the sarcolemma. This induces the opening of voltage gated Na^+ channels which causes a rapid inward movement of Na^+ (phase 0) driven by their electrochemical gradient (I_{Na}), which depolarizes the sarcolemma, and triggers the inactivation of the Na^+ gate. This is followed by phase 1, in which K^+ moves outwards driven by both their concentration and the electrical gradient (I_{to}), which partially repolarizes the sarcolemma. During phase 2, a balancing current is established by inward movement of Ca^{2+} (I_{Ca}) through a voltage gated Ca^{2+} channel (L-type Ca^{2+} channel). This influx of Ca^{2+} triggers the release of Ca^{2+} through intracellular calcium ryanodine receptor (RyR2) channels from sarcoplasmic reticulum by a process known as Ca^{2+}-induced Ca^{2+} release. This inward flux of calcium ions is balanced by an outward flux of potassium ions mediated by two types of channels referred to as delayed rectifier potassium channels (I_{Kr}, I_{Ks}). Once the L-type Ca^{2+} channels are closed, there is no more inward flux of ions to balance the outward of the potassium ions, and thus the sarcolemma becomes completely repolarized again during phase 3 to reach the resting negative potential in phase 4 (**Figure 12**).

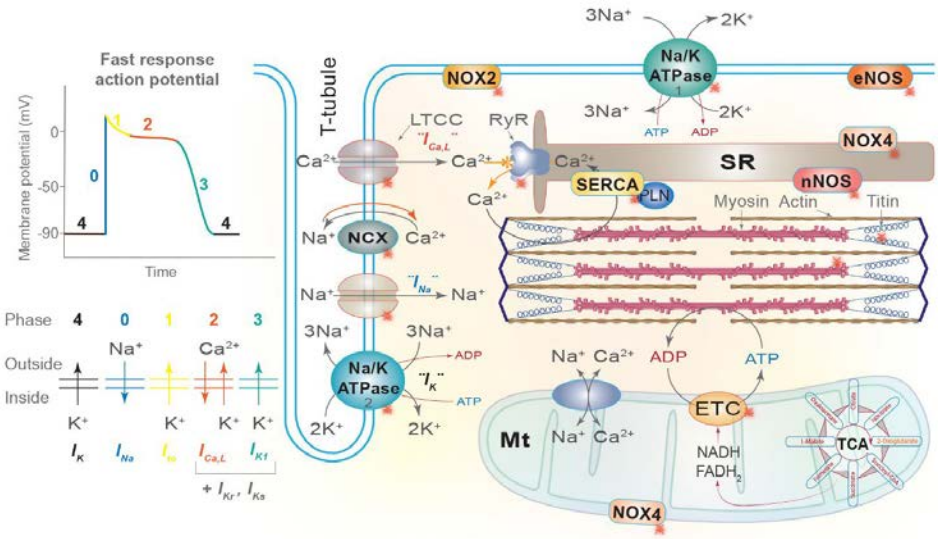

Figure 12: Excitation-contraction coupling (EC coupling) in cardiomyocytes.

I_{to} : transient outward current, I_{Kr} and I_{Ks} delayed rectifier potassium current, LTCC: L-type Ca^{2+} channels ✳ indicates potential sources for oxidative species. The figure is adapted from a tutorial video clip by Eric Strong (Strong, 2021), and from Wiessman *et al.,* (Weissman and Maack, 2021).

The calcium released in phase 2 through RyR2 activates the myofilaments via troponin C, which induces cardiomyocyte contraction. During diastole, cytosolic Ca^{2+} is mainly cleared by re-uptake into SR, which is mediated by the SR Ca^{2+} ATPase SERCA2a (Weissman and Maack, 2021).

1.4.1 Redox-depended posttranslational modifications

Many other proteins and gated channels that are involved in the EC coupling are not mentioned here for simplicity. However, several proteins in the EC coupling are either post-translationally modified by redox moieties, or their activities are modulated by oxidative species.

RyR2 is one of these proteins, which has approximately 90 cysteine residues, many of which are subjected to modifications with different redox moieties, including **S-glutathionylation**, **S-nitrosylation**, disulfide cross-linking, or other type of redox-triggered modifications, such as phosphorylation (Santos et al., 2011).

In this regard, S-nitrosylation was found to be required for RyR2 activation, and to be increased upon subjecting cardiomyocytes to sustained stretch *ex-vivo*. Moreover, both eNOS and nNOS, which produce ˙NO, were found to coimmunoprecipitate with RyR2. These observations

indicate that both eNOS and nNOS can directly modulate the activity of RyR2 through a reversal S-nitrosylation by •NO during every cardiac cycle (Lim et al., 2008).

Moreover, $O_2^{\bullet-}$ produced by NOX2 has been suggested to affect RyR2 function. NOX2, as mentioned earlier, is an enzyme that localizes to the sarcolemma and produces $O_2^{\bullet-}$ as its primary function, but it is generally quiescent and requires activation. Physiological stretch rapidly activates NOX2 to produce $O_2^{\bullet-}$ in a microtubule-dependent process to trigger a burst of Ca^{2+} release through RyR2 (Prosser et al., 2011). In fact, this effect on Ca^{2+} release through RyR2 might be mediated by $O_2^{\bullet-}$ through S-glutathionylation of a specific cystine residue in RyR2. Indeed, Sánchez et al. proposed that tachycardia (accelerated heart rates) increases the activity of RyR2 by stimulating its S-glutathionylation through NOXs enzymes (Sanchez et al., 2005).

One might think that NOX4 could play a similar role as NOX2. But NOX4 in fact differs from NOX2 substantially in both being continuously active in producing ROS at low levels, and in its localization to the membrane of sarcoplasmic reticulum in cardiomyocytes. Its role in the heart is not fully resolved, but it was suggested to play a protective mechanism (Santos et al., 2011; Weissman and Maack, 2021). However, these unique features of NOX4, in comparison to NOX2, would suggest that NOX4 continuously regulates the EC coupling during every cardiac cycle, and not only in response to physiological stretch, as NOX2 does.

1.4.1.1 The complexity of redox-depended posttranslational modification

The production of new oxidative species through the reaction between different ROS and/or RNS (explained in section 1.1.1), may explain the functional purpose of co-localizing both NOSs and NOXs in proximity to each other and to RyR2. Different species of ROS or RNS can either induce different redox modifications, or the same modification, but through different mechanisms under different conditions. An oxidative reaction is always needed before a subsequent reductive reaction can occur that attaches a redox moiety to a protein.

For example, •NO can induce S-glutathionylation of cysteine residues in RyR2, in addition to the S-nitrosylation described above. Nitrosative species induced by •NO can react with GSH to produce S-glutathionylated cysteine, either directly or through S-nitrosoglutathione (GSNO) (**Figure 13**) (Xiong et al., 2011). However, it would be interesting to experimentally validate this interesting hypothesis for RyR2 and for other proteins as well.

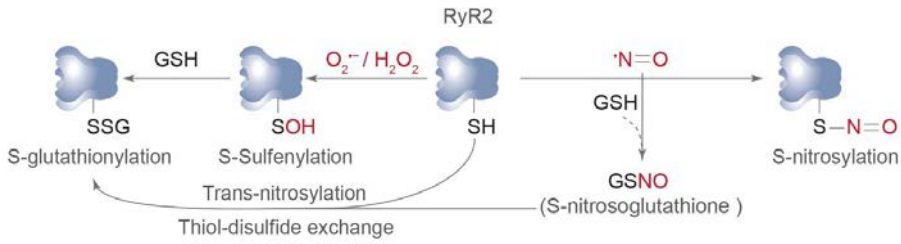

Figure 13: Examples of redox-dependent posttranslational modifications for Ryanodine Receptor 2.
The figure is constructed based on the information provided in the text above.

RyR2 is not the only protein involved in EC coupling that is post-translationally modified by redox moieties. S-glutathionylation and S-nitrosylation are also not the only redox-dependent modifications of proteins. Several other proteins involved in the EC-coupling or in other molecular mechanisms are either redox-modified or require redox in their microenvironment for optimal function. I chose RyR2 as an example because it is an important protein for a specific function in a specific cell type of my immediate interest. I chose it to challenge the traditional view on redox, as discussed above, and to highlight the importance and crucial functions of redox in protein modifications and their functions, contrary to the traditional view of oxidative species being just unwanted by-products, and that reductants exist only to detoxify oxidants.

Disulfide bonds represent an essential structural and functional modification in numerous proteins. Disulfide bonds form through oxidation, reduction and isomerization reactions that take place in the endoplasmic reticulum (ER). Achieving a correct disulfide bond in ER is dependent on the redox status within the ER. Therefore, maintaining redox homeostasis in the ER is essential for correct protein folding (Espinosa-Diez et al., 2015).

In addition to S-glutathionylation, S-nitrosylation and disulfide bond, cysteine residues undergo multiple other types of modifications, such as S-succinylation, S-palmitoylation, S-cysteinylation and other, each having a distinct biological impact (**Figure 14**). Moreover, other amino acids in proteins can also undergo numerous redox-dependent modifications. They will not be discussed here, but they can be reviewed elsewhere. However, they deliver the same message about the importance of the reductive system beyond its antioxidative properties.

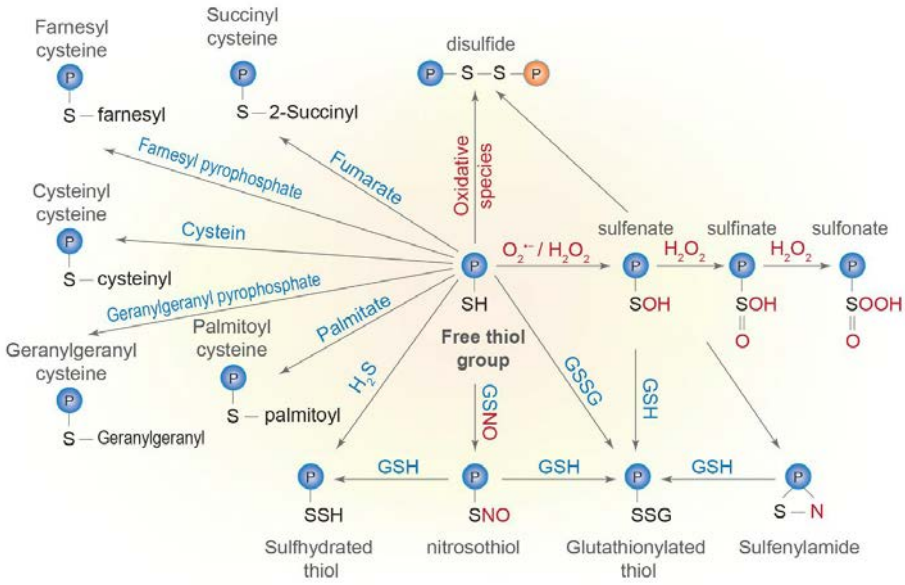

Figure 14: Some redox-dependent posttranslational modifications of cysteine residue in proteins.
The figure is adapted from multiple publications (Auclair et al., 2013; Blaskovic et al., 2013; Charron et al., 2013; Chung et al., 2013; Frizzell et al., 2011; Meng and Li, 2021).

In addition to modifying proteins with redox-derived moieties, the regulation of protein **phosphorylation** is another crucial biological function of oxidants. Phosphorylation is an essential reversible posttranslational modification of proteins that regulate their functions. Phosphate groups are covalently added to certain amino acid residues in the protein by kinases and removed by phosphatases. For example, protein tyrosine phosphatases contain a redox controlled cysteine residue in their conserved active domain. This residue catalyzes the dephosphorylation of proteins, but it can itself also be subjected to oxidation by H_2O_2, rendering the phosphatase inactive, and thus increasing phosphorylation. Moreover, the activity of several protein kinases, e.g., the mitogen-activated protein kinases (MAPKs), is also regulated by ROS (Espinosa-Diez et al., 2015).

1.4.1.2 Redox dependent signaling

In addition to the role of the redox system in post translational modification of protein, redox also mediates cellular signaling.

The major source of oxidative species in cells, *i.e.*, **mitochondrial $O_2^{\bullet-}$** (explained in section 1.2.1.1), are not accidentally generated as previously thought. Some studies have instead shown that electrons do not leak “by accident” from the electron transfer complexes (ETC), but that it is a controlled mechanism that mediates feedback signaling to the nucleus, where it

subsequently transcriptionally regulates the capacity of ETC and the TCA cycle in order to meet cellular needs (Moreno-Loshuertos et al., 2006; Munro and Treberg, 2017). This redox-mediated crosstalk between different intracellular organelles is a fascinating and emerging topic.

Redox-mediated mitochondrial-nuclear crosstalk is at the essence of our recent work (Elbeck et al., 2022); and therefore, the second part of this overview will be dedicated to this interesting topic.

In conclusion, redox biology is essential for many basic mechanisms that control and regulate almost all cellular processes, either through direct redox modifications of proteins and metabolites, or through providing the optimal redox milieu for biomolecular reactions.

1.4.2 Pathogenic mechanisms promoted by oxidative species

Excessive production of ROS might be injurious, but this would be similar to the excessive presence of almost any metabolite, or even protein, regardless of their nature. However, the magnitude of induced damage might differ based on the nature of the molecule and other factors. Some ROS, such as hydroxyl radical ($^{\bullet}OH$), have high reactivity, while others, such as superoxide ($O_2^{\bullet-}$), have low reactivity. In contrast to general belief, the injurious part of ROS and other oxidative species in diseases is not caused by ¨random¨ reactivity but is rather due to modulation of the redox milieu of biomolecular reactions, or to effects on natural redox-mediated modifications of proteins and metabolites. Cardiomyocytes (and probably also other cell types) are equipped with a potent antioxidative capacity even under severe conditions such as heart failure or myocardial infarction. In our recent work, we showed that cardiomyocytes can survive very high concentrations of oxidants and maintain redox homeostasis during heart failure (Elbeck et al., 2022). Moreover, I present in the result section of this monograph evidence for maintained redox homeostasis in the myocardium of human patients with end stage DCM (see section 5.1).

As described above, redox modifications are essential for the function of numerous proteins, and therefore, any shift in redox homeostasis would have deleterious subsequences. For example, an optimal reductive milieu is required for a correct disulfide bond formation and ensuing protein folding. A diversion or disruption in redox homeostasis would result in substantial increase in misfolding of proteins in the ER lumen. This induces ER stress and the activation of the unfolded protein response to restore normal ER function (Minamino and Kitakaze, 2010). Severe or chronic stress would induce autophagy to remove damaged proteins

and organelles, and ultimately leads to apoptosis to eliminate the damaged cells (Sozen et al., 2015).

Many other redox mediated modifications and cellular signaling would likely also be affected by alterations in redox homeostasis, with pathological consequences and/or the activation of protective or maladaptive mechanisms to repair or adapt to the damage. One should note here that a shift in redox homeostasis is not the main cause of diseases, but rather a secondary consequence, which may however contribute to the pathogenesis. Apart from mutations in enzymes that directly regulate redox homeostasis, excessive ROS production would be an expected consequence.

1.4.3 Redox targeting for therapeutic purposes

The overlooked physiological roles of oxidative species, together with numerous experimental evidence supporting a wide production of oxidative species in several diseases, have boosted the interest in potential treatments of diseases through targeting oxidative species. Over the past decades, several preclinical and clinical trials aimed to ameliorate oxidative stress in heart failure were carried out, either by exogenous supplement of antioxidant, by exogenous inhibition of the production of oxidative species, or by enhancing the endogenous antioxidative capacity. However, despite some promising results in preclinical tests, all such clinical trials hitherto conducted in patients with heart failure have failed (van der Pol et al., 2019; Zhou and Tian, 2018). In patients with chronic kidney disease adverse effects towards heart failure development have even been reported (de Zeeuw et al., 2013).

Many reasons have been suggested to explain this failure, such as that more potent inducers of antioxidative capacity are needed. In addition, it was thought that a certain type of heart failure patients, or heart failure at a certain stage of the disease development, might respond better to antioxidative therapies than patients with acute myocardial infarction, which were initially targeted (van der Pol et al., 2019). However, regardless of these ideas we are left with the fact that in spite of extensive efforts, there is currently no approved redox drug targeting oxidative species on the market.

The main reason for this failure may lie in the now-recognized physiological importance of cellular oxidants and reductants, which may have been overlooked before. Redox therapies may aberrate the delicate balance between oxidants- reductants as an off-target, and therefore impact almost all cellular functions, and eventually worsen the disease phenotype instead of improving it (**Figure 15**).

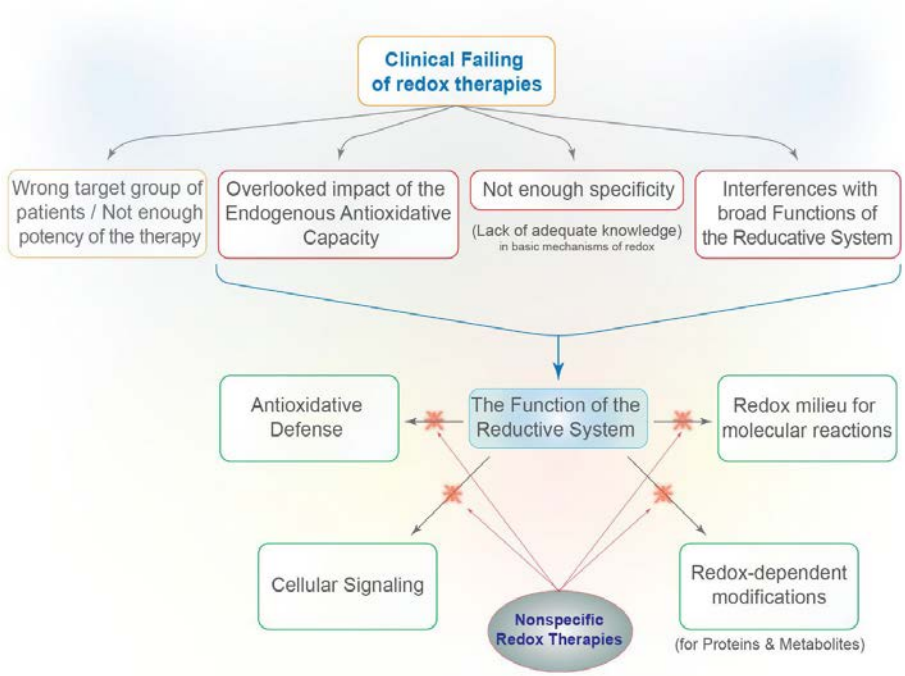

Figure 15: summary over potential actual reasons for the failing of redox clinical trials in cardiovascular diseases

✱ indicates potential interferences of antioxidative treatments with the broad functions of the reductive system.

This view is rather attested by multiple reports indicating adverse effects of antioxidative therapies (Cunnington et al., 2012; de Zeeuw et al., 2013; Vasquez-Vivar et al., 2002). In our own studies, we have observed that the treatment of neonatal cardiomyocytes with 3 mM of the antioxidant NAC induced significant cell death before surviving cells adapted to the NAC treatment (Elbeck et al., 2022). This is even in line with previous observations that constitutive activation of NRF2 by knocking out KEAP1 is lethal but rescued by simultaneous knockout of NRF2 (Wakabayashi et al., 2003), while knocking out NRF2 alone had a mild effect. These observations may indicate that antioxidants are not necessarily safe compounds, and therefore that their utilization requires caution. Altogether, this further emphasizes the hypothesis presented here, namely that the failure of antioxidative therapies might be attributed not to the lack of any effects, but to unwanted interference with general redox homeostasis.

It could be concluded here that an isolated focus on oxidative species as injurious byproducts is far too naïve and overlooks the essential roles of oxidants, or collectively of redox homeostasis, in almost all biological functions. Moreover, the failure of redox treatments in cardiovascular diseases should not discourage further efforts in this area, but such efforts

should be taken into consideration of the growing understanding of the endogenous redox capacity. Ideally, this would enable the selection of an extremely precise mechanism to target instead of a whole pathway (**Figure 15**). This would open new approaches for individualized and precise medicine.

1.5 REDOX MEDIATES FUNCTIONAL INTRACELLULAR COMMUNICATIONS AND CROSS TALK

Intermediates and derivatives of TCA cycle are not only important for biosynthesis and energy production but also for cellular signaling. Most metabolites are biosynthesized through redox-dependent reactions, and therefore their levels are highly modulated by redox homeostasis. For example, mitochondrial $O_2^{\bullet -}$, which is generated through electrons outflowing of the electron-transfer-complexes (ETC), has been shown to mediate feedback signaling to the nucleus. In return, the nucleus responds by transcribing genes that regulate mitochondrial biogenesis and function to adjust for the cellular needs. (Moreno-Loshuertos et al., 2006; Munro and Treberg, 2017).

L2-hydroxyglutare (L2HG), which we studied in our recent work (Elbeck et al., 2022), represents another example of redox-dependent intracellular crosstalk. L2HG is a mitochondrial metabolite that mediates robust cardiac antioxidative defense and signaling through a feedforward loop involving 2-oxoglutarate. The loop mediates an unconventional way of cellular communications through regulating intronic DNA hydroxy-methylation (Elbeck et al., 2022). Before going into more background and details about L2HG, I provide below an introduction to cardiac metabolism, particularly under heart failure, and a brief background about the enzymes that control the levels of L2HG.

1.5.1 The etiology of heart failure

Heart failure is a complex clinical syndrome with high etiological and clinical heterogeneity associated with a variety of comorbidities. Heart failure is defined as the inability of the heart to pump adequate amounts of blood and oxygen into the circulation and tissues due to weaknesses in the cardiac muscle. Cardiomyopathies encompass myocardial diseases that are associated with structural or functional defects in the cardiac muscle, which lead to heart failure. Three subtypes of cardiomyopathies were originally described: hypertrophic (HCM), dilated (DCM), and restrictive (RCM). Subsequently, many other subtypes were added, including arrhythmogenic right ventricular and left ventricular noncompaction cardiomyopathies. However, individual patients usually have overlapping phenotypes of multiple cardiomyopathies. Cardiomyopathies that are associated with mutations affecting the

structure or the function of cardiomyocytes are termed *genetic cardiomyopathies* (McKenna et al., 2017).

Traditionally, heart failure has been diagnosed based on assessment of the ejection fraction of the left ventricle (LVEF). Based on LVEF, heart failure patients are categorized as having heart failure with reduced EF (HFrEF) when LVEF is lower than 40%, mid-range EF (HFmrEF) when LVEF is between 40–49%, or preserved EF (HFpEF) when LVEF exceeds 50%. However, this classification oversimplifies the complex heterogeneity of heart failure (Groenewegen et al., 2020).

A more accurate diagnosis relies on interpreting the entire echocardiogram to assess cardiac geometry. For example, the reduced ejection of left ventricles of patients categorized under HFrEF results in most cases from eccentric hypertrophy, such as in DCM, in which cardiac walls become thinner (**Figure 16**). Thinner walls imply less force to pump blood, and therefore systolic dysfunction. HFpEF, on the other hand, may be associated with hypertrophy, which could be either concentric hypertrophy when the overall LV mass is increased, or concentric remodeling when the LV mass is normal (**Figure 16**). Thicker walls in hypertrophy impair the normal relaxation of the cardiac muscle, and therefore, it is usually associated with diastolic dysfunction (Gaasch and Zile, 2011; Jefferies and Towbin, 2010). However, the above classification is based on broadly acceptable and common knowledge; there are no general guidelines for definitive classification, and therefore many other classifications may be found in different reports, such as the categorization of concentric hypertrophy with HFrEF in a small subset of patients under DCM (Nauta et al., 2019).

Consequently, biomarkers are increasingly being utilized as tools for accurate diagnosis of the cardiomyopathy phenotype, for monitoring the prognosis of the diseases, and for optimal selection of suitable treatments (Hage et al., 2017; Sarhene et al., 2019).

In this regard, oxidative stress, imbalance of myocardial substrate metabolism and energy deficit are common features of heart failure, despite the wide clinical and etiological heterogeneity of heart failure (Bertero and Maack, 2018). However, the regulation of redox homeostasis would likely differ in different types of heart failure, as we showed in our recent work for the paradoxical regulation of IDH2. IDH2 expression is significantly downregulated in DCM with eccentric hypertrophy, but not in hypertrophic cardiomyopathy (Elbeck et al., 2022). Thus, defining unique molecular pathways to characterize each different type of heart failure will help to advance both diagnostic and therapeutic approaches, including antioxidative therapies.

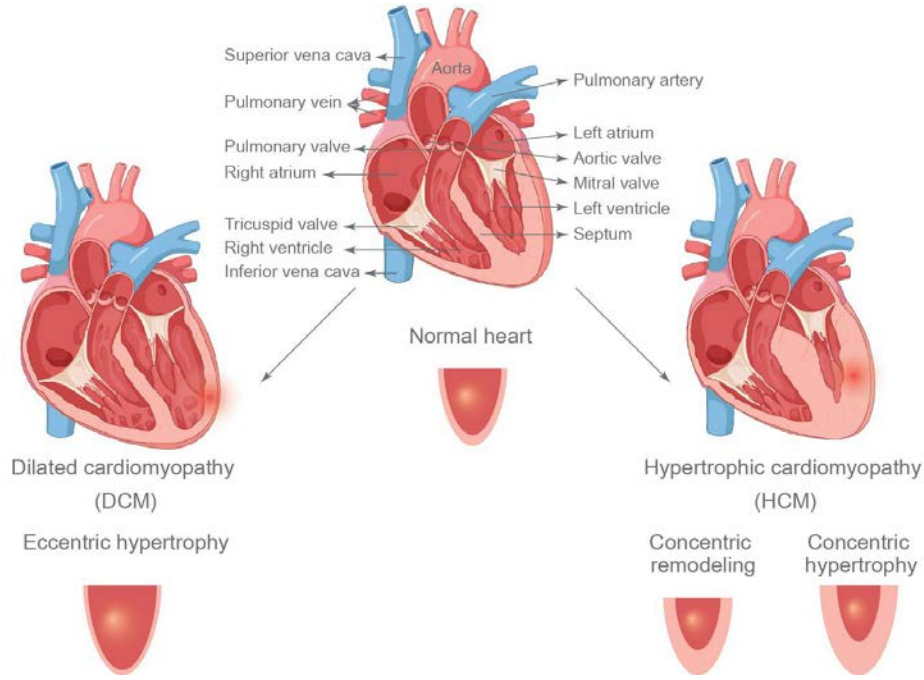

Figure 16: Cardiac geometries in different types of cardiomyopathies

The icons of complete hearts were imported from BioRender.com.

1.5.2 Cardiac metabolism

Under physiological conditions, the healthy heart is metabolically flexible and utilizes free fatty acids (~70%) through fatty acid β-oxidation, and glucose (~30%) through pyruvate oxidation, as sources for carbon in cellular respiration through the Krebs cycle (Bertero and Maack, 2018). Other sources, such as glutamine, likely have negligible contributions to cardiac metabolism, as the heart contains non-dividing cardiomyocytes. In fact, glutamine represents a prominent source for carbon in rapidly dividing cells such as cancers, but not cardiomyocytes (Comte et al., 2002).

Subsequently, through the TCA cycle, NADH and NADPH are regenerated and utilized in mitochondrial oxidative phosphorylation (OXPHOS) to generate ATP and maintain redox homeostasis. OXPHOS supplies cardiomyocytes with more than 95% of their ATP needs, while the remaining small percentage is contributed through glycolysis and to a much lesser extent through the tiny amounts of ATP produced directly in the TCA cycle (Doenst et al., 2013). ATP and phosphocreatine represent the energy pool of cardiomyocytes.

Phosphocreatine is a compound with high-energy bond phosphates, which serves as a rapidly mobilizable reserve to regenerate ATP from ADP (Yi-Dan et al., 2021).

In heart failure, the transport of fatty acids to mitochondria is impaired. This impairment is not accompanied by a decrease in the cardiomyocyte's uptake of fatty acids, which consequently leads to the accumulation of fatty acids and eventually to lipid toxicity in the cardiomyocytes. On the other side, glucose uptake and glycolysis increase in heart failure without an increase in mitochondrial glucose oxidation, which may induce also glucotoxicity (Bertero and Maack, 2018).

Consequently, despite the increase in energy demand during the terms of elevated cardiac preload and/or afterload in heart failure, the net mitochondrial oxidation (fatty acid + glucose) decreases, and therefore the TCA cycle is not able either to sustain adequate supply of NADH and FADH2 to the electron transfer chain for ATP generation, nor to adequately supply NADPH for maintaining redox homeostasis (Munzel et al., 2017).

1.5.3 L2-hydroxyglutarate

In addition to regenerating NAD(P)H and FADH2, the TCA cycle generates multiple intermediate metabolites such as L-2- and D-2-hydroxyglutarate (L/D2HG). L/D2HG are two enantiomeric metabolites derived from the reduction of 2-oxoglutarate (2OG). Until very recently, L/D2HG were referred to as oncometabolites or as metabolic waste byproducts. However, emerging research indicates pivotal molecular roles for both of L/D2HG in numerous cellular functions, including redox hemostasis and the modulation of epigenetic functions (Elbeck et al., 2022). However, there is still very little known about their precise mechanism(s) of action and biological functions.

The precursor metabolite of both L/D2HG is 2OG which is the central metabolite of the Krebs cycle. It is mainly produced by isocitrate dehydrogenases (IDH) in mitochondria and subsequently catabolized by 2-oxoglutarate dehydrogenase complex OGDHc. In addition to its role in the TCA cycle, 2OG is a cofactor for several 2OG-dependent dioxygenases that catalyze the hydroxylation of a range of molecules, including nucleic acids, chromatin, proteins, lipids, and metabolites (Islam et al., 2018).

1.5.3.1 Biosynthesis and catabolism of 2OG

As mentioned above, 2OG is mainly produced by IDHs from isocitrate in cardiac mitochondria, as its other source *i.e.*, glutamine metabolism through glutamate dehydrogenase (GDH), has a negligible contribution to cardiomyocyte energetics, as explained above.

1.5.3.1.1 Isocitrate dehydrogenases (IDH)

Mitochondrial isocitrate dehydrogenases (IDH) are an essential family of enzymes in the TCA cycle that catalyzes the oxidative decarboxylation of isocitrate to 2-oxoglutarate (**Figure 17**). The members of this enzyme family belong to two subclasses; one $NADP^+$ dependent (IDH1/2) and one NAD^+ dependent (IDH3A, B and G)(EMBL-EBI, 2019). IDH2 and IDH3A are highly expressed in the heart compared to other tissues (NCBI, 2019a, b), and therefore, their activities would be expected to have pronounced effects on cardiac function. IDH2 and IDH3 are mitochondrial isoforms, while IDH1 is cytoplasmic.

IDH2 was recently recognized as the main direct source for mitochondrial NADPH in cardiac myocytes (Nickel et al., 2015). Moreover, through 2OG coupled with OGDHc and NNT, IDH2 also constitutes another indirect but important source for mitochondrial NADPH (Wagner et al., 2020) (**Figure 17**). Thus, IDH2 represents an essential component of the antioxidative system, which is not only due to its prominent production of NADPH, but also its role in L2HG metabolism (**Figure 17**) (Elbeck et al., 2022).

The activity and stability of IDH2 are modulated through redox-dependent posttranslational modifications, such as glutationylation, succinylation and acetylation. Oxidative stress was found to induce glutationylation of IDH2, which reduces its activity but at the same time protects it from degradation, hence increasing its stability (Kil and Park, 2005). In contrast, oxidative stress has been found to increase the activity of IDH2 by deacetylation and desuccinylation of its lysin residues through SIRT3 and SIRT5, respectively (Yu et al., 2012; Zhou et al., 2016).

The importance of IDH2 for the heart is further attested by the modulation of the cardiac phenotype observed in animal models deficient in IDH2. The induction of chronic and persistent loss of IDH2 activity is associated with cardiac hypertrophy development in spontaneously hypertensive rats (Benderdour et al., 2004). Moreover, homozygote *Idh2*$^{-/-}$ mice develop age-dependent cardiac hypertrophy (from ≈ 6 months) (Ku et al., 2015). *Idh2*$^{-/-}$ mice exhibit significant increase in intracellular H_2O_2 levels, myocardial lipid peroxidation, LDH activity and apoptosis, but no clear mitochondrial structural aberration (Ku et al., 2015). However, in heart failure, IDH2 does not seem to be deficient. In dilated cardiomyopathy with eccentric hypertrophy, we have found that IDH2 expression was slightly downregulated; however, this was accompanied by an increase in its enzymatic activity due to post-translational modifications. (Elbeck et al., 2022). This balance between expression and activity may be a

way to achieve an adequate antioxidative response without overwhelming the cell with reductive equivalents.

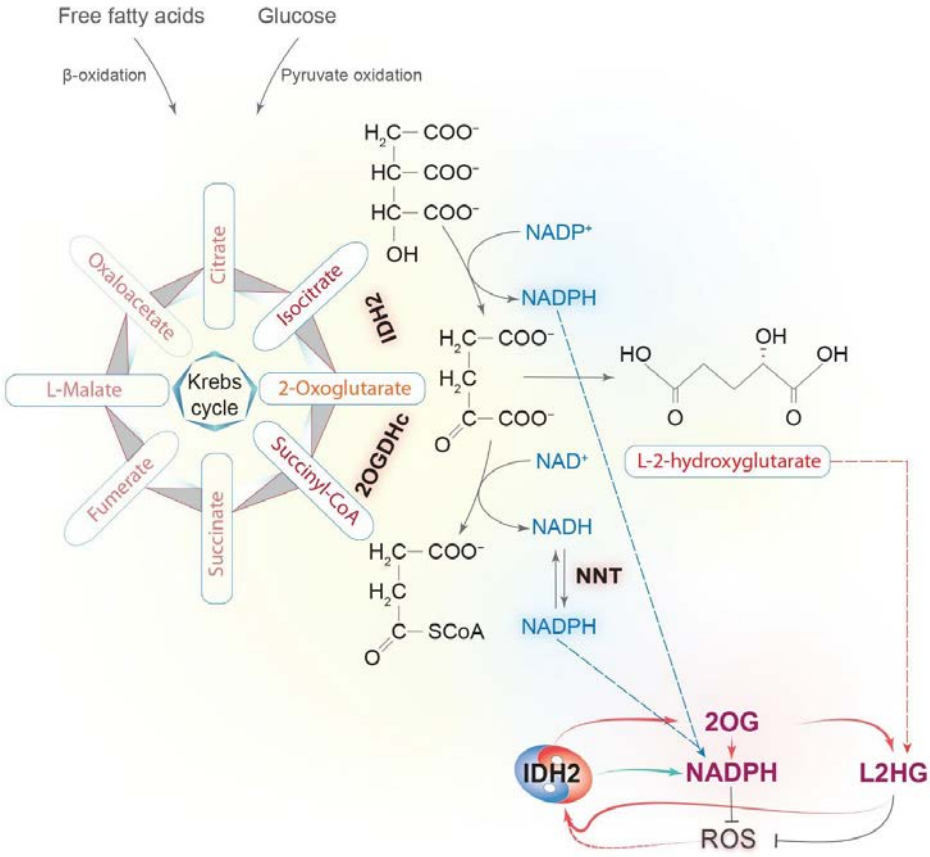

Figure 17: IDH2 is the main direct and indirect sources of NADPH in cardiac mitochondria

In cardiac mitochondria, NADPH is prominently produced by IDH2 directly, and also indirectly from NADH through IDH2-derived 2OG coupled with OGDHs and NNT.

1.5.3.1.2 2-Oxoglutarate dehydrogenase complex (OGDHc)

The enzymatic complex of 2-oxoglutarate dehydrogenase catalyzes the oxidative decarboxylation of 2-OG to succinyl-CoA producing one NADH molecule within the TCA cycle (**Figure 17**). The complex consists of three enzymes: 2-oxoglutarate dehydrogenase (OGDH), dihydrolipoyl succinyltransferase (DLST), and dihydrolipoyl dehydrogenase (DLD). OGDHc localizes to the mitochondrial inner membrane toward the matrix and binds to complex I of the electron transfer chain (Maas and Bisswanger, 1990).

OGDHc acts as a crucial control point in the TCA cycle, as its activity is regulated by multiple mechanisms. It is inhibited by its own products, *i.e.*, succinyl CoA and NADH (high $NADH/NAD^+$ ratio) and activated by ADP and Ca^{2+} (Starkov, 2013).

The dihydrolipoamide dehydrogenase (DLD) component of the OGDHc appears to be a significant contributor to mitochondrial ROS production in the brain, an effect that is further enhanced under pathological conditions that alters $NADH/NAD^+$ ratio (Chen et al., 2016; Starkov, 2013; Starkov et al., 2004). A similar role for cardiac OGDHc has been postulated in some reports (Lucas and Szweda, 1999; Mailloux et al., 2016; Oldford et al., 2019), but refuted in a recent study that found that OGDHc is a negligible contributor to cardiac mitochondrial ROS. Instead, OGDHc plays a substantial role in the antioxidative defense, as the NADH produced by OGDHc is specifically shuttled to NNT to produce NADPH (**Figure 17**) (Wagner et al., 2020). This antioxidative role of OGDHc further supports the antioxidative role of R-α-lipoic acid, which is part of OGDHc (discussed in a previous section 1.3.1).

1.5.3.2 Biogenesis of L2 and D2 hydroxyglutarate

L2HG is produced by L-malate dehydrogenase and lactate dehydrogenase. Its levels increase under hypoxia (Intlekofer et al., 2017; Oldham et al., 2015). Whereas the other enantiomer, *i.e.*, D2HG, is produced by multiple ¨incidental side reactions¨ of multiple enzymes such as 3-phosphoglycerate dehydrogenase and hydroxyacid-oxoacid transhydrogenase (Fan et al., 2015; Kaufman et al., 1988). High levels of D2HG are also produced by mutated IDH1/2 that have a neomorphic activity, which leads to abnormal reduction of α-ketoglutarate to the D2HG (Cairns and Mak, 2013). The levels of L/D2HG are regulated through two specific mitochondrial dehydrogenases that oxidize them back to 2-OG, *e.g.*, L2HGDH and D2HGDH, respectively (**Figure 18**). In a subsequent section (1.5.3.3) of this monograph, I discuss in further detail why I consider the term ¨incidental side reactions¨ misleading.

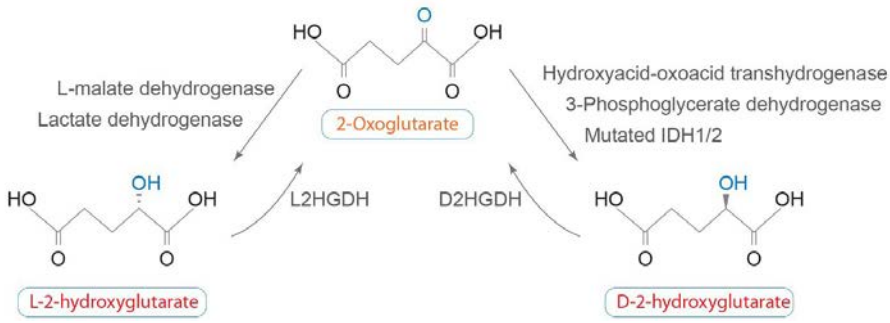

Figure 18: Chemical structure and enzymatic sources of L2HG and D2HG

1.5.3.3 Biological roles of L2 and D2 hydroxyglutarate

The current view in the literature on the molecular mechanisms of L/D2HG holds that both enzymes mediate similar functions, *i.e.,* inhibiting their precursor-dependent dioxygenases (2OGDD), but with slight differences in their potency (Xu et al., 2011). This idea has no solid experimental evidence, however, and most likely originates from the observation that enantiomers have identical chemical and physical properties, and as some of the biological functions are mediated through these properties, such as redox reactions. However, although enantiomers have identical physiochemical properties, they differ in their steric conformations. This is an important factor for their biological functions, especially those that require specific structural complementary between substrates/cofactors and enzymes, such as the interaction of L/D2HG with 2OGDD family of enzymes. Thus, contrary to the common view, L2HG and D2HG have distinct functions, although some of them partially overlap.

Hypoxia induces elevation of L2HG, which affects a broad range of metabolic pathways, including energy production and redox homeostasis. The increase of L2HG in hypoxia is accompanied by a simultaneous increase in 2OG and $NADH/NAD^+$ ratio. Therefore, 2HG and 2OG might inter-convert to provide the cells with a redox reservoir (Oldham et al., 2015). However, hypoxia-induced L2HG was found to originate from glutamine-derived 2OG, not from IDH2-derived 2OG (Intlekofer et al., 2015).

In our recent work (Elbeck et al., 2022), we found that L2HG levels are elevated in cardiac tissues in conjunction with heart failure in a hypoxia-independent manner. We further found that L2HG originates from IDH2-derived 2OG. Elevation of L2HG is a part of a feedforward loop that regulates the antioxidative defense, together with 2OG and IDH2 (Elbeck et al., 2022). The discrepancy observed between our results and Intlekofer *et al.,* (Intlekofer et al., 2015) could be attributed to multiple reasons.

Most importantly, although L2HG induction was originally discovered in hypoxia, hypoxia *per se* is not the inducer of L2HG. We did not observe the induction of HIF-1α target genes in the myocardium of patients with end-stage non-ischemic genetic DCM or in $Mlp^{-/-}$ mice that develop DCM, but we observed an induction in L2HG (Elbeck et al., 2022). It is important to emphasize here that hypoxia is not a characteristic of heart failure, except for ischemic myocardial infarction that represents a specific subtype of heart failure. The presence of hypoxia in the myocardium of patients with non-ischemic cardiomyopathies is controversial, even in end-stage patients with non-ischemic DCM (Dass et al., 2015). Therefore, L2HG is not directly induced by hypoxia, but rather induced by a distinct mechanism associated with

hypoxia and also with heart failure, and it is most likely linked to remolding of redox homeostasis.

As mentioned above, cancer cells (that were utilized by Intlekofer *et al.*, (Intlekofer et al., 2015)) have very low expression levels of IDH2 and rely mostly on glutamine as a source of carbon for the TCA cycle. Conversely, glutamine derived-2OG is negligible in cardiomyocytes, which also have the highest levels of expression of IDH2 among all other cell types. Therefore, normoxic L2HG may originate from both IDH2- and glutamine-derived 2OG, which is dependent on the metabolic profile of the cell type. This conclusion also lends supported from Intlekofer *et al.* own results (**Figure 19**) (Intlekofer et al., 2015). In their data, isotopic labelling suggested that SF188 cancer cells fed with ^{13}C-glucose have substantial induction of L2HG in normoxia, representing almost 30% of that in cells fed with 13C-glutamine, which is proportional to their prominent metabolic reliance on glutamine rather than glucose.

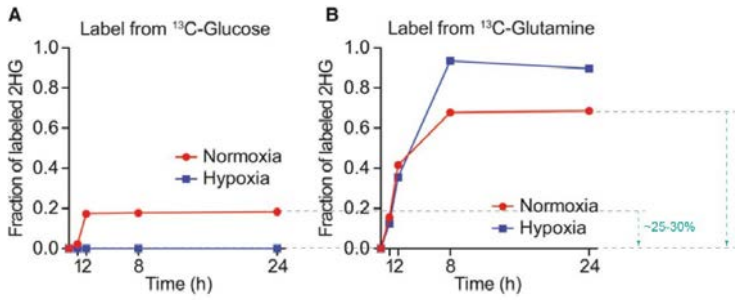

Figure 19: The origin of the precursor of 2OG-derived L2HG in Normoxia and hypoxia.

The figure is cropped from Figure 2A in Intlekofer et al. (Intlekofer et al., 2015) with permission. The figure shows that nomoxic cells fed with glucose exhibit a ~25-30% induction of L2HG, in comparison to cells fed with glutamine, pointing toward that L2HG can be derived from 2OG originated from IDH2, which is a downstream enzyme in glucose metabolism. Dashed lines are added to the figure to illustrate this difference.

To the best of my efforts, I have not been able to find published work discussing the physiological roles of D2HG. Available reports instead investigate its pathological roles associated with cancer cells carrying mutations in IDH1 or IDH2, or in cells having loss of function-mutations in D2HGDH. However, emerging physiological roles of L2HG would imply that D2HG also plays a significant role in normal cellular functions, and that its production is not due to incidental side reactions as it is currently viewed.

1.5.3.4 Pathological roles of L2 and D2 hydroxyglutarate

Highly elevated levels of D2HG were initially detected in patients with tumors-bearing mutations in IDH1 or IDH2 (Cairns and Mak, 2013), and thus D2HG was branded as an oncometabolite. A similar feature was also assigned for L2HG, as it was detected at high levels in some tumors, such as renal cell carcinoma, due to decreased expression of L2HGDH (Shelar et al., 2018). L2HG and D2HG elevations are also associated with the neuro-metabolic disorders L-2-hydroxyglutaric aciduria and D-2-hydroxyglutaric aciduria, due to mutations in L2HGDH and D2HGDH, respectively (Steenweg et al., 2010; Struys et al., 2005).

Some patients with a severe type of D-2-hydroxyglutaric aciduria experience cardiomyopathy, associated with high levels of D2HG in their plasma due to mutations in IDH2 (Kranendijk et al., 2012). This observation spurred subsequent studies that also described cardiac effects in transgenic mice overexpressing mutants of *Idh2*$^{(R140Q\ \&\ R172K)}$ (Akbay et al., 2014; Karlstaedt et al., 2016).

Hearts from the *Idh2*$^{(R140Q\ \&\ R172K)}$ transgenic mice exhibit increased dilation and apoptosis, alteration in TCA cycle metabolites, and alterations in histone methylation and glycogen deposition (Akbay et al., 2014). The observed heart failure phenotype in these studies and the latency of the phenotype have been correlated with the levels of 2HG (Akbay et al., 2014; Karlstaedt et al., 2016). Some of these alterations were found to be reversible after lowering D2HG levels in reversibly inducible transgenic mice (*Idh2*$^{(R140Q)}$), which was found to improve heart function (Akbay et al., 2014).

These studies may suggest a link between very high levels of D2HG and cardiac pathology, but they did not investigate the underlying molecular mechanism for the observed effects. Our recent work, which describes a positive role for both L2HG and D2HG in modulating redox homeostasis, may however indicate that previously observed negative cardiac effects associated with very high levels of D2HG may be caused by an impact of elevated D2HG on redox homeostasis (Elbeck et al., 2022).

1.5.4 2-hydroxyglutarate regulates epigenetics

Intermediate metabolites of the TCA cycle take part in numerous intracellular processes. Several of these metabolites, such as 2OG, its reduced enantiomers L2HG and D2HG, succinate, and fumarate are essential cofactors for 2OG-dependent dioxygenases (2OGDDs). In addition to 2OG, 2OGDDs also require Fe^{2+} and molecular oxygen as other essential cofactors for their functions (Xu et al., 2011). There are more than 70 members of these dioxygenases, among them are both the JMJD family of histone's demethylating enzymes and

the ten-eleven translocation (TET) DNA hydroxymethylation enzymes. The latter convert 5-methylcytosine (5mC) to 5-hydroxymethylcytosine (5hmC) in genomic DNA (gDNA), see **Figure 20** (Koivunen and Laukka, 2018).

Evidence supporting the role for L2HG in modulating DNA methylation has been observed in numerous studies. Both L2HG and D2HG inhibit TET1/2 activities *ex vivo*, with L2HD being more potent than the D enantiomer (Xu et al., 2011). Hypoxia has in multiple cell lines been associated with a loss of TETs activity and a subsequent reduction in 5hmC levels in a time- and O_2-concentration-dependent manner. Hypoxic tumors have significantly higher hypermethylation than other tumors, especially tumors that carry *IDH* mutations (Thienpont et al., 2016). As hypoxia is associated with inducting the elevation of L2HG levels (Oldham et al., 2015), the effects of hypoxia observed by Thienpont *et al.* (Thienpont et al., 2016) on TETs could be very much attributed to L2HG.

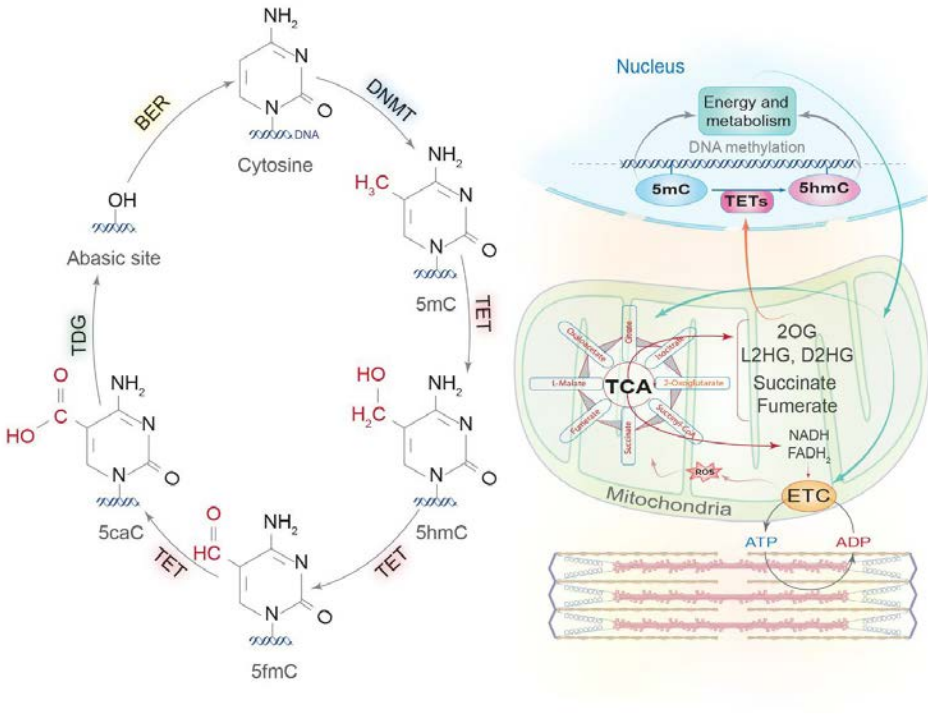

Figure 20: Intermediates metabolites of the TCA cycle mediates intracellular communications

TDG: Thymine-DNA glycosylase, BER Base excision repair. 5mC: 5-Methylcytosine, 5hmC: 5-Hydroxymethylcytosine, 5fC: 5-Formylcytosine, 5caC: 5-carboxylcytosine.

To my knowledge, no direct studies have reported on the impact of mitochondrial metabolites, including L2HG, on epigenetics in cardiovascular diseases. In heart failure, the accumulation

of mitochondrial calcium is decreased due to alterations in cytosolic calcium deposition from the sarcoplasmic reticulum (Munzel et al., 2017). These alterations would impact the levels of 2OG and L2HG, and hence promote epigenetic changes, as both IDHs and OGDHc are highly regulated by mitochondrial calcium levels.

We could recently establish an indirect link between the elevation of cardiac L2HG and the remolding of gDNA 5hmC in a murine model of heart failure. We could also show that modulating Tet1/3 activities through knock-down in cardiomyocytes affects genes that are regulated by L2HG, such as *Idh2*. This highlights the crucial role of 2OG and L2HG in mitochondria-epigenome bi-directional crosstalk, especially in the physiology and pathology of cardiomyopathies.

1.5.5 Epigenetics in heart failure

The heart is a specialized organ with terminally differentiated cardiomyocytes. Still, the heart responds and adapts to a variety of stimuli. To what extent epigenetic changes, such as histone and gDNA methylations, may play an important role in regulating cardiac function, has not yet been well explored.

1.5.5.1 Current advances in profiling of methylome in association to heart failure

DNA methylation was until recently thought to be a stable type of epigenetic modification. However, dynamic DNA methylation plays important roles in regulating cardiac metabolism. Active changes in DNA methylation and histone modifications of genes encoding specific gene programs have been observed in both murine and human cardiomyocytes during both development and heart failure (Gilsbach et al., 2014; Gilsbach et al., 2018).

During heart development, genes involved in cardiac contraction or mitochondrial function exhibit loss of methylation, whereas genes involved in embryonic pattern specification and morphogenesis gain methylation. These alterations are more pronounced in some genetic regions than in others, such as in enhancer and gene body regions (Gilsbach et al., 2014; Gilsbach et al., 2018). Similarly, remolding of heart failure is associated with alterations in DNA methylation, involving genes implicated in cardiac muscle development and energy metabolism (Gilsbach et al., 2014; Pepin et al., 2019a; Pepin et al., 2019b).

Genes with higher enrichment of 5hmC in their gene bodies are associated with higher expression and the presence of active histone marks. In a murine model of heart failure caused by transverse aortic constriction, the distribution of cardiac 5hmC in different genetic regions was found to be epigenetically remodeled in ways that resemble the embryonic pattern. Genes

affected by this remodeling are mainly involved in biological processes associated with tricarboxylic acid (TCA) cycle, fatty acid metabolism and the generation of energy, and exhibit a loss in 5hmC in their gene bodies accompanied by repressed gene expression (Greco et al., 2016).

Greco *et. al.*, utilized a method to infer the distribution of 5hmC, i.e., Hmedip that has ~200-300 bp resolution. The exact localization of 5hmC in the genetic regions could therefore not be determined. Two recent methods were developed to determine 5hmC at a single-nucleotide resolution when combined with bisulfite treatment and sequencing, *i.e.*, Tet-Assisted Bisulfite Sequencing (TAB-seq) and Oxidative bisulfite sequencing (oxBS-Seq), with the latter likely being much more accurate. Both methods rely on an indirect quantification method (*i.e.*, bioinformatic subtraction) to deduce 5hmC, and therefore, achieving a correct subtraction requires extremely high sequencing coverage (> 200X) for both parallel prepared libraries, making the methodology enormously costly.

In our recent work (Elbeck et al., 2022), we utilized an available data set of whole genome BS and OxBS sequencing at single-nucleotide resolution of myocardium from a murine model of DCM ($Mlp^{-/-}$) to infer alterations in the distribution of 5hmC and gene expression. However, the sequencing depth of these data was not optimal (~ 10X) precluding single-nucleotide resolution. Nevertheless, through developing a novel computational approach, we were at least able to link some effects associated with heart failure to the levels of intronic 5hmC in genes coding for metabolic processes (Elbeck et al., 2022). This represents a higher level of resolution than the gene-body level previously achieved (Greco et al., 2016).

1.5.5.2 Current available technologies for methylome analysis

The available technologies for methylome profiling have greatly evolved during recent years; from simple methods utilizing restriction enzymes that differentially cut epigenetically modified DNA sequences, to the current second and third generation sequencing technologies with the capacity to unveil epigenetic modifications in the whole genome.

Low resolution methods, such as immunoprecipitation, have been extensively utilized and provided novel insights, especially into the biological roles of 5hmC. Mdip and hMedip are examples of these approaches, which utilize antibodies against 5mC (Medip) and 5hmC (hMedip) to enrich gDNA fragments carrying these modifications, followed by a subsequent sequencing step. These methods can identify the approximate position of modification (within ~200-300 bp resolution) and enable quantification of relative levels to a control sample, but not

absolute values. These methods are highly prone to artifacts and have very low resolution, which limits their ability to map modification to the exact DNA region. Numerous variants of the methods that utilize immunoprecipitation or restriction enzymes have been developed, but all of them suffer drawbacks in accuracy, reproducibility, or lack of capability to distinguish 5mC and 5hmC.

Although whole genome bisulfite sequencing (BS) may provide single-nucleotide resolution, it cannot distinguish 5mC from 5hmC. However, as mentioned above, two recent methods were developed to enable the detection of 5mC and 5hmC at a single-nucleotide resolution, *i.e.*, TAB-seq and oxBS-Seq, when combined with BS sequencing (**Figure 21**). Both methods are indirect methods, however, and rely on bioinformatic subtraction to infer levels and distributions of 5hmC, and therefore they require high sequencing coverage. Both methods are accurate and reproducible in profiling whole genome 5hmC, especially OxBS-Seq, but they are not able to detect the other two cytosine modifications, *i.e.*, 5-formylcytosine (5fC) and 5-carboxylcytosine (5caC).

Third-generation sequencing, such as Nanopore, is an emerging innovative technology that enables long read-sequencing with a direct and simultaneity identification of the exact position and levels of all DNA modifications (*i.e.*, 5mC, 5hmC, 5fmC and 5caC). However, this technology is still at a very early stage of development. Its currently biggest drawback is the low accuracy of modified-base calling. Moreover, it is very expensive.

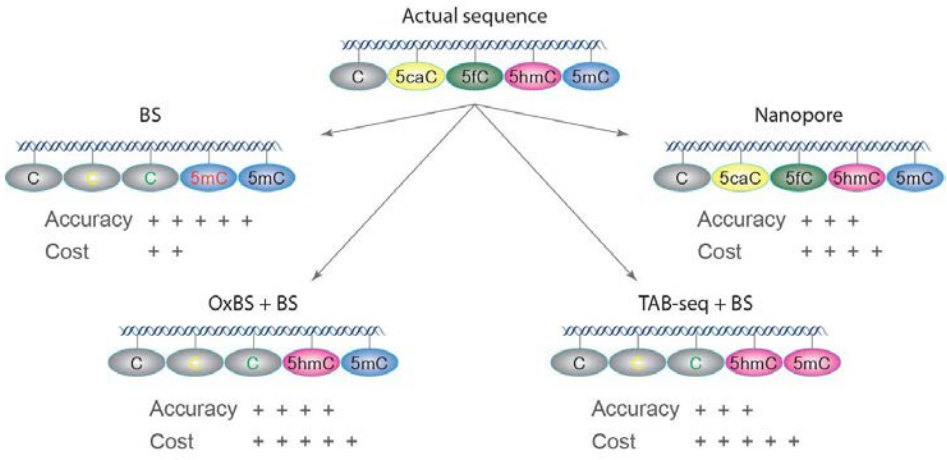

Figure 21: Schematic representation of available methods for single-nucleotide resolution analysis of different types of DNA methylation

The schematic representation depicts how the modification would be read after the bioinformatic analysis of the raw sequencing data. The depicted scale of the accuracy and cost is composed of 5 grades, where 5 pluses indicate the most accurate and the most expensive. Estimations of accuracy and cost are based on my own experience.

1.5.5.3 Current challenges and future perspective

Despite all advances in the field of methylome research, whole genome profiling of cardiac methylome is still at a primitive stage in comparison to *e.g.*, transcriptomic analysis. Underlying reasons are mainly associated with current technical limitations, but also with the nature and complexity of the methylome, perhaps especially in the heart.

5hmC exists in the cardiac genome at low levels. Of total CpGs, only 4.4% of them contain 5hmC. In comparison, 58.7% of the CpGs contain 5mC (Elbeck et al., 2022). The low percentage will make any changes in amount of 5hmC associated with heart failure hard to detect using low resolution methods that distinguish 5hmC from 5mC, or totally masked by only bisulfite analysis.

However, the low levels of 5hmC are not the only hinder to the exploration of its biological functions. Many other factors contribute. Most importantly are probably the dynamics of 5hmC changes associated with chronic diseases, such as heart failure. Heart failure may span decades before reaching an end-stage congestive heart failure. Therefore, expected alterations of 5hmC associated with chronic metabolic and structural remodeling might affect less than 1% of total methylated CpGs. This implies that sequencing at high depth may be required to accurately document small changes.

Such small changes would probably be possible to observe in studies of animal models, which usually have identical genomic sequence and a homogenous lifestyle with controlled environmental impacts. In this case, achieving high sequencing coverage for a relatively low number of samples might be sufficient.

However, this would be far more complicated in humans, who show large variations in both the genetic background (single nucleotide polymorphisms (SNPs)), and environmental factors. All these factors would impact the methylome. Therefore, a high *n* number would be required to obtain interpretable data.

Accomplishing an adequate coverage for BS and OxBS sequencing for analyzing the alterations of 5hmC on the whole genome level would cost ~ 40 000 Euro for **one** sample only, as per May 2022. Even if an adequate number of patients were sequenced the required subsequent computing power needed for processing such a data set would pose a next challenge. Taking these challenges together the time might not yet be ripe for this type of question.

Biological challenges add to these technical hurdles. The function of a DNA sequence is highly dependent on the modification type and the genetic position of that modification, as well as the type of the cell or organ being studied (Ponnaluri et al., 2017). Different DNA modifications selectively attract or repel distinct transcription factors or functional proteins (Spruijt et al., 2013). In addition, the function of the modification within a gene might be highly region dependent. For example, methylation of the promoter is associated with repressed gene expression, but with increased gene expression when present in the gene body (Yang et al., 2014).

All these concepts highlight that the generation of a meaningful set of methylation data requires a method with high resolution and sufficient accuracy. Therefore, low resolution methods for studying whole genome methylome, such as Medip and hMedip should be avoided, as the level of information that they can generate could be considered meaningless. To justify experiments of this type, one could possibly consider using the extremely costly whole-genome BS and OxBS sequencing at a single-nucleotide resolution for screening a low number of samples, with the aim of finding potentially novel methylation sites, which can then be subsequently validated in additional samples and explored for their biological effects by utilizing a targeted approached, such as pyrosequencing.

Illumina's Methylation Arrays with a predefined sets of CpGs represent a cost-effective way to do genome-wide association studies. The biggest drawback for these arrays is the low numbers of covered CpGs and the bias toward certain genetic regions. These arrays can currently analyze 800,000 out of ~ 25 million CpGs sites that exist in the genome, but they are continuously and rapidly being improved.

It's worth noting that sequencing provides a snapshot of the current 5hmC levels and does not capture the dynamic flux state over time. This is an important perspective, as inferred effects of 5hmC would constitute both; a unique function of 5hmC itself, and an effect associated with alleviation of 5mC levels, as 5hmC also represents as an intermediary stage in the process of demethylation, involving the conversion of 5mC to unmodified cytosine.

Finally, the field of methylome, and the knowledge that has been generated in the recent few years have substantially developed from the initial belief that the methylome is a random process to the current view of specific functions associated with the positions of each specific modification. However, the current obstacles regarding the availability of proper methodologies, and probably the greediness of dominating sequencing companies, have delayed these advances. Nevertheless, emerging disruptive innovations, such as third

generation sequencing would induce an explosion of novel discoveries in the field of epigenetics, which will undoubtedly unveil novel molecular mechanisms and aid in developing novel therapies for multiple diseases, including heart failure.

2 RESEARCH AIMS

The overall aim of the work presented in this monograph was to investigate the impact of different components of the reductive system on the endogenous antioxidative capacity and on the intracellular crosstalk between the mitochondria and the nucleus (*i.e.*, epigenetics), in connection to cardiac remodeling/reverse remodeling associated with heart failure.

2.1 STUDY-I: Protective antioxidative mechanisms and reversed remodeling of heart failure

The aim of this study was to unveil a novel molecular mechanism of IDH2 in regulating the endogenous reductive system in cardiomyocytes. We sought also to investigate sexual dimorphism in the regulation of cardiac redox homeostasis, and the degree to which cardiac endogenous antioxidative capacity is compromised under heart failure, as well as their subsequent response to exogenous antioxidative treatments. Moreover, we aimed to study the redox-related mitochondrial-nuclear crosstalk, mediated by the mitochondrial metabolite L-2-hydroxyglutarate and the ensuing DNA hydroxy-methylation.

2.2 STUDY-II: The role of cardiac miR-208b in regulating redox defense

The aim of this study was to study the impact and potential targets of a highly expressed micro-RNA in the myocardium of patients with heart failure, *i.e.*, miR-208b-3p. Moreover, we aimed to assess whether miR-208b-3p plays a role in regulating redox homeostasis in cardiomyocytes.

2.3 STUDY-III: Novel isoforms of MLP and their role in the remodeling of heart failure

The aim of this project was to look for potential translatable isoforms of MLP from non-canonical start codons in $Mlp^{-/-}$ mice. $Mlp^{-/-}$ mice have elevated levels of cardiac *Mlp* transcripts that lack exon 2, and thus lack the canonical start codon required for the translation of full-length MLP. We also aimed to investigate the potential biological and pathological impacts of these novel isoforms of MLP.

3 MATERIALS AND METHODS

All studies included in this monograph and the attached manuscript posted at BioRxiv that utilized animals or samples from humans were performed according to the relevant ethical permits described in the supplementary materials of Elbeck *et al.* (Elbeck et al., 2022).

3.1 STUDY-I: Protective antioxidative mechanisms and reversed remodeling of heart failure

A detailed description of all methods utilized in the first part of this study, which constitutes the manuscript published as a preprint on BioRxiv (Elbeck et al., 2022), is available through the following link, and also attached to the end of the booklet format of this monograph:

https://www.biorxiv.org/content/10.1101/2022.03.26.485908v1

All additional new data presented in this study were re-analyses of sequencing data included in the preprinted manuscript at BioRxiv. All utilized lists of differentially expressed genes will be publicly available once this manuscript is accepted for publication in a peer-reviewed journal.

The code utilized to produce the data displayed in Figure I-3 in the Results section of this monograph was the same code that was utilized to produce Figure 1D in Elbeck *et al.*, 2022 after excluding the list of genes coding for Mitochondrial Metabolic Enzymes. Data utilized for IPA analyses presented in Figure I-4 were produced with Excel, by intersecting the indicated different sets of genes by using the function ¨vlookup¨. All IPA analyses were performed according to the method described in the Supplementary Materials of Elbeck *et al.*,2022.

3.2 STUDY-II: The role of cardiac miR-208b in regulating redox defense

3.2.1 *In vivo* study

LNA-modified antagomir against miR-208b-3p and a scrambled control sequence were obtained from Qiagen (miRCURY LNA^{TM}) (Table 1). The sequence of the antagomir was obtained from a previous study by Zhou *et al.* (Zhou et al., 2017), while the sequence of the scrambled control was provided by Qiagen. The study was designed and performed in accordance with the PREPARE guidelines (Smith et al., 2018).

Table 1: The sequence of utilized antagomirs and scramble control.

Target	sequences	Cat. No
I-MMU-MIR-208B-3P	C*T*T*T*T*G*T*T*C*G*T*C*T*T*A	339203 YCI0201031-FZA
MMU-MIR-SCRAMBLE	A*C*G*T*C*T*A*T*A*C*G*C*C*C*A	339203 YCI0202044-FZA

* indicate phosphorothioate bonds

The potency of utilized antagomir in lowering the levels of miR-208b-3p *in vivo* was already validated by Zhou *et al.*, (Zhou et al., 2017). Moreover, the predicted improvement of cardiac function in *Mlp*$^{-/-}$ mice was small, due to the extensive variability in the disease severity of these animals (Arber et al., 1997; Elbeck et al., 2022). We therefore argued that useful data could not be achieved from treating just a few animals. Hence, we skipped the pilot step, and instead directly treated 8 animals in each group (antagomir/scramble), which we estimated to be enough to observe a significant improvement in the cardiac function if lowering miR-208b-3p level would have beneficial effects. This assumption was based on our previous experience from similar experiments.

Mlp$^{-/-}$ animals, at the age of 8 weeks, were randomized into two groups based on their body weights (see Figure II-4A for the experimental design of the study). Each animal received 4 injections of 80 mg/kg of antagomir or scrambled control at days 1, 7, 14 and 28. Echocardiography was performed on days 0, 14 and 28. The study was terminated immediately after the last echocardiographic examination, and the hearts were dissected and frozen immediately for subsequent biochemical analyses. No animals died before terminating the study, and there were no observable changes on their behaviors or body weight. The experimenters were blinded to the treatment groups during different procedures. The examination with echocardiography was performed with the exact same procedure described in the supplementary materials of Elbeck *et al.* 2022.

3.2.2 *In vitro* transient overexpression of miR-208b-3p

HEK 293 (HEK) cells were plated in 12-well-plates (Corning) with the growth medium (DMEM, 10% FBS, Pen/Strep). Plated cells at a confluency of 70% were transfected with a mammalian shRNA knockdown vector carrying a hsa-miR-208b-3p. The expression of the small RNA was driven by the U6 promoter. A transcript of enhanced green fluorescent protein (EGFP) was added to the construct under the human phosphoglycerate kinase 1 promoter to visualize transfected cells by green florescence. For scramble control, cells were transfected with a mammalian gene expression vector carrying an enhanced green fluorescent protein (EGFP) transcript under the human eukaryotic translation elongation factor 1 α1 promoter (Table 2). This was the same control vector that was utilized in study-III.

Table 2: Sequences of ShRNA utilized in the current work

Construct ID	Target gene	ShRNA sequences	Map
VB201215-1116kpk	hsa-miR-208b-3p	ACAAACCTTTTGTTCGTCTTAT	https://en.vectorbuilder.com/vector/VB201215-1116kpk.html
VB180823-1120qay	Scramble, EGFP	-	https://en.vectorbuilder.com/vector/VB180823-1120qay.html

The transfection was performed with Lipofectamine™ 3000 reagents (Invitrogen) according to the manufacturer's instructions. In short, cells were washed with PBS and incubated in 400 µl of Opti-MEM™ reduced serum (#31985062, Gibco) for 1 h to starve the cells. Then an additional 100 µl of Opti-MEM™ reduced serum was added, containing the lipofectamine transfecting reagents and 250 ng of the plasmid currying the miR-208b-3p or scramble constructs. Next day, 500 µl of fresh growth medium was added to each well. Thereafter, the growth medium was replaced daily with a fresh medium until day 5, when EGFP expression was examined under a florescence microscope, and then the cells were washed twice with PBS, and lysed with 90 + 60 µl of TRIzol for extracting the RNA. The TRIzol method is the same as described in the supplementary materials of Elbeck *et al*. (Elbeck et al., 2022).

Negative controls consisting of untransfected cells were simultaneously treated with the same procedure as those cells that were transfected with the plasmid carrying the miR208b-3p construct, but without having any DNA in the transfection reagents.

3.2.3 Quantitative PCR

For the first strand synthesis of cDNA, SuperScript IV First-Strand Synthesis System (Invitrogen) was utilized with poly-T primers. The qPCR analyses displayed in all figures of this project (except for miR-208b-3p) were performed utilizing SYBR Green using the same procedure as described in the supplementary materials of Elbeck *et al.* (Elbeck et al., 2022). The primers utilized for quantifying murine *Idh2*, *Hmox1*, *Nqo1*, and *Osgin1* were the same as described in that supplementary method file. The primers for the murine *Myh6*, *Myh7*, and the human *IDH2* are shown in Table 3 below.

Table 3: qPCR primers utilized in the study

Gene	Forward primer	Reverse primer	Species
IDH2	GCGAAGCCCGTGGTGGAGAT	AGTCTGGTCACGGTTTGGGA	Human
Myh6	CCAACACCAACCTGTCCAAGT	AGAGGTTATTCCTCGTCGTGCAT	mouse
Myh7	CTCAAGCTGCTCAGCAATCTATTT	GGAGCGCAAGTTTGTCATAAGT	mouse

Data from the qPCR analyses that are displayed in figures II-2 B and C were obtained from the same cardiac tissues of $Mlp^{-/-}$ animals utilized in Figure 2A,B and C in Elbeck *et al.*, (Elbeck et al., 2022). Correlated percentages of ejection fraction with expression level of miR-208b-3p, which are displayed in Figure II-2 C, were also derived from the same previously mentioned animals, and the utilized echocardiographic data in this correlation is the same data displayed in Figure 4 G,H and I in Elbeck *et al.* (Elbeck et al., 2022).

For the synthesis of the cDNA of miR-208b-3p and U6 snRNA, TaqMan™ Fast Advanced Master Mix (#4444557, ThermoFisher Scientific) was utilizes according to the manufacturer's

instructions, with the flowing thermal program (reverse transcription at 16°C for 30 min and then 42°C for 30 min, stop reaction 85°C for 5 min and then hold at 4°C).

For quantitative analysis of miR-208b-3p, the TaqMan™ MicroRNA assays; hsa-miR-208b (#4427975, Assay ID 002290) and U6 snRNA (#4427975, Assay ID, 001973) from Thermo Fisher Scientific were utilized, according to the manufacturer's instructions. The thermal program was (UNG activation at 50°C for 2 min, then enzyme activation at 95°C for 10 min, 40 cycles of [denature at 95°C for 15 sec, then Anneal /Extend 60°C for 60 sec, plate read].

Both cDNA synthesis and subsequent qPCR analyses of miRNA were performed in 384-well-plates utilizing CFX384 Touch™ Real-Time PCR Detection System (BioRad, US). For the cDNA synthesis, the reaction volume in each well was scaled down to 40% of the total recommended volume, and later diluted with water after the synthesis was done. In the qPCR reactions, the volume was scaled down to 80%. These reductions in volumes were optimized to save on reagents. No negative effects on efficiency or accuracy were observed.

3.2.4 RNA Sequencing

3.2.4.1 - Small RNA sequencing

Enriched small RNA fractions were extracted from the myocardia of 3 *Mlp*$^{-/-}$ mice and 3 WT littermate controls using mirVana™ miRNA Isolation Kit, following the manufacturer's instructions. The quantity of enriched small RNA fraction was estimated by Qubit™ through utilizing the RNA High Sensitivity Kit (Thermo Fisher Scientific), and the quality of the RNA was assessed through utilizing the Bioanalyzer Agilent Small RNA Kit. The samples were sent to SciLifeLab for preparing Small RNA libraries by utilizing TruSeq® Small RNA Library Prep Kit, and subsequently sequenced on HiSeq (rapid) Flowcell (1x50 bp reads) to yield ~15M reads per sample. Raw sequencing data were bioinformatically processed (by Xidan Li, ICMC) using a standard method to obtain a list of differentially expressed miRNAs.

3.2.4.2 Sequencing of mRNA

Total RNA was extracted from the myocardium of *Mlp*$^{-/-}$ mice treated with miR-208b-3p antagomir or scramble control by using TRIzol as described in the supplementary material of Elbeck *et al.* (Elbeck et al., 2022). A standard SmartSeq 2 protocol was utilized for preparing mRNA libraries for sequencing (Picelli et al., 2014), as described in the supplementary materials of Elbeck *et al.* (Elbeck et al., 2022) except that 8 technical replicates, instead of 4, were prepared and sequenced from each sample. The raw data of all 8 technical replicates were merged and analyzed (by David Brodin, BEA facility) utilizing the same bioinformatic codes

described in the supplementary materials of Elbeck *et al.* (Elbeck et al., 2022) to obtain the differential expressed list of genes.

3.3 4-3- STUDY-III: Novel isoforms of MLP and their role in the remodeling of heart failure

3.3.1 Quantitative PCR

RNA from the myocardium of *Mlp*$^{-/-}$ and WT littermate controls was extracted using the RNeasy Fibrous Tissue Mini Kit (Qiagen). The subsequent synthesis of cDNA and the qPCR analyses of different exons of *Mlp* transcripts were performed as described above (section 3.2.3) utilizing the primers described in Table 4.

Table 4: qPCR primers utilized in study III

Gene	Forward primer	Reverse primer	Species
Mlp_{ex2}	GTCTTCACCATGCCAAACTG	CCCATTGCACTGGATTTCTT	Mouse
Mlp_{ex3}	AAAGCTCTGGACAGCACCAC	AACTGCAGGCCAAGATGCT	Mouse
Mlp_{ex6}	GAAGCTGCCTGCTTTCTCAC	ACTTCGGTGCAGCCTATGAC	Mouse

3.3.2 Long-reads Oxford-nanopore sequencing

3.3.2.1 Targeted sequencing of Mlp transcripts

As there are only two potential stop codons in the transcript of *Mlp* mRNA located in exon 6, we predicted that all potential novel transcripts that encode for translatable proteins of murine MLP would have exon 6 included in their mRNA. Therefore, we thought to develop a method that could enrich all these transcripts, and then unveil their sequence and their 5′ end by long-read Nanopore sequencing.

The SmartSeq2 protocol enables cDNA synthesis and subsequent amplification of all polyadenylated mRNA transcripts. In the canonical protocol, the 3′ end of the Oligo (dt) primers and the 5′ end of the template switching oligos (TSO) contain complementary sequences, and therefore the subsequent amplification of the cDNA is done with a single primer that anneals to both ends (ISPCR). However, to enable the amplification of a specific transcript, the sequence of the 3′ end should not be complementary to that of the 5′ end. This can be done by designing a different oligo (dt) primer, or different TSO. For our experiment, we used a different oligo $dt_{30,b}$ primer, which was kindly provided by Omid Faridani at ICMC.

The SmartSeq2 protocol with the new oligo $dt_{30,b}$ primer was utilized to obtain whole transcriptomic cDNA library, which was then amplified using ISPCR and another complementary primer to the 3′ end of the oligo $dt_{30,b}$ primer (primer 414, also kindly provided by Omid Faridani at ICMC). Amplified cDNA was then purified with Ampure XP beads.

Thereafter, the cDNA of all *Mlp* transcripts that share exon 6 was enriched through a PCR amplification using a ISPCR as a forward primer, and a sequence corresponding to exon 6 of *Mlp* (mMlp.ex6-R, ACTTCGGTGCAGCCTATGAC) as reverse primer (**Figure 22**). The reaction product, enriched for *Mlp* transcripts, was then purified with Ampure XP beads, quantified, and used as input for library preparation according to the 1D^2 sequencing of genomic DNA kit (with SQK-LSK308, Oxford Nanopore) following the manufacturer's instructions, and with skipping the optional step of DNA repair. The library was then sequenced on MinION Sequencer (Oxford-nanopore).

The cDNA synthesis and the sequencing were done together with the master student Dominique Koppenhöfer, whom I supervised, and the raw data of the sequencing was analyzed by Humam Siga at ICMC, by utilizing algorithms provided by Oxford-nanopore.

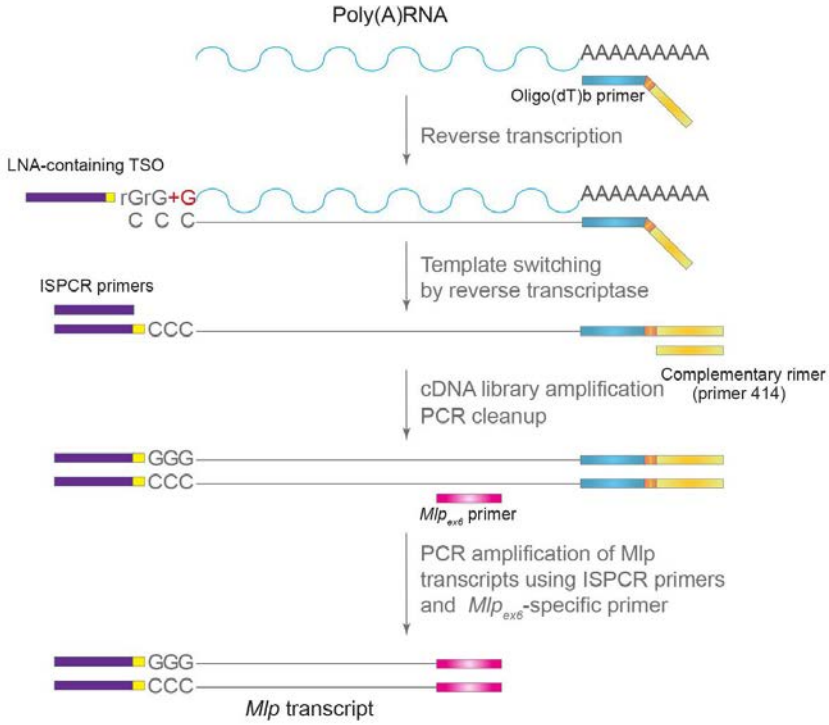

Figure 22: A scheme over targeted approach to enrich for 5'-unknown *Mlp* novel transcripts
The figure is adapted from SmartSeq 2 protocol (Picelli et al., 2014) with modifications .

3.3.2.2 Direct RNA sequencing

To verify the presence of novel *Mlp* transcripts, which were identified using the targeted sequencing approach described above, and to verify that no additional transcripts lacking exon

6 had been missed, we utilized Nanopore direct RNA sequencing technology. This technique sequences the mRNA itself without converting it to cDNA.

The mRNA was enriched from the total RNA by using the NEBNext Poly(A) mRNA Magnetic Isolation Module according to the manufacturer's instructions. The quantity of enriched mRNA was assessed with Qubit HS RNA Assay, and its quality was examined using a bioanalyzer and the Agilent RNA 6000 Nano Kit (**Figure 23**). When needed, the enriched mRNA was concentrated with RNA clean XP beads (1:2, mRNA:beads) to achieve the required concentration for the subsequent application. Enriched mRNA was then used for library preparation using the Direct RNA Seq Kit according to the manufacturer's instructions, and thereafter sequenced on MinION Sequencer (Oxford-nanopore). This experiment was also done together with the master thesis student Dominique Koppenhöfer, and the raw data of the sequencing was also analyzed by Humam Siga, by utilizing algorithms provided by Oxford-nanopore.

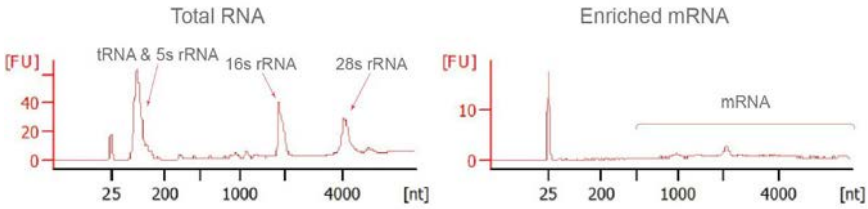

Figure 23: Bioanalyzer traces of enriching total RNA for mRNA

The figure is from one of the experiments that I performed for the direct RNA sequencing.

3.3.3 Western blotting

Protein lysates were prepared with RIPA buffer, as described in the supplementary methods of Elbeck *et al.* (Elbeck et al., 2022). An electrophoresis system from BioRad was utilized for whole project III; *i.e.*, Laemmli sample buffer supplemented with 10% β-mercaptoethanol, Mini-PROTEAN® TGX Stain-free gels 4-15 %, Precision Plus Protein Dual Color Standards, and Tris/Glycine/SDS for the running buffer. After electrophoresis, proteins were transferred to 0.2 µm PVDF membrane using the Trans-Blot® Turbo™ with Mini PVDF Transfer Packs (BioRad). The membrane was subsequently fixed with 0.4% formalin, and washed with PBS, TBST and blocked with milk, as described in the Supplementary Methods in Elbeck *et al.*, 2022.

The membranes were blotted with different primary antibodies (see Table 5), and subsequently blotted with their corresponding secondary antibodies. The different incubation times indicated for the antibodies against Mlp are for different experiments. For example, blotting of Mlp from

Mlp$^{-/-}$ required a long period of incubation to enhance the signal, whereas overnight incubation was enough to detect Mlp from overexpressing constructs. A chemiluminescent signal was detected with ChemiDoc™ gel imaging system (BioRad). When needed, the membranes were stripped with harsh or mild stripping buffers (for their composition, please see Supplementary Methods in Elbeck *et al.* (Elbeck et al., 2022), and then reblotted using another primary antibody.

Table 5: Primary and secondary antibodies utilized in the study.

Antibody	Reference number	Provider	dilution	Incubation
Mlp (Rabbit)	10721-1-AP	Proteintech®	1:500	4°C, 3 days/ overnight
Mlp (Rabbit)	ab155538	Abcam	1:500	4°C, 3 days/overnight
GAPDH (Mouse)	MA5-15738	Invitrogen	1:2500	4°C, overnight
GFP (Chicken)	ab13970	Abcam	1:5000	4°C, overnight
Secondary anti-rabbit IgG		GE Healthcare	1:5000	1 h, RT
Secondary anti-mouse IgG		Abcam	1:5000	1 h, RT
Secondary anti-Chicken IgG		Abcam	1:5000	1 h, RT

3.3.4 *In vitro* overexpression of Mlp isoforms

HEK cells were transfected with plasmids carrying constructs coding for different isoforms of Mlp (Table 6). Transfection was done by utilizing Lipofectamine™ 3000 reagents (Invitrogen) with the procedure described in section 3.2.2, except that cells were collected 3 days after the transfection. The cells were then lysed with RIPA buffer and subsequently analyzed for Mlp level by Western blotting.

Table 6: Plasmids encoding different isoform of Mlp

Number*	Transcript	Plasmid name	Plasmid ID	Map
Scramble		pRP[Exp]-Puro-EF1A-eGFP	VB180823-1120qay	https://en.vectorbuilder.com/vector/VB180823-1120qay.html
1	Mlp (Full length)	pRP[Exp]-Puro-EF1A-mCsrp3 WT	VB180823-1134ban	https://en.vectorbuilder.com/vector/VB180823-1134ban.html
2	Δex(1 and 2) Mlp	pRP[Exp]-Puro-EF1A-mCsrp3 C-term. Isof.	VB180823-1133yhw	https://en.vectorbuilder.com/vector/VB180823-1133yhw.html
3	Δex2 Mlp (201)	pRP[Exp]-Puro-EF1A-mCsrp3 201 Δex2-T2A-eGFP	VB180823-1132hzt	https://en.vectorbuilder.com/vector/VB180823-1132hzt.html
4	Δex2 Mlp (202)	pRP[Exp]-Puro-EF1A-mCsrp3 202 Δex2-T2A-eGFP	VB180823-1129avy	https://en.vectorbuilder.com/vector/VB180823-1129avy.html
5	Δex2 Mlp-Arf	pRP[Exp]-Puro-EF1A-mCsrp3 202 Δex2-eGFP	VB180823-1130eju	https://en.vectorbuilder.com/vector/VB180823-1130eju.html
6	Δex 2 Mlp + UTR	pRP[Exp]-Puro-EF1A-mCsrp3 202 Δex2+UTR-T2A-eGFP	VB161103-1013cck	https://en.vectorbuilder.com/vector/VB161103-1013cck.html

* The number of the construct indicated in Figure III-10

3.3.5 Immunoprecipitation and mass spectrometric analyses:

Protein lysates were prepared from myocardial tissues with either RIPA or NB-40 buffers. Mlp was immunoprecipitated from the lysate using Dynabeads Protein G (#10003D, ThermoFisher) according to the manufacturer's instructions. Antibodies against Mlp (Abcam or Proteintech, Table 5) were chemically crosslinked to the beads through treatment with BS_3 reagent. IgG control (Abcam, ab27478) was used as a negative control.

In the final step, precipitated proteins on the beads were boiled with sample buffer and then electrophoresed. Gels were stained with either SimplyBlue™ SafeStain (#LC6065, Thermo Fisher), or SilverQuest Silver Staining Kit (#LC6070, Thermo Fisher) to visualize protein bands. Bands corresponding to the expected molecular weight of Mlp novel isoforms were excised from the gel and sent for protein fingerprinting by mass spectrometry at the Proteomics Biomedicum core facility. Mass spectrometric data was kindly analyzed by Akos Vegvari (Proteomics Biomedicum, KI).

3.3.6 Immunofluorescence analysis

Immunofluorescence was performed as described in the supplementary materials for Elbeck *et al.* (Elbeck et al., 2022). The utilized primary antibodies against Mlp were (ab155538, Abcam) and against α-actinin were (A7811, Sigma-Aldrich). The corresponding secondary antibodies were Alexa Fluor Donkey anti mouse 488 (ab150105) and Alexa Fluor Donkey anti rabbit 568 (ab175470, Abcam). The mounting Medium contained DAPI (Fluoroshield, ab104139, Abcam).

Images were acquired using a Zeiss Axio Observer Z1 florescence microscope, and Zeiss EISS LSM 880 confocal microscope equipped with Airyscan.

4 METHODOLOGICAL CONSIDERATION

I have spent considerable effort and PhD training time to try to optimize suitable methods to yield trustful and meaningful results. Problems that I encountered included lack of proper basic knowledge in some concepts, technical limitations, or time constraints. However, I did my best, and I used my biochemical and molecular background to understand the purpose of every single component I used in every experiment done. It required substantial time and effort and involved ample troubleshooting, but in return helped me break deadlocks in important projects, while simultaneously avoiding other projects that contained flawed hypotheses or methodologies.

I try to avoid using commercially available kits from companies that refuse to disclose the actual components of their kits, especially when alternatives are available. I have learned that companies often use very simple reagents but refuse to disclose them for commercial purposes (I am not against them making money, but that should be in exchange for deep expertise and reliable service). Research methodologies must be possible to adjust to fit to the research question or a novel application. There is nothing that should be difficult to understand, or data that do not make sense. To me, the required acquisition of basic knowledge could be easily gained, when needed. Therefore, I mostly utilized homemade or optimized reagents and developed my own protocols and methods, which I have disclosed transparently in my work.

Below, I give some examples of a few of the simple techniques that I spent considerable time developing and optimizing. Some of these examples also show how additional supportive and useful conclusions could be inferred from same set of experiments without efforts beyond a good understanding of the experiments combined with some accurate and precise work.

4.1 Ethical considerations

I perceive that utilizing animals in research is necessary for the study of complex molecular crosstalks between different types of cells and organs. Although physiological studies in vitro may be quite complex and involve for example heterotypic cell cultures and organoids of high cellular complexity, it would probably never be possible to substitute live animals for all biomedical research applications, especially the complex ones dealing with multiple organs. I personally do not want to be the subject of a pre-clinical trial, but I also do not want to suffer from a treatable disease. Therefore, improving the well-being of lab animals is essential for several aspects. However, despite all efforts that have been invested in this regard in recent decades, I think that the current regulations are still insufficient to achieve the ultimate goals of the 3R principles (**R**eplacing animals when it is possible, **R**efining experimental procedures to minimize suffering of experimental animals and **R**educing number of animals used).

Among the shortcomings of current regulatory measures, are for example that there are yet no legal consequences for researchers who have exerted scientific misconduct in general, or specifically involving animals. The ultimate purpose of medical research is to improve human health, and not only to promote own career with faking data, killing innocent animals, and wasting research funds and resources. In my opinion, such actions should be prosecuted in courts of law, which is not the case in Sweden today.

Moreover, the broad practice of ignoring negative data, or to hide experimental details or data should be strongly discouraged (Hofseth, 2018). Negative results are always as important as positive ones, as they delineate new routes, or may represent positive data in other circumstances or for other researchers. Ethical boards and funding agencies should develop a mechanism to retrospectively follow major experiments, especially those involving animals or clinical materials, and make sure that their data are accessible to the broad scientific community. This would save a huge number of animals or research efforts and resources. In addition, sharing complete raw data and metadata that would enable subsequent re-utilization of data should also be more encouraged by funding agencies.

4.2 Profiling of gene expression

4.2.1 RNA extraction

RNA extraction represents the initial basic step for all subsequent assays of profiling gene expression, including qPCR, microarrays, and all types of sequencing. Therefore, correct profiling of gene expression requires the best possible and consistent qualities of extracted RNAs.

There are multiple available methods to extract and purify RNA. All applications require an initial step to break cellular membranes and proteins to release the RNA. This step might be sufficient for some applications that work with crude extracts such as single RNA-seq, but most other applications require subsequent purification of the RNA.

Breaking cellular membranes can be done with different methods, most of which rely on hypotonic solutions, or surfactants to solubilize lipids and denature or break down proteins to release the RNA, such as detergents, proteases, phenol, or others. Whereas the subsequent purification of the RNA utilizes one of two methods; either precipitating the RNA into a pellet, or capturing RNA molecules with a silica-based membrane that reversibly absorbs the RNA.

Methods that utilize silica-based membranes yield extremely good quality and pure RNA, and they also enable the fractionation of different species of RNA based on their length. However,

they recover lower amounts of RNA and increase the chances of RNA degradation through the multiple steps of purifications when the RNA is not in a precipitated state (protected from enzymatic degradation by RNases), and they are usually expensive and laborious.

On the other hand, methods based on precipitating the RNA are fast and inexpensive. They also yield substantially higher amounts of RNA and minimize the risk of RNA degradation by RNases. However, it is usually not that easy to see the precipitated pellet, which is then readily getting lost, especially when extracting small amounts of RNA without adding glycogen. Glycogen is a highly branched polysaccharide, insoluble in ethanol solution. Adding glycogen to aquatic phase during RNA extraction and subsequently adding ethanol precipitates the glycogen, which traps RNA molecules and forms a solid ethanol-insoluble easily visible pellet (R0551, Thermo Scientific).

Commercially available kits for extraction and purification of RNA use different combinations of protocols to break cellular membranes and to purify the RNA. However, based on the heart being fibrotic tissue, using a phenolic-based method such as TRIzol (a monophasic solution of phenol and guanidinium isothiocyanate) omits the need for treatment with proteases to break cellular membranes. Phenol solubilizes proteins, causing the cellular component to dissolve in TRIzol, especially when mechanical sheering is applied (with tissuelyzer, vortexing, pipetting or sonication).

Moreover, I found that scaling down utilized amounts of TRIzol reagents facilitates performing the extraction in strips of small 0.2 tubes, and therefore enabling the handling of a large number of samples simultaneously (up to 72 samples). These small adjustments enabled me to develop a high-throughput protocol, which yielded very good quality of RNA, was highly reproducible and fast, and saved substantial amounts of reagents, cost, and samples.

The simultaneous extraction of multiple samples, with a consistently high yield of high-quality total RNA, enabled me to identify changes in recovered RNA yields also when their magnitude was small, for example in association with the death of few cells or changes in their morphology upon redox treatments (Elbeck et al., 2022). This simply provided me with additional data that allowed me to monitor the quality of the experiments and obtain supportive data at almost no additional effort, data that I would most likely have missed using commercial kits, or it would have required considerable time and efforts to optimize some sophisticated and specialized methods to investigate it, such as xCELLigence®.

However, kits that utilize silica-based membranes are still very useful when digestion of contaminating traces of gDNA is needed, or to fraction or enrich certain RNA species such as

small RNAs (>200 nt). Digestion of contaminating gDNA is important when investigating rare non-poly-adenylated protein noncoding RNAs by qPCR or by total RNAseq, as even traces of contaminating gDNA would interfere with the results.

Fractionation of RNA species is based on differential ethanol precipitations of RNA molecules based on their sizes, where the smaller RNA requires higher percentages of ethanol to precipitate. Therefore, it is very important to adjust the accurate percentage of ethanol, and to use a fresh and well-preserved ethanol solution, as small percentages of moisture absorbed from the atmosphere would change the percentage of ethanol. Most kits use 30% ethanol to precipitate big RNA (< 200 nt). It is very important to realize here that this 200 nt is not a cutoff size, as most would think, but a mean value of a size range. This is crucial for some applications, such as qPCR analyses of miRNA (~ 21 nt), which uses a longer RNA species as control for the normalization such as U6 snRNA (~ 100 nt). Therefore, fractionation of the RNA should definitely be avoided when not needed.

4.2.2 Quantification of RNA

The second important step in profiling gene expression is to achieve a correct estimation of the quantity and quality of the extracted RNA. Nanodrop represents a cheap method to obtain a rough estimate of the RNA purity and quality. However, it is hugely inaccurate for, and usually overestimates, the amounts of RNA. In contrast, fluorometric assays, such as Qubit, represent the best available method for specific and accurate quantitative estimation of RNA, but it is expensive. One way that I found useful to overcome the high cost is to re-use the same solution of Qubit several times to quantify subsequent samples (2-3 times), until the amount of the RNA in the quantifying solution reaches the higher range of the standards. Then, a subsequent subtraction of the previous value each time gives the actual value.

Bioanalyzer is a practical and accurate method for assessing the quality of RNA, but it is also very expensive. I found that by gaining increased experience with RNA extraction, and by using TRIzol, the quality of recovered RNA was so rarely compromised that measuring RNA quality could be omitted for most subsequent applications. If RNA degradation would occur in a few samples, it could be spotted by Qubit quantification when extracting from equal amounts of tissues or cells. The latter also represents an important and crucial practice.

4.2.3 *qPCR*

Quantitative PCR represents a very simple, sensitive, and accurate method for profiling a small number of genes but requires a number of considerations in order to deliver reliable data.

As mentioned, accurate quantitative estimation of RNA is crucial, as normalization with housekeeping genes such as GAPDH does not compensate for large differences in the concentrations of input RNA between samples, as one might think. This is because the amplification curve of targeted fragments is not exactly exponential, even in the "exponential phase". It differs slightly from gene to gene based on the initial number of cDNA molecules of the target genes, their sequences, utilized primers, and the length of the fragments being amplified. Housekeeping genes used for normalization are usually very highly expressed in comparison to the target genes, which would impose differences to their amplification curves, and therefore, even small differences in the concentrations between samples would be magnified, even after normalization. This would be particularly important when investigating biological effects associated with small differences in gene expression (**Figure 24**).

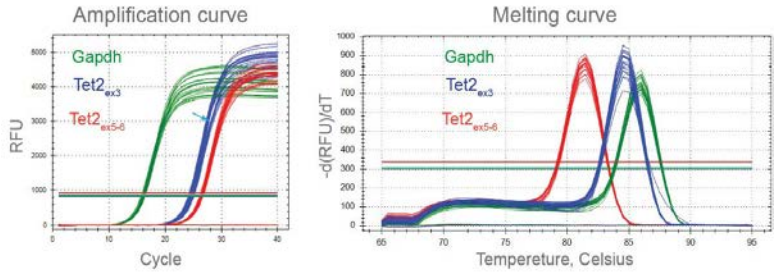

Figure 24: Accurate estimation of RNA concentrations yields reliable qPCR results, even for small differences

This figure is from one of my qPCR experiments, where Tet2 was knocked down with shRNA targeting its exon 3. *Tet2* is an extremely long and rare transcript in cardiac cells, which makes both its targeting and the validation of the targeting not easy. In the example shown in this figure, the accurate quantification of extracted RNA from multiple biological replicates yielded consistent quantification cycle (Cq) for all samples, which can be observed from the narrow variation of amplification curves of *Gapdh*. Primers targeting exon 5-6 junction of *Tet2* transcript did not show any difference in the treated group. However, a primer targeting the target exon of the ShRNA located farther to the ploy A-tail (*i.e.,* exon 3) could detect a 20% reduction in the level of *Tet2* transcript (Quantification is not shown but it can be inferred from the increase in the width of the amplification curves of $Tet2_{ex3}$). Melting curves show that there were no primer-dimers.

Designing optimal primers with low primer-dimer artifacts is also important. The position of annealing of the designed primer is also another important factor (**Figure 24**). For example, qPCR analyses of transcripts longer than 7000 nt with primers located very close to the 5′ UTR would not work when the cDNA is synthesized utilizing the poly-T primers, as most cDNA reverse transcriptases would not transcribe longer fragments (this issue is not related to the experiment shown in **Figure 24**, where both amplified fragments of Tet2 with both set of primers are shorter than 7000 bp). The melting curve is usually a useful tool to assess both the presence and the interference of primer-dimers (**Figure 24**, right panel).

Moreover, the quantification cycle (Cq) in qPCR can give additional useful information than the relative gene expression value if the experiment is designed and performed correctly. It can

give, for example, some information about the quality of the RNA (especially when the quality check of the extracted RNA is skipped, as mentioned earlier). It can also give information about the biological variation of a studied mechanism through careful observations of the control group.

As an example, in our recent work, when treating NRCMs with H_2O_2 (**Figure 25** and (Figure 2 in (Elbeck et al., 2022))), the expression of oxidative-stress-induced genes *Hmox1*, *Nqo1* and *Osgin1*, were increasing with increased doses of H_2O_2. However, at very high doses of H_2O_2, i.e., 100-300 µM, their expression decreased dramatically, especially in cells that were collected 6 h after treatment (**Figure 25**). Looking at the Cq values of *Gapdh* (**Figure 25**), I concluded that this decrease resulted from H_2O_2-induced RNA degradation, as the Cq values dropped in all biological replicates treated with these doses.

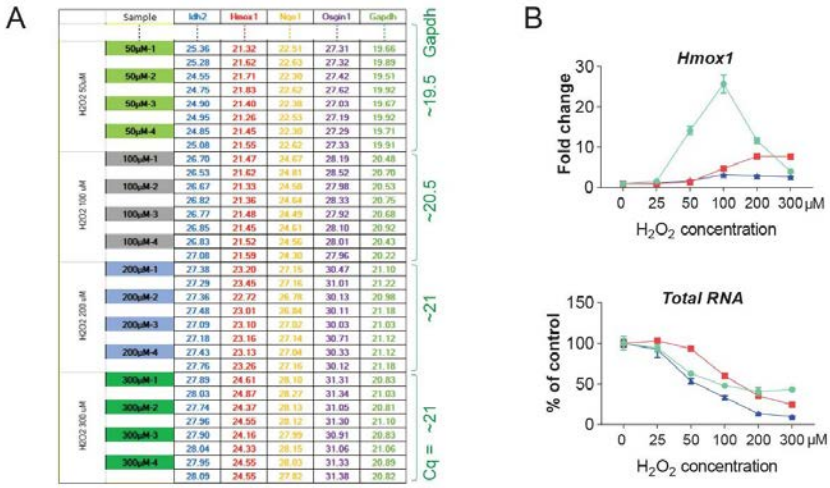

Figure 25: H_2O_2 induced degradation of RNA inferred from Cq values of qPCR analysis

A: Screenshot from the raw Cq values of qPCR analysis of NRCMs treated with increasing doses of H_2O_2 in our recent work. A drop of Cq=1 is equivalent to ~ 50% reduction in the initial quantity of the transcript. The two rows for each sample represent technical replicates **B**: qPCR analysis of *Hmox1* expression in NRCMs treated with H_2O_2, and the recovered amounts of RNA from these treated cells. This loss of RNA exerted no impact on gene expression observed, since 5 ng of total RNA was employed in all qPCR reactions. Figure B is taken from our recent publication (Elbeck et al., 2022) with permission. The curves for *Nqo1* and *Osgin1* show similar trends to *Hmox1*, and therefore are not shown here.

Most cells would not be able to scavenge high concentrations of hydrogen peroxide, which would then cause the fragmentations of RNA and DNA, and subsequent immediate death of cells without having time to undergo apoptosis. As cardiomyocytes adhere firmly to the culture dish surface, and because they are large cells, dead cardiomyocytes would need more than 6 hours to detach. The method that I used to extract RNA (TRIzol) would recover all mRNAs

including fragmented molecules, but the subsequent cDNA synthesis should not copy fragmented mRNAs that have lost their poly A-tail. Equal amounts utilized for the qPCR reactions refers to total RNA amounts, not cDNA (that can't be measured). Therefore, the genes will appear as downregulated at the high concentrations of H_2O_2 at the 6 h time point. However, after 24 h or 48 h, these dead cells will be washed off, and newly dying cells will be fragmented and detached by apoptosis. The data are normalized to the untreated cells in each individual time point.

Moreover, qPCR can give an indication about different types of biological variations of studied mechanisms. Normal biological variation can be inferred from the standard deviation of the control group, which would differ from the added-on variation induced by the condition being investigated, and which (the latter) can be also inferred from the standard deviation of the treated group. However, a common mistake that prevents visualizing Normal biological variation is when the values of the fold changes in the control group are set to ¨1¨ and subsequent mean fold change lacks error bars. This is a very common mistake found in numerous published papers.

The fold changes of the control are not 1, but rather the logarithmic values of subtractions of ΔCq values of each sample from each other sample in the control group (**Figure 26**). This would give each control sample n subtractions (ΔΔCq) (n is the number of samples in the control group), and a total number of subtractions in the control group equal to n^n. As an example, if there are 3 samples in the control group (C1, C2, C3), each sample would have 3 ΔΔCq values (for C1 for example: ΔCq_{C1}-ΔCq_{C1}, ΔCq_{C1}-ΔCq_{C2} and ΔCq_{C1}-ΔCq_{C3}), and the number of ΔΔCq values for the whole control group would of be 3^3=9 in this example. The sum of these 9 values is 0, but individual values are not 0 (except for ΔCq_{C1}-ΔCq_{C1}, ΔCq_{C2}-ΔCq_{C2} and ΔCq_{C3}-ΔCq_{C3}) (**Figure 26**). Then, the average of all ΔΔCq values for each sample should be calculated (in our example, for control sample $\overline{\Delta\Delta Cq}_{C1}$ = [((ΔCq_{C1}-ΔCq_{C1}) + (ΔCq_{C1}-ΔCq_{C2}) + (ΔCq_{C1}-ΔCq_{C3}))/3] ≠ 0). Then the logarithmic value of this average is calculated, which give n number of averaged fold changes (in our example we get 3 values), which none of them should have the exact value of 1, but the average of all of them (n) would be equal to the exact value of 1. Having n number of fold changes with variable values would enable the calculation of standard deviation, which would then reflect the biological inter-variation of the investigated mechanism in the control group. The same principle would also be applicable to the treatment group.

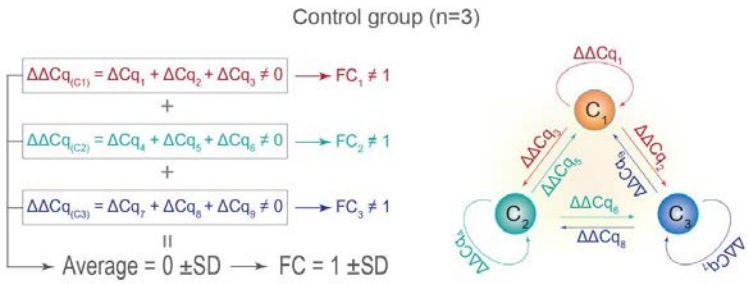

Figure 26: Fold changes (FC) of the control group does not equal to 1 in qPCR analysis or other assays

The illustration explains a common mistake in some publications, which do not show standard deviation for the fold change of the control group.

This common mistake would not only omit the information about the inter-variation of the investigated mechanisms in the control group, but it would also unintentionally falsify the subsequent statistics for the whole experiment, as comparing treated group with control group that has SD = 0 would give very low, but false, *p* values.

4.2.4 *Sequencing*

RNA sequencing represents an efficient way to profile the whole transcriptome, in comparison to only one or a few genes using qPCR or some microarrays (microarray analysis has become obsolete for plain transcription profiling techniques, but some had become close to genome-wide). It also enables the detection of novel transcripts, without requiring any prior knowledge of their presence or sequence.

4.2.4.1 Next and third generation sequencing

Both next (second) and third generation sequencing techniques are used for transcription profiling. Each of these techniques has its advantages and disadvantages. Next generation sequencing (NGS) is usually proceeded by a library preparation that fragments the RNA, ligates primers, and reverse-transcribes the fragments to cDNA followed by an amplification step. SmartSeq2, one of these techniques (Picelli et al., 2014), is a relatively cheap, and may utilize homemade reagents. These advantages make SmartSeq2 an optimal method for modification and adaptation to a variety of applications (such as the method that we developed in section 3.3.2.1). However, the main disadvantage of this technique is the high number of amplification rounds required to obtain sufficient quantity from the cDNA and from its subsequent library, which would, if not perfectly optimized, result in high number of PCR duplicates or unmappable reads.

Another main disadvantage of SmartSeq2 is that it does not accurately estimate the expression of extremely long transcripts (> 7000 nt) such as TET1-3. This is mainly due to the fact that Superscript II attach 3-4 non-template-derived cytidine residues to the 3′ end of the cDNA during first-strand synthesis in the presence of a high concentration of magnesium (**Figure 22**). These added cytosines are then utilized for the subsequent template switching of the transcription. Thus, Superscript II would not reach the 3′ end of the extremely long and unfragmented mRNAs, and therefore these partially synthesized and stalled cDNAs will not be appended with these cytosines. However, the sequencing library would still contain some cDNAs of formerly fragmented mRNAs of the long transcripts, which still have the poly A-tail. This incidental fragmentation of the mRNA usually results during RNA extraction and the subsequent handling procedures, which might not be consistent among all investigated samples.

On the other hand, commercially available kits for library preparations yield much better results. The starting input of RNA is usually much higher, and they additionally fragment the RNA before synthesizing the cDNA and after depleting rRNAs. Their libraries, therefore, requires less amplification steps (6-7 *vs.* > 20 cycles in SmartSeq 2), and include all transcripts, regardless of their length. However, these kits are very expensive, and it is not possible to modify them to fit for custom purposes other than what they have been designed for. Some of these kits generate libraries from total RNA after depleting ribosomal RNA, and others target only polyadenylated transcripts. I always prefer total RNAseq, and not only the mRNAseq, as the former would also provide information about non-poly-adenylated long-noncoding RNAs at no extra effort. Even if one might not be interested in them at the time, they would be useful for other researchers, or for future projects. The field of non-coding RNA is moving rapidly, and novel discoveries are made at a high pace.

Third generation sequencing enables sequencing of long reads, including full transcripts. Therefore, they enable the detection of novel transcripts (as we have done in the 3rd project) without requiring any prior knowledge about their presence, or their spliced forms, which would not always be possible in NGS as the RNA is either fragmented, or only the 5′-UTR ends are sequenced. However, the accuracy of correct base-calling of the sequencing data is much less than that of the NGS, but they are being continuously developed and improved.

4.2.4.2 Small RNA sequencing

Small RNA sequencing represents an efficient way to profile whole differentially expressed miRNA transcriptome, and to detect novel putative miRNAs. As described in a previous

section, correct profiling of miRNA would also require optimal extraction and purification methods of RNA.

In my experience, Qiagen kits provide good quality of the extracted RNA. Therefore, I initially utilized miRNeasy Kit from Qiagen to extract an enriched fraction of small RNA. However, subsequent quality control of the extracted small RNA fraction by using a bioanalyzer did not show an observable peak for miRNA, although the adjacent peak for tRNA was very evident and of a high quality (a close example is shown in the subsequent **Figure 27**).

My initial thoughts after consultation with SciLifeLab was to try a different kit. Therefore, I tested extracting total RNA from the same sample using two additional kits, *i.e.*, mirVana™ and E.Z.N.A.® Micro RNA Kit, both of which utilize silica-based spin columns similar to Qiagen kit. However, subsequent bioanalyzer analyses failed to detect a peak for the miRNA in all three samples.

To subsequently investigate whether the extracted RNA contained any miRNA, I ran a qPCR analysis for miR-1, which is a cardiac specific miRNA, using miScript PCR kit (Qiagen). MiR-1 was detected in all samples of RNA extracted with all kits, but with a slightly higher expression with the RNA extracted with the mirVana™ kit, and I therefore decided to subsequently use this kit. However, it seems that there is something specific to the heart, as if it appears to contain huge amount of tRNA that masks the peak of the miRNA peak (**Figure 27**).

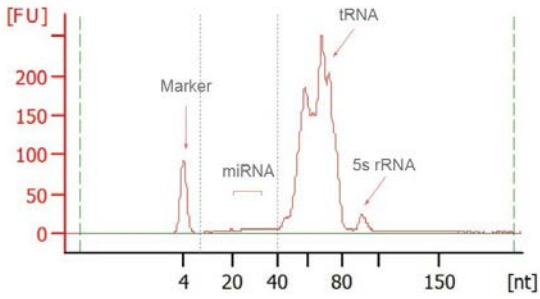

Figure 27: Bioanalyzer traces for small RNA enriched fraction

The small RNA enriched fraction was extracted from a myocardial tissue using mirVana™ kit.

Moreover, as we observed that the relative percentage of miRNAs appeared to be low even in the enriched small RNA fraction, we considered preparing small RNA libraries from the enriched fraction of small RNA instead of total RNA. Illumina TruSeq Small RNA kit uses adaptors that specifically target mature miRNAs that are modified with 5′-phosphate (5′-P) and 3′-hydroxyl (3′-OH) ends, and the miRNA fraction is further enriched by a subsequent size

selection step of the final libraries. Therefore, the staring materials can be total RNA, but we thought instead that using enriched fraction of the small RNA would increase the chances of successful targeting of the primers to mature miRNA in our case. The initial purpose of this sequencing project was to look for novel miRNAs.

4.2.4.3 Pathway analyses

Pathway analysis of NGS transcriptomic data provides an oversight over biological pathways induced or suppressed by the investigated treatment or disease. However, pathway analysis does not provide direct proof for the involvement of a biological function in the process investigated, but rather gives an indication that can be used to formulate a hypothesis for further investigation. This is since these analyses are biased by the data used to train the algorithm. Therefore, one needs to apply a certain degree of common sense when interpreting and selecting relevant significantly enriched pathways, which should be ultimately supported by some other data acquired by different experiments. For example, finding in cardiac transcriptomic data an enriched pathway related to a disease in the brain, such as Alzheimer's disease does not imply that Alzheimer's disease exists in or affects the heart. It instead indicates that a pathway that shares some common features with Alzheimer's is activated in the heart, such as unfolded protein response, or ER stress.

4.3 Western blotting

Western blotting is one of the basic and essential methods in molecular biology used to determine specific protein expressions. Although several variants of this method have appeared during recent years, such as capillary and automated Western blotting, the conventional method remains superior for a number of reasons. Western blotting does not only provide information about the protein characteristic, but it also an impression about the integrity and the validity of the whole work, as it only requires sharp eyes and a critical mind to spot any deviations from a reliable result and good practice of the method, not only in own data, but also in publications.

Western blotting might seem a simple technique, but in reality, it is not, as it requires many optimizations for several aspects for each new target. Many considerations should be taken in Western blotting when designing new experiments, interpreting their data, and visualizing them.

The most important element in Western blotting is choice of antibody, the source of which is most often a company. Said company should always be able to provide the exact peptide(s) utilized to raise the antibody and provide information about how they optimized their validation of the antibody. The size of the detected band should be always close to the expected size from

the calculated molecular weight, if not there should be a valid explanation. In this regard, I will show in a subsequent section of this monograph an example of some of the troubles that I had when optimizing antibodies against some targets.

The second important aspect is to optimize a suitable lysis buffer for preparing protein lysate of a tissue or cells, as well as choosing a suitable gel and running buffer for the electrophoresis. It is worth mentioning here, that the visual size indicated by the protein ladder on the gel might differ slightly from the actual size, according to the type of gel and running buffer being utilized, and therefore, companies usually provide a table for the apparent Mw in different conditions.

When it comes to data presentation, it is extremely important to show both the target protein and the loading control from the same membrane, and not to use a ¨representative¨ image of the experiment without the cognate loading control. The aim of visualizing equal loading is to enable the reader to assess and validate the integrity of the work and to independently discover mistakes or flaws. A loading control is usually a "housekeeping protein" known to remain constant under experimental conditions. The choice of such a control should therefore be made carefully, as common types, *e.g.*, β-actin and GAPDH, may vary in certain contexts. However, they are usually highly expressed, and a substantial fraction of them would remain on the membrane after multiple rounds of stripping and reblotting. Therefore, there is normally no reason that prevents the experimenter from showing a loading control from the same membrane that was used to blot the target protein. It is also important to avoid cutting the membrane into smaller pieces, although this is a common practice, justified by saving time and reagents. Cutting the membrane means cutting away important controls of data quality, such as molecular weight markers, cross-reactions, and others. When quantifying the intensity of bands blotted on multiple membranes, values originating from different membranes should be normalized prior to merging them, similar to the normalization method that we described in our recent work (Elbeck et al., 2022).

Finally, one should remember that Western blotting is not a quantitative method, but a semiquantitative one. Therefore, one should not over-interpret the results, or blindly trust statistically significant data.

4.3.1 An example of optimizing antibodies for L2hgdh *and* D2hgdh

In our recent work (Elbeck et al., 2022), *in vitro* induction of L2HG and D2HG through knocking down L2hgdh and D2hgdh in neonatal rat cardiomyocytes (NRCMs) was an essential

experiment to unveil the regulatory role of L2HG on Idh2. Therefore, I needed to validate that knocking down RNA levels resulted also in a reduction in the levels of the cognate proteins.

For this purpose, I initially tested two antibodies, one against L2HGDH (#PA5-104318) and one against D2HGDH (#PA5-100063, Invitrogen) on protein lysates form the myocardium of *Mlp*$^{-/-}$ mice, and a protein lysate prepared from plain NRCMs, before testing them on precious lysates prepared from ShRNA-transduced cells. The expected Mw for the two alternatively spliced isoforms of L2hgdh is 50 kDa and 48 kDa, respectively. L2hgdh can also appear at ~45 kDa due to the cleavage of a 51aa mitochondrial-targeting transit peptide, while the expected and observed Mw of D2hgdh is 56 kDa.

The results of Western blotting indicated that the antibody against D2hgdh appeared to detect a band around 56 kDa (*i.e.*, the expected size) in both lysates prepared from murine heart and NRCMs (**Figure 28A**, right panel). While the antibody against L2hgdh detected 4 bands, two of them (bands 2 and 3 in **Figure 28A** left panel) appeared to be close to the expected molecular weight of L2hgdh ~45 kDa, and even band 2 seemed to have less intensity in those lysates prepared from *Mlp*$^{-/-}$ in comparison to those prepared from the WT littermate controls (**Figure 28A**), which agreed with the RNA-seq data obtained from those hearts.

However, previously published Western blotting results of L2hgdh from several organs of *L2hgdh*$^{-/-}$ mice (except the heart) shows the presence of several unspecific bands for L2hgdh, some of them even close to the predicted Mw of L2hgdh (Ma et al., 2017). Therefore, it was not possible to conclude that observed band 2 in my blot (**Figure 28A**) was indeed L2hgdh. Moreover, band 2 did not appear to be exactly 45 kDa, although it was close. Therefore, I thought to validate whether band number 2 corresponds to L2hgdh by testing same cardiac lysates with a new antibody against L2hgdh, which was used by Ma *et al.* (i.e., 15707-1-AP from Proteintech).

Surprisingly, blotting with the new antibody from Proteintech against L2hgdh gave a different pattern of bands to those previously obtained with the antibody from ThermoFisher, where the suspected band 2 in the previous blotting in (**Figure 28A** left panel), did not appear to be present when blotting with the antibody from Proteintech (**Figure 28B**). However, bands 3 and 4 seemed to appear in both blots.

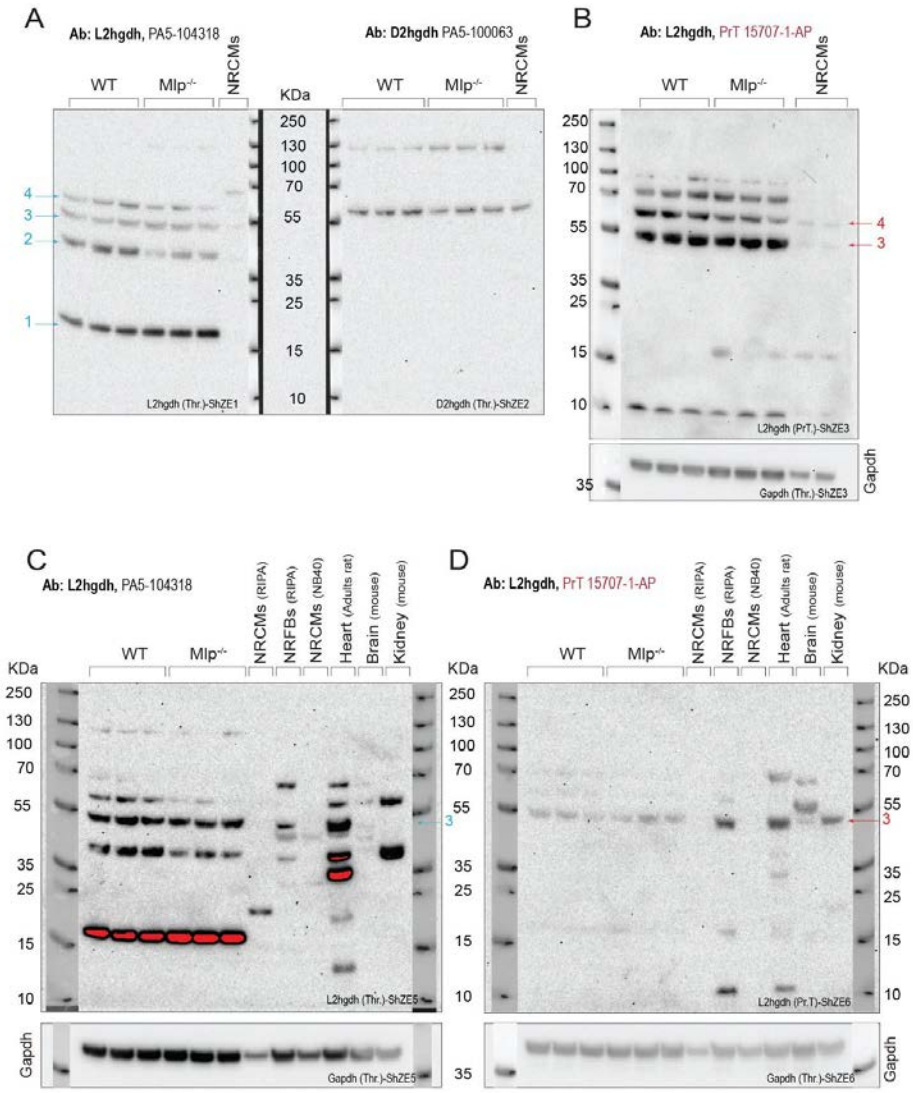

Figure 28: Optimizing Western blotting of L2hgdh and D2hgdh

Thr. :ThermoFisher scientific. PrT: Proteintech.

Therefore, I consulted with the technical support of Proteintech (they have an excellent customer support), and their recommendations were to try incubating the membrane with a higher concentration of their antibody, but at room temperature instead of 4°C, and for only 1-2 h to minimize unspecific bindings (my own initial thought was that incubation overnight at 4°C would minimize unspecific bindings). I tested that, and additionally included lysates from different murine and rat organs to compare the pattern of different bands to those published by Ma *et al.*, in *L2hgdh*$^{-/-}$ mice (Ma et al., 2017) (**Figure 28C and D**).

Most of the bands seen when blotting with the antibody from Proteintech against L2hgdh (**Figure 28B**), got fainter when the membrane was blotted for a short period at room temperature, except band 3. Therefore, this band 3 most likely corresponded to L2hgdh as it appeared in all investigated tissues that were blotted with the antibody from Proteintech (**Figure 28D**).

The most surprising finding here was that band 3 appeared to be absent in the protein lysate from kidney when blotted with the antibody from Thermo Fisher (blue arrow), but not when blotted with the antibody from Proteintech (red arrow) (**Figure 28C and D**), despite that the Mw of both bands (blue and red arrows) appeared identical. Therefore, it appeared as if L2hgdh antibody from ThermoFisher was probably detecting a different protein than L2hgdh, but of same size.

Before proceeding with testing the expression of L2hgdh in transduced NRCMs with ShRNA against *L2hgdh* with the antibody from Proteintech, I also wished to try to enhance the signal of the band obtained with NRCMs through modifications of the lysis buffer. After multiple optimizations, the signal improved substantially when NRCMs were lysed with NB-40 buffer accompanied with multiple cycles of freezing and thawing to break cellular membranes, and with subsequent exposure of the blotted membrane for UV light (up to an hour) when imaging the chemiluminescence signal.

I then used the above optimized conditions to test L2hgdh levels, utilizing the antibody from Proteintech, after knocking down L2hgdh with shRNA. The results showed a gradual downregulation of L2hgdh with increasing shRNA transduction, while no downregulation of L2hgdh was observed when D2hgdh was knocked down (**Figure 29A**).

Coming back to the D2hgdh antibody from Thermo Fisher, which initially gave a band at the expected size ~ 56 kDa (**Figure 28A** right panel), I incubated the same membrane utilized in **Figure 29A** with this antibody after stripping L2hgdh antibodies. Surprisingly however, blotting with PA5-100063 antibody (Thermo Fisher) supposed to be specific for D2hgdh showed downregulation of bands in cells transduced with ShRNA against L2hgdh, but not with ShRNA against D2hgdh (**Figure 29B**). The pattern of the decrease in the bands' intensity upon increasing viral titrations appeared to be very similar to the one obtained when using the antibody against L2hgdh (**Figure 29A**). However, these bands did not have the same Mw, as the band appeared below the 55 kDa marker when blotting for L2hgdh, while above when blotting for D2hgdh. The only reasonable explanation for this is that PA5-100063 D2hgdh

antibody (Thermo Fisher) probably recognizes a different isoform of L2hgdh, not D2hgdh, for an unknown reason.

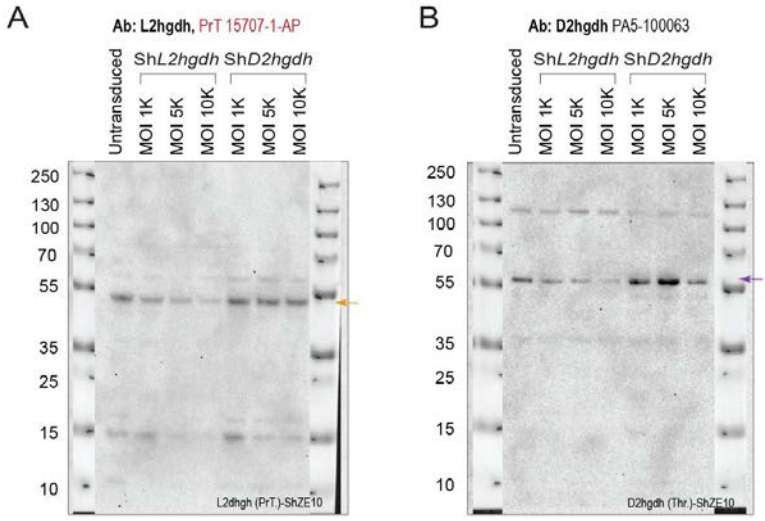

Figure 29: Testing optimized antibodies for Western blotting of L2hgdh and D2hgdh in NRCMs transduced with ShRNA

Thr. :ThermoFisher scientific. PrT: Proteintech.

However, in the analyzed batch of NRCMs (**Figure 29A** last three lanes) exposed to ShRNA against *D2hgdh*, I only reached 20% knockdown of the mRNA level using the highest MOI titer. Therefore, I subsequently designed new ShRNAs against *D2hgdh* which could achieve ~70% knockdown of D2hgdh. Despite this, western blotting for D2hgdh using the PA5-100063 antibody with the new batch of transduced NRCMs did not show any downregulation of D2hgdh.

I thought that these data provided enough evidence for something wrong with PA5-100063 antibody against D2hgdh, and that it would consequently not be worth doing further optimization work or seeking help from Thermo Fisher. I therefore decided to instead try another antibody from a different company (Proteintech) against D2hgdh (13895-1-AP). This antibody was previously utilized by Lin et al (Lin et al., 2015). Nevertheless, utilizing this antibody did not either give any specific bands for D2hgdh that could appear to be getting downregulated in NRCMs transduced with ShRNA against D2hgdh when the viral titrations were increased (Data not shown).

However, the full images of Western blotting's membranes, provided by Lin *et al*. in their supplementary data, revealed that 13895-1-AP antibody (Proteintech) detects a very highly

expressed but unspecific protein located above the specific band for D2hgdh, however, with a very close molecular weight to D2hgdh (Lin et al., 2015). Lin et al used a different composition of gel and running buffer than the ones I used, which helped them to clearly resolve these two bands. I tried to instead mask the position of this prominent unspecific band on the membrane with an aluminum foil to block its interference with the chemiluminescent signal, which finally enabled me to detect a lower Mw adjacent band that appeared to have substantially less intensity in cells transduced with shRNA against D2hgdh (**Figure 30**). However, subsequent quantifications of these bands' intensities were not feasible due to the high interference in the background from the signal of the masked unspecific upper bands. Nevertheless, at the same time, I was able also to measure D2HG levels in these cells by a targeted mass spectrometric approach, which confirmed that it was induced (Elbeck et al., 2022). Therefore, I thought that this proof was enough for my purpose, and there was no need for any further optimizations.

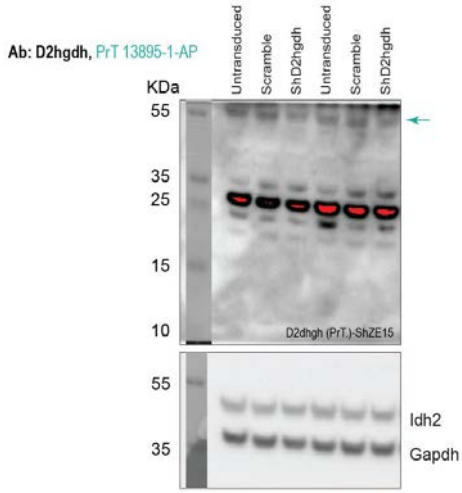

Figure 30: Testing optimized antibodies for Western blotting for D2hgdh in NRCMs transduced with ShRNA
PrT: Proteintech. The upper part of the membrane was not cut, but it was masked during the imaging of the chemiluminescence signal to reduce the background signal of an upper unspecific band.

Therefore, to conclude this case, none of the identified bands for L2hgdh and D2hgdh in the initial Wester blotting results presented in figure 28A, seemed to be identical to what had been reported earlier. However, I am careful to not overinterpret and conclude that all bands in **Figure 28A** originated from unspecific binding of the antibodies, as this statement would require mass spectrometric analysis for proof, which was out of scope in this study. Instead, I wish to emphasize the importance of validating all antibodies utilized for Western blotting. This case was not about bad luck in a singular case, as I have had similar experiences with many other antibodies from different companies. It boils down to is all about a very common

thing in molecular biology, which might probably explain a huge proportion of irreproducibility of published materials (Baker, 2015).

4.4 Cell transfection and transduction

Knocking down or knocking in protein-coding nucleic acid sequences are basic molecular tools for studying molecular functions of proteins or their associated metabolites. Cardiomyocytes are usually difficult cells to transfect or transduce as they do not divide.

In some experiments, where we did not need to study the protein or miRNA in their specific cellular context, we instead utilized other cell types that were easier to transfect. However, in most studies, we wanted to study the biological impacts of a specific protein or metabolite in cardiomyocytes, and therefore we had to utilize primary neonatal cardiomyocytes. Transducing cardiomyocytes is usually much more efficient than transfecting them, but the former requires stricter procedures and permissions to work with viruses.

I was able to further increase the efficiency of transducing NRCMs by keeping the viruses in the culture media for several days. Moreover, I aimed to culture NRCMs for a long period after the transfection, as I wanted to *in vitro* mimic the state of chronic diseases, which are usually associated with chronic alterations in molecular mechanisms. With some optimization to the culturing medium and surface, I was able to keep NRCMs healthy for over a week.

4.4.1 Analyses of metabolites

My initial trials for extracting mitochondrial metabolites from NRCMs with a conventional method of extraction did not yield detectable levels upon targeted mass spectrometric analysis. However, a tiny modification in the extraction method improved it substantially. The usual extraction solution utilizes 80% aqueous methanol, which precipitates proteins, and thus probably traps metabolites within aggregates of mitochondrial proteins. However, lysing the cells in pure water by repeated thawing and freezing cycles, and then subsequently adding the methanol improved the yield substantially.

4.5 Characterization of mitochondrial structure and function

4.5.1 Mitochondria isolation

During the preparations for our recent work (Elbeck et al., 2022), qPCR, RNA seq and Western blotting of Idh2 indicated that there were small differences in its expression level in the myocardium of *Mlp*$^{-/-}$ in comparison to their littermate control. Therefore, I thought that I would

need to have a high *n* number of animals to be able to show a reliable trend of dysregulation of Idh2 activity.

Available published methods for isolating mitochondria required fresh tissues for the isolation. I tried them and found it very laborious to isolate cardiac mitochondria from more than five animals per day. Moreover, I did not have the proper equipment to handle higher number of samples with huge amounts of tissues (like whole heart). Therefore, I thought to develop a reproducible method to isolate mitochondria from low amounts of frozen cardiac tissues.

I had access to TissueLyser (Qiagen), which had however not been used before for isolating mitochondria. However, TissueLyser can homogenize a high number of samples simultaneously. After extensive optimizations, and through utilizing a combination of different sizes of metallic balls (instead of conventionally utilized glass pestles) with multiple dissociation times and frequencies of vibration, I was finally able to isolate a mitochondrial fraction with a good quality and high purity. Although, the yielded amounts were low, they were enough for measurement of Idh2 activity. I also had to optimize the measurement procedure to adapt it from the conventional used spectrometric cuvettes to wells of a specific 384-well plate, and hence I could use less amounts of mitochondria and simultaneously measure large numbers of samples with several technical replicates.

It is worth to mention here, that the isolated mitochondria that I got with the above-described method were mostly subsarcolemmal. There are several studies showing that there are substantial differences in the characteristic and functions between the two subtypes of mitochondria in the heart and in skeletal muscles (*i.e.*, subsarcolemmal and interfibrillar mitochondria, **Figure 2**) (Palmer et al., 1977). Therefore, I thought that it would be important to characterize Idh2 activity in the interfibrillar mitochondria as well. However, isolation of interfibrillar mitochondrial fraction requires treatment with a protease (Nagarse) to break the myofibers and release the mitochondria; a process that was not easy to optimize within the above-described method but would be interesting to optimize for future work.

4.5.2 Transmission electron microscopy (TEM)

TEM represents a method for ultrastructural morphological analysis. Hence it is applicable to the study of mitochondrial structures and their potential alterations in diseases. The method depends on ultrasectioning of investigated tissues, which is slow and has low throughput and therefore makes it difficult to observe small differences with sufficient reproducibility. A testimony to these problems is the extremely low number of publications that describe alterations in mitochondrial structure associated with cardiomyopathies.

Moreover, recent research shows that mitochondria are organized in tubular network, the structure of which is not possible to observe by TEM sectioning. It requires a 3D-ultra-high resolution florescence microscopy such as STED, accompanied by tissue-clearing technology. Even so, cardiomyocytes are densely packed with mitochondria, which make them more difficult to study also with this technology in comparison to other cells and tissues.

4.6 Florescence microscopy

Florescence microscopy represents a useful tool to evaluate the transfection/transduction efficiency, and to study the localization of different proteins by immunofluorescence staining. The latter, and especially for low expressed proteins, requires higher resolution than many other applications. During my work on the third project, I first had access to a Zeiss microscope that utilizes Airyscan for super-resolution microscopy (a technique that enable resolving objects smaller than the diffraction limit of light), and later to a Leica microscope that utilizes mathematical deconvolution to achieve super-resolution. Both microscopes have extremely good features, but for my project purpose, where I was most interest in the resolution, I found that Airyscan was probably better, as it provides real optical resolution, as opposed to deconvolution, which is based on approximation and mathematical equations which is less transparent to users without specialized knowledge.

5 RESULTS AND DISCUSSION

5.1 STUDY I: PROTECTIVE ANTIOXIDATIVE MECHANISMS AND REVERSED REMODELING OF HEART FAILURE:

5.1.1 Background:

Heart failure is a major cause of morbidity and mortality worldwide (World Health Organization (WHO, 2019)). HF is a complex clinical syndrome with high etiological and clinical heterogeneity associated with a variety of comorbidities. Oxidative stress and imbalance of myocardial substrate metabolism are common features of HF (Bertero and Maack, 2018). However, several approaches aiming to ameliorate oxidative stress in heart failure could not achieve clinical success, despite the promising results from the pre-clinical stages (van der Pol et al., 2019; Zhou and Tian, 2018). One explanation could be that excessive quenching of physiological levels of reactive oxygen species (ROS), which act as cellular signaling molecules, might lead to adverse effects (Santos et al., 2011; Song et al., 2014). In our recent work (Elbeck et al., 2022), we highlighted that the potency of the endogenous antioxidative capacity could be a possible contributing factor for the failure of clinical trials, a concept that has not received much attention before.

5.1.2 An epigenetic circuit links mitochondrial redox homeostasis and cardiac function

In our recent work (Elbeck et al., 2022), we unveiled that mitochondrial isocitrate dehydrogenase 2 (IDH2) governs an extensive regulatory mechanism in cardiac mitochondria. We showed that IDH2 coordinates other antioxidative elements such as NRF2 through a feedforward cycle involving 2-oxoglutarate (2OG) and L2-hydroxyglutarate (L2HG) (**Figure I-1**).

We observed that IDH2 expression is significantly downregulated in the myocardia of patients with eccentric dilated cardiomyopathy (DCM) and in *Mlp*$^{-/-}$, a murine model of DCM. We also found that neonatal rat cardiomyocytes exposed to pro-oxidants exhibited downregulation in *Idh2* in a dose and time-dependent manner. These observations were at first puzzling, as it was unclear how a downregulation of an essential component of the antioxidative defense would counteract oxidative stress. However, we subsequently demonstrated that the downregulation of IDH2 observed in the cardiac muscles was actually accompanied by an increase in its enzymatic activity due to post-translational modifications associated, a mechanism preventing overwhelming the cell with antioxidants, while adequately mitigating oxidative stress.

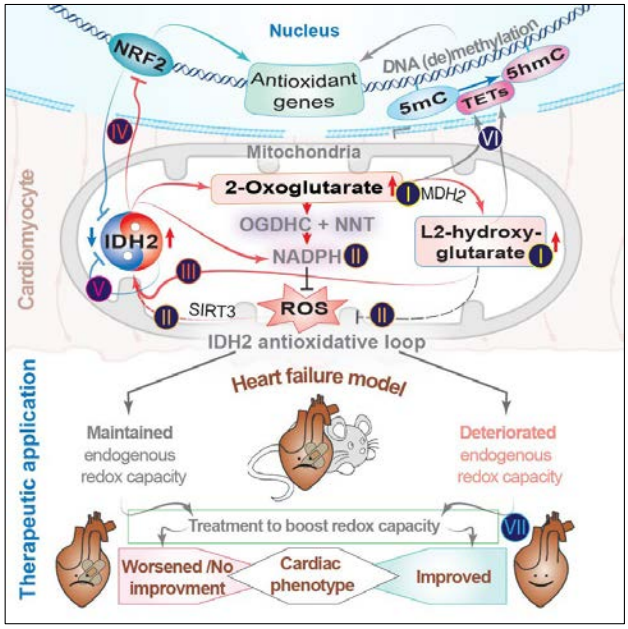

Figure I-1: A Graphical summary over the proposed novel molecular mechanism in Elbeck *et al*. (Elbeck et al., 2022)
The numbers in Latin indicate the bullet points described in the main text below.

The antioxidative feedforward loop described in Elbeck *et al.* can be summarized in the following bullet-points, indicated by a Latin number that is depicted in (**Figure I-1**):

I[1]**-** L2HG is produced from 2OG when there are elevated concentrations of 2OG. L2HG/2OG forms a redox couple that mitigates oxidative damage (Intlekofer et al., 2017; Oldham et al., 2015; Wise et al., 2011). We observed increased levels of L2HG and 2OG in the myocardia of *Mlp*$^{-/-}$ mice.

II[1]**-** In cardiac myocytes, IDH2 is the main enzyme to regenerate mitochondrial NADPH, which is required for the enzymatic elimination of H_2O_2 (Nickel et al., 2015; Wagner et al., 2020). ROS, in its turn, induces the activation of IDH2 through desuccinylation (Zhou et al., 2016). We showed that IDH2 is desuccinylated in the myocardium of patients with DCM.

[1] *The data presented in **I** & **II** form a cycle (IDH2-2OG-L2HG-ROS) to mitigate oxidative stress.*

III [2]- We demonstrated that L2HG induces the expression of IDH2, and the activation of proteins involved in counteracting oxidative stress.

IV[2]- The activities of IDH2 and NRF2 are mutually interconnected in cardiomyocytes: inducing one represses the activity of the other—a mechanism that prevents overwhelming the cell with antioxidants. [3]

V[2]- The activity of IDH2 is modulated by the antioxidative status of the cell through modulating its expression and posttranslational modifications. We found that increasing the antioxidative capacity induces *IDH2* downregulation as a negative feedback loop.

VI[2]- The ratio 2OG/L2HG is a potent modulator of TET1-3 enzymatic activities (Xu, Yang et al. 2011). We found that the antioxidative feedforward loop modulates the activity of TETs and subsequently the epigenetic landscape, and particularly antioxidative genes including *IDH2*.

VII- We next explored the possible implications of these findings for the treatment of patients with heart failure, taking into consideration previously failed clinical trials that aimed to ameliorate oxidative stress associated with heart failure. We first demonstrated that there are differences in the antioxidative defense between males and females, with females having more robust antioxidative defense system. A phenomenon that was even reflected on the phenotype of heart failure, with female having less severe DCM than males. We next employed this sex difference to test our hypothesis, through utilizing a novel molecule (AZ925) to activate the NRF2 pathway. We concluded that boosting antioxidative capacity – only when endogenous one is deteriorated - improves cardiac function, highlighting new utilities in precision medicine.

5.1.3 Potential protective redox mechanisms in human DCM patients:

In our work in Elbeck et al 2022, we highlighted that left ventricular (LV) myocardium of patients with end-stage DCM shares some signatures of differentially expressed genes related to mitochondrial function and oxidative phosphorylation with *Mlp*$^{-/-}$ (figures 1A and 1B in Elbeck et al., 2022).

However, hearts of patients with end-stage DCM and *Mlp*$^{-/-}$ differ substantially in the magnitude of severity and in the stage of progression toward heart failure. Human DCM have more severe phenotype than *Mlp*$^{-/-}$, as *Mlp*$^{-/-}$ mice usually have a survival rate similar to that of

[2] *The data presented in III-VI indicates a regulatory role for the cycle (IDH2-2OG-L2HG-ROS), mutually regulating the antioxidative defense in the cardiomyocytes, together with other antioxidative elements.*

WT littermate controls, while human DCM samples were explanted from patients who were already in their final stage of heart failure and needed to undergo heart transplant.

A very clear difference in gene signature can be spotted in (Figure 1E in Elbeck et al., 2022) between human DCM patients and *Mlp*$^{-/-}$ in the opposite expression trend of oxoglutarate dehydrogenase like (*OGDHL*). It is upregulated in human DCM, while it is downregulated in *Mlp*$^{-/-}$, while its paralog *OGDH* is downregulated in both data sets (**Figure I-2**).

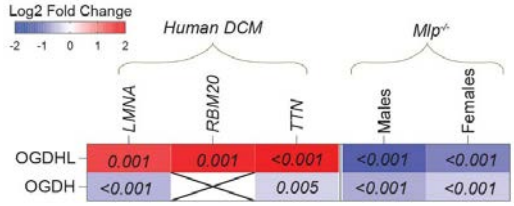

Figure I-2: Expression of *OGDHL* and *OGDH* in the myocardium of patients with DCM and in *Mlp*$^{-/-}$
The expression was assessed by RNA sequencing. The human data set is a published transcriptomic data from left ventricular (LV) myocardium of patients with end-stage heart failure with characterized mutations in *LMNA*, *RBM20* and *TTN* (Sielemann et al., 2020). Transcriptomic data of *Mlp*$^{-/-}$ is obtained from (Elbeck *et. al.,* 2022). Numbers in italic inside the boxes indicate *p*-values.

OGDHL is a component of the 2-oxoglutarate dehydrogenase complex (OGDHC) and shares high similarity (85%) to OGDH (Bunik and Degtyarev, 2008). The exact difference in the function between OGDH and OGDHL is still unknown. However, knocking down OGDHL was found to enhance cancer cell survival through increasing the antioxidative capacity, whereas overexpressing it increased ROS generation and apoptosis (Dai et al., 2020; Sen et al., 2012). Thus, the downregulation of *Ogdhl* observed in *Mlp*$^{-/-}$ may indicate a defense mechanism aiming to increase the antioxidative capacity, while the upregulation of *OGDHL* observed in the human samples may reflect a more severe stage of DCM in the human patient than *Mlp*$^{-/-}$, and it may appear as a deleterious mechanism. However, upregulating *OGDHL* may actually be a maladaptive mechanism trying to recover part of the impaired oxidative metabolism of the TCA cycle in heart failure, but probably at the expense of increased ROS generation, similar to what has been observed in cancer cells (Dai et al., 2020).

To try to elucidate general differences in gene signatures between human end-stage DCM and *Mlp*$^{-/-}$, I intersected the transcriptomic data sets from left ventricle myocardium of *Mlp*$^{-/-}$ and patients with end-stage DCM harboring mutations in *LMNA*, *RBM20* or *TTN*, as it is shown in figure (**Figure I-3**)

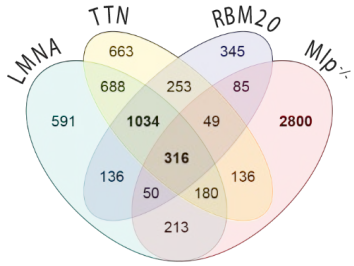

Figure I-3: Venn diagram of intersected differentially expressed genes in heart failure

The expression was assessed in the LV myocardium of patients with DCM and *Mlp*$^{-/-}$ through RNA sequencing. The human data set is obtained from published transcriptomic data (Sielemann et al., 2020). Transcriptomic data of *Mlp*$^{-/-}$ is obtained from (Elbeck et al., 2022). The number inside each intersection indicates the number of differentially expressed genes (DEGs) shared between the data sets forming this intersection. The numbers highlighted in Bold indicate the three unique intersections that I will focus on in my subsequent analysis in figure I-4. The transcriptomic data set of *Mlp*$^{-/-}$ was a merged data set of males and females. Only DEGs with $p<0.05$ and adjusted p-value < 0.01 were included in this analysis.

In order to elucidate the molecular pathways underlying each distinct intersection, I performed IPA comparative analysis, where I only focused on three distinct intersections (**Figure I-4**):

- Genes that are uniquely dysregulated in the DCM patients regardless the mutation (**1,034 DEGs**): This would represent a list of distinct genes representative for human patients with end-stage genetic DCM.
- Genes that are uniquely dysregulated in *Mlp*$^{-/-}$ (**2,800 DEGs**)
- Genes that are commonly dysregulated among all four data sets investigated (**316 DEGs**): This list would highlight DEGs that are unique to genetic DCM regardless the disease stage.

Subsequent ingenuity pathway analysis (IPA) of shared and distinct genetic expression revealed that shared signatures of genetic DCM in both human and murine model encoded for proteins involved in pathways related to mitochondrial function (**Figure I-4** upper panel), supporting our previous observations in Elbeck *et al.* 2022. Whereas genes that were either uniquely dysregulated in DCM patients or in *Mlp*$^{-/-}$ encoded proteins involved in multiple pathways with opposite activation trends (**Figure I-4** lower panel), such as EIF2 signaling, TGF-β signaling, autophagy and unfolded protein response.

Pathways including EIF2 signaling, autophagy and unfolded protein response are linked to endoplasmic reticulum (ER) stress and protein misfolding, which are processes strongly related to heart failure and oxidative stress. Misfolded proteins accumulate in the ER lumen upon aberrant regulation of calcium homeostasis and oxidative stress, which induces ER stress. Thereafter, ER stress activates unfolded protein response in an attempt to recover normal ER function (Minamino and Kitakaze, 2010). Although this process seems to give the cell a chance

to repair the damage, severe or chronic stress would induce autophagy to remove damaged proteins or organelles, and ultimately induce apoptosis to eliminate the damaged cells (Sozen et al., 2015).

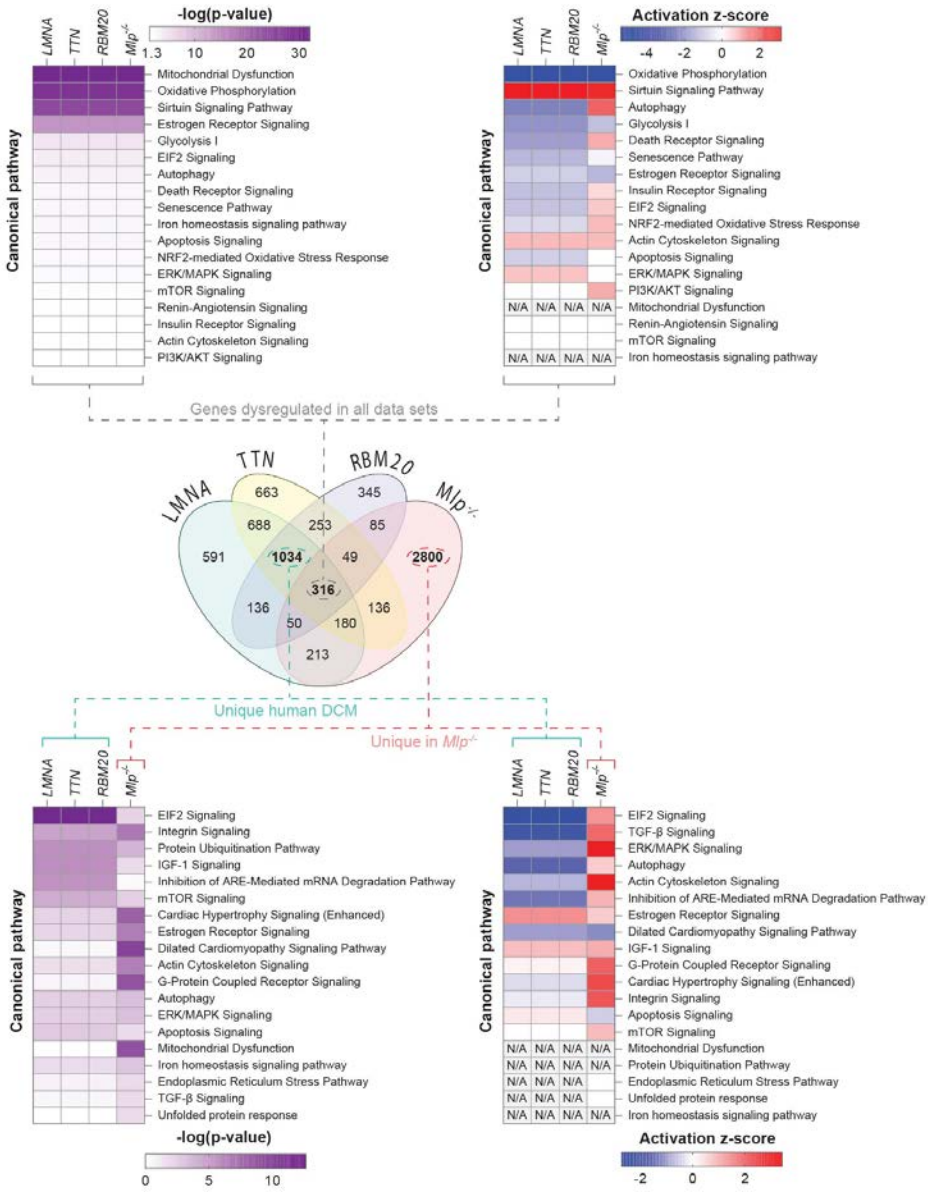

Figure I-4: IPA enrichment analysis of distinct transcriptomic intersections between patients with DCM and *Mlp*$^{-/-}$

Selected pathways from IPA enrichment analysis on DEGs that were included in the intersections analysis among patients with DCM (Sielemann et al., 2020) and *Mlp*$^{-/-}$ (Elbeck et al., 2022). The intersection analysis was described in Figure I-3.

Intriguingly, I observed that RNAs encoding proteins involved in pathways related to ER stress and autophagy were inactivated in the human patients with end-stage DCM (**Figure I-4** lower panel). Moreover, the subsequently triggered unfolded protein response did not seem to be significantly enriched or even have any activation trend in these patients with DCM, confirming the observation about inactivating pathways related to ER stress and autophagy (**Figure I-4** lower panel). In contrast, these pathways had the opposite trend in *Mlp*$^{-/-}$ and were strongly activated.

The inactivation of these crucial pathways related to ER stress and autophagy in the patients with DCM made me wonder about the underlying reason. My hypothesis is that the myocardium, and even under DCM, may still have an adequate capacity of endogenous antioxidative defense system to handle deleterious excessive oxidative stress, as a part of the mechanism trying to recover part of the impaired oxidative metabolism.

In support of this scenario, RNAs encoding proteins involved in pathway related to NRF2-mediated oxidative stress response appeared to be deactivated in the transcriptomic data of end-stage human DCM samples (**Figure I-4** upper panels). The latter is further supported by a previous study indicating that left ventricle myocardium of patients with idiopathic DCM do not show elevated activity or expression of intracellular enzymes involved in the elimination of ROS (Baumer et al., 2000). This was also supported by our observation that *HMOX1*, a downstream target gene for NRF2, was significantly down-regulated in patients with end-stage human DCM with mutations in TTN and RBM20 (**Figure I-5**) resembling the expression trend of *Hmox1* in neonatal rat cardiomyocytes exposed to the antioxidant NAC (**Figure 4B** in Elbeck *et al.*, 2022). These observations support a notion that the heart, even under end-stage DCM, may still have an adequate antioxidative system under resting conditions.

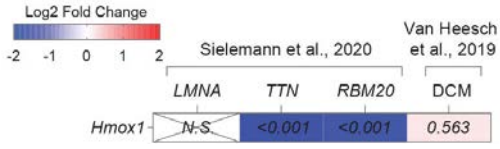

Figure I-5: Expression of *HMOX1* in the myocardium of DCM patients

The expression of *HMOX1* were assessed by analyzing published transcriptomic data from left ventricular (LV) myocardium of patients with end-stage heart failure (Sielemann et al., 2020; van Heesch et al., 2019).

However, if oxidative damage would occur, then it would require extreme oxidative condition, such as perfusing the heart with cumene hydroperoxide (Janssen et al., 1993). The latter would occur only when the endogenous scavenging system of the heart cannot cope with the amounts of free radical generated. Even experimental ischemic reperfusion of hearts is not enough to

induce such condition or to cause the accumulation of detectable levels of lipid peroxidation (Janssen et al., 1993). The presence of reduced cellular GSH at extremely high levels is for a reason, *i.e.*, to protect the heart from oxidative injuries under extreme work overload conditions. Nevertheless, I believe that transient and localized oxidative damage would still occur in heart failures, when excessive ROS generated under extreme work overload and myocardial infarction temporarily exceed the capacity of the endogenous antioxidative system in their microenvironment to handle, and therefore might induce a localized damage.

5.1.4 Opposite trends of activation between patients with DCM and *Mlp*$^{-/-}$ may indicate same purpose

As discussed above, ROS in cardiomyocytes is preliminary generated from the mitochondria during ATP regeneration. Cardiomyocytes from both human and mice have very similar mitochondria, but they have substantial differences in the cardiac workload under resting conditions.

The human heart beats ~70 times per minute, while murine heart beats ~300-700 times per minute. The high murine heart rate may therefore appear as an extreme work-overload compared to humans. Moreover, the slower electron flow through the human ETC would imply more potential electron ¨leakage¨ in human ETC compared to mouse. Thus, in addition to some specific adaptations in the human/murine cardiac contracting machinery, it appears as if the human/murine antioxidative systems would need to have unique mechanisms to handle this relative increase in accompanying ROS production in different places. However, humans and mice share high similarity in the majority of translated proteins and biomolecules. Therefore, the same set of proteins may be arranged in unique sets to form pathways with unique functions or adjustments in humans or mice to fit their needs. Hence, opposite trends of activation of the same pathways observed in *Mlp*$^{-/-}$ and human DCM samples (**Figure I-5**) may therefore still actually indicate protective mechanisms in both cases. These insights highlight the caution needed when extrapolated conclusions for mechanisms in human are drawn from data generated in animal models. Different stages of DCM development may also impose different adaptations strategies that enable the cells to survive, albeit at the expense of some optimal functions, which might also explain the different trends of activation of same pathways.

Moreover, reverse remodeling, which we found to improve cardiac function in female *Mlp*$^{-/-}$ mice, has also been reported to improve cardiac function in a subset of human DCM patients (Merlo et al., 2018). Even patients with end-stage DCM were also observed to undergo substantial reverse remodeling associated with improvements in cardiac function upon left

ventricle assist device implant (LVAD) (Ambardekar and Buttrick, 2011; Burkhoff et al., 2021), reducing the deleterious effects of work overload. Interestingly, these observations suggest that the presence of operational cardioprotective mechanisms may be elicited also in end-stage DCM.

In conclusion, potential protective mechanisms, described above, indicate that the heart, even under end stage DCM, possesses several powerful defense mechanisms that do not only ameliorate stress, but also continuously try to repair induced damages. Hence, there is a need to deepen our understanding of the molecular basis of cardiac redox regulation to be able to develop optimal therapeutic strategies for heart failure patients. Furthermore, since the spectrum of heart failure etiologies and phenotypes is diverse and complex (Triposkiadis et al., 2019), a personalized approach may be required to identify the right patients who may benefit from interventions in mitochondrial metabolism and redox regulation. Moreover, antioxidative compounds are not always beneficial substances, as they do basically induce injuries to cardiomyocytes when they are inadequately used (Santos et al., 2011; Song et al., 2014). The latter is also supported by the observation from our recent study where we observed that the antioxidant NAC induced some loss of cardiomyocytes, as inferred from the recovered RNA levels in NAC treated cells (**Figure 4D** in Elbeck et al., 2022). This emphasizes the importance of assessing relevant endogenous protective mechanisms before therapeutical intervention to avoid potential side effects.

5.2 STUDY II: THE ROLE OF CARDIAC MIR-208B IN REGULATING REDOX DEFENSE

5.2.1 Background

Since their discovery in C. elegans, micro-RNAs (miRNA) have emerged as essential post-transcriptional modulators for gene expression and cellular functions. MiRNAs are a family of short non-coding RNAs of ~22 nucleotides, transcribed directly from genes, or derived from introns or long noncoding RNA as primary miRNA (pri-miRNA), and subsequently processed into a precursor miRNA (pre-miRNA), and finally to a mature miRNA (**Figure II-1**). Mature miRNA can arise from the 5′ arm of the pre- miRNA hairpin (termed miRNA-5p) or from the 3′ (termed miRNA-3p). Each miRNA possesses a seed sequence (2^{nd}-8^{th} nucleotides at the 5`end), which has strong complementarity to the miRNA-target site on the 3′-UTR of the targeted mRNA. Mature miRNA is loaded on the AGO complex, and bind to the target site on the 3′-UTR of the mRNA and silence the gene through repressing the translation or inducing mRNA decay (Gebert and MacRae, 2019).

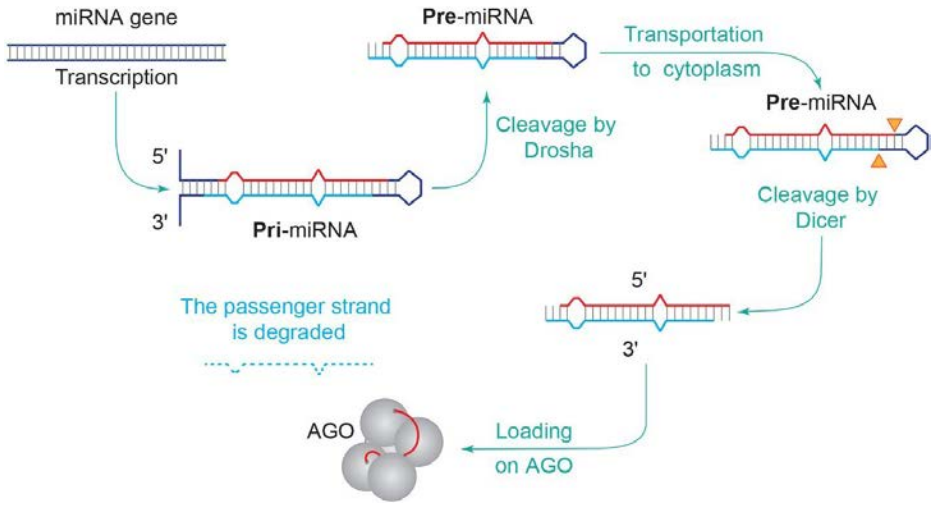

Figure II-1: A cartoon over miRNA biogenesis

The figure was adapted from Gebert *et al.* (Gebert and MacRae, 2019) with modifications.

MiRNAs regulate genes involved in almost all cellular processes and functions, therefore they have emerged as important biomarkers for diagnosis and as targets for therapies. Multiple miRNAs have been implicated to play a role in the development and progression of cardiovascular diseases and heart failure. MyomiRs are a family of miRNAs, which are specific to the muscles. Members of this family, such as miR-208a-3p, miR-208b-3p, miR-499 regulate the antithetical expression of cardiac myosin heavy chain (MHC) genes *MYH6* and *MYH7* (van

Rooij et al., 2009). MHCs are the main components of cardiac contractile machinery. The two isoforms are 93% homologous in their sequence, but MYH6 has substantially higher contractile velocity and actin attachment than MYH7. In heart failure, contraction-relaxation dysfunction is associated with a decrease in the percentage of MYH6 in ventricles from 5-10% to below <2%, which is known as the MHCs switch, or as the fetal gene pattern (Palmer, 2005).

Moreover, miRNAs have been implicated to mutually regulate redox responses. These miRNAs were termed as redoximiRs (Cheng et al., 2013; Fierro-Fernandez et al., 2016). RedoximiRs regulate redox homeostasis by modulating the levels of key cellular redox regulators, such as NRF2, or by modulating the levels of ROS-generating enzymes, such as NOX4. Mutually, miRNA are also themselves regulated by cellular redox state. ROS influences the expression of miRNA by modulating the epigenetic landscape of miRNA genes through histone deacetylases and DNA methyltransferases. ROS even directly impact miRNA biogenesis through affecting the activities of both Dicer and DGCR8/Drosha-complex (Cheng et al., 2013).

Several miRNAs have also been reported to regulate the levels of *IDH2*, a key regulator for the antioxidative defense in cardiomyocytes, such as mi-R183, mi-R144 and miR-1285 (Fu et al., 2014; Liao et al., 2022; Tanaka et al., 2013).

5.2.2 MiR208b-3p is strongly upregulated in DCM

In our recent work (Elbeck et al., 2022), we observed that oxidative stress induces downregulation of IDH2 (**Figure 2E** in Elbeck *et al.*, 2022). To investigate whether the downregulation of IDH2 is mediated by a post-transcriptional microRNA (miRNA) targeting, we profiled miRNA in *Mlp*$^{-/-}$ hearts by small RNA sequencing. However, we did not observe substantial dysregulation in any of the experimentally validated miRNAs targeting *Idh2* (*i.e.*, mi-R183, mi-R144 and miR-1285).

Nevertheless, we identified miR-208b-3p to be strongly elevated (~20-fold) in *Mlp*$^{-/-}$ compared to WT littermate controls (**Figure II-2A and B**). Moreover, we found that the levels of miR208b-3p were strongly negatively correlated ($r = -0.713$, $p < 0.001$) with the left ventricular ejection fraction (LVEF%) in both male and female *Mlp*$^{-/-}$ (**Figure II-2C**), suggesting a link between miR208b-3p and the severity of the cardiac phenotype.

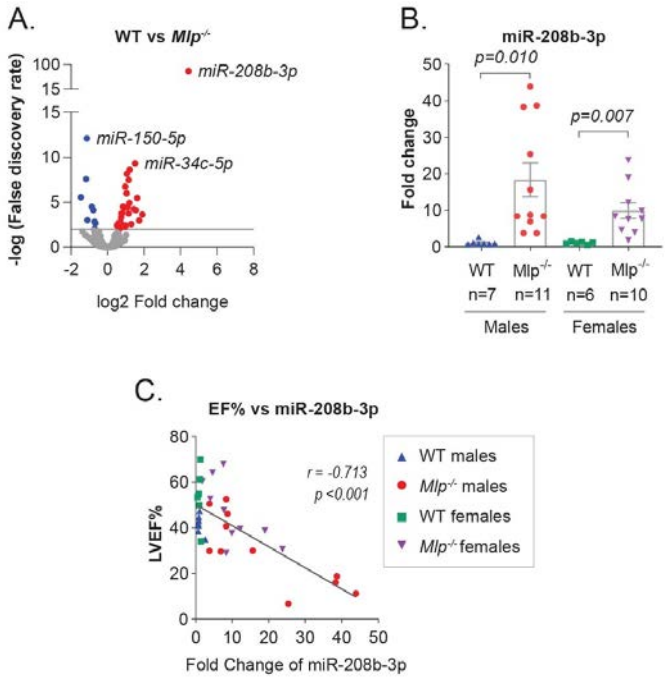

Figure II-2: miR-208b-3p is upregulated in the myocardium of *Mlp*$^{-/-}$

A. Volcano plot of transcriptomic data of small RNA sequencing on cardiac tissues from *Mlp*$^{-/-}$ (males, 12 weeks old, n=3). **B.** qPCR analysis of miR-208b-3p expression in LV myocardium of *Mlp*$^{-/-}$ males and females (12 weeks old). The fold change was normalized to the levels in the WT littermate controls. Bars are the mean values ±SEM with unpaired two-tailed *t*-test. **C.** Person correlation between the left ventricle ejection fraction (LVEF%) and the corresponding levels of miR-208b-3p in the LV myocardium of WT and *Mlp*$^{-/-}$, estimated by qPCR analysis.

In contrast, miR208b-**5p** originating from the 5p-arm of same pre-miR208b showed very low expression. It was upregulated in *Mlp*$^{-/-}$ (**Figure II-3**) but to a much lesser extent than miR-208b-**3p**. The low number of reads of miR-208b-**5p** *vs.* miR-208b-**3p** (≈10 reads *vs*. ≈20,000) suggests that miR208b-**5p** does not have a functional role beyond being a passenger strand with expected degradation when miR-208b-3p gets loaded onto the AGO complex (**Figure II-3**).

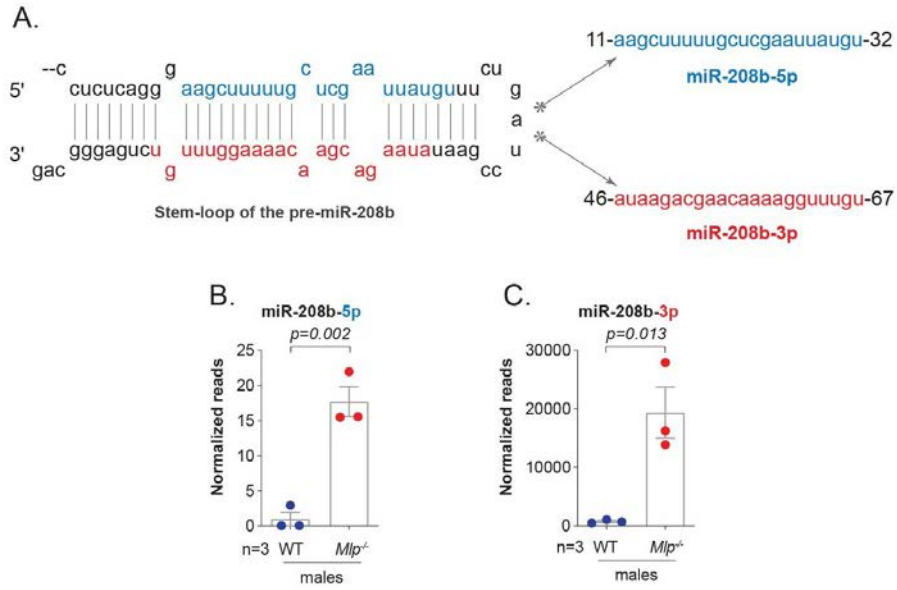

Figure II-3: A comparison between the expression of the 3p and 5p arms of the pre-miR-208b in *Mlp*$^{-/-}$

A. The sequence of the stem loop of pre-miR-208b, and its 5p and 3p mature miRNAs. The sequences are obtained from miRbase (Accession ID MI0005552). **B** and **C.** The expression of miR-208b-5p and miR-208-3p in the myocardium of *Mlp*$^{-/-}$ estimated by small RNA sequencing (males, 12 weeks old). Bars are the mean values ±SEM with unpaired two-tailed *t*-test.

5.2.3 The role of MiR208b-3p in cardiac reverse remodeling

MiR208b-3p is a cardiac specific microRNA, transcribed from an intronic region of *MYH7*, and has an identical seed-sequence to miR208a-3p that is transcribed from an intronic region of *MYH6*. Both microRNAs regulate myosin heavy chains expression under heart failure (van Rooij et al., 2009). MiR208b and miR208a are elevated in cardiac DCM patients, and their levels were found to be reduced in patients who respond to β-blocker treatment and undergo reverse remodeling associated with improved cardiac function (Sucharov et al., 2017). However, miR-208a levels, but not miR-208b, were positively correlated with both fibrosis and poor clinical outcome of the DCM (Satoh et al., 2010), suggesting a potential protective role for miR-208**b**-3p, but not for miR-208**a**-3p. This potentially different roles of these two miRNAs with identical seed sequence but difference in their 3´ side is supported by recent observations that miRNAs with identical seed sequences can be directed to different target sites based on the contribution from the 3´ half of the miRNA also (Broughton et al., 2016; Gebert and MacRae, 2019; Moore et al., 2015).

Nevertheless, a recent study showed that *in vivo* knocking down of miR-208b-3p ameliorated the progression of fibrosis associated with hypertrophic response in a DCM model induced by angiotensin-II treatment of heterozygous (HET) knock-in mice of *Ttn* with the insertion

mutation (c. 43628insAT) (I will use the abbreviation AngII-*Ttn*$^{mut/+}$ to refer to this murine model in my subsequent texts). Moreover, miR208b-3p knockdown prevented the hypertrophic progression toward DCM in these mice (Zhou et al., 2017).

These conflicting data between the potential protective observations in human DCM patients, the deleterious effect in the study utilizing AngII-*Ttn*$^{mut/+}$ mice, and the high expression of miR208b-3p in *Mlp*$^{-/-}$ mice makes the role of miR-208b-3p in cardiac pathology unclear. We therefore sought to investigate its function in heart failure through knocking down its elevated levels in *Mlp*$^{-/-}$ *in vivo*.

For this purpose, we treated *Mlp*$^{-/-}$ males with LNA-modified miR208b-antagomirs for 4 doses under one month (**Figure II-4A**) and led to more than 70% reduction in the levels of miR208b-3p at the end of the study (**Figure II-4B**). Nevertheless, despite this significant reduction in miR208b-3p levels, we did not observe changes in the cardiac function, or left ventricle diameter or wall thickness (**Figure II-4C and D**). However, anti-miR-208b-3p treatment induced a significant downregulation of *Myh7* expression, but no change in *Myh6* expression (**Figure II-4E and F**).

I attributed the discrepancy between our results and those reported by Zhou *et al.*, 2017 upon miR-208b-3p knockdown to multiple factors. In fact, the two mouse models utilized in the two studies have substantial differences in the DCM phenotype. Both *Mlp*$^{-/-}$ and AngII-*Ttn*$^{mut/+}$ mice develop a DCM phenotype associated with eccentric hypertrophy, in which there is an increase in left ventricle diameter, associated with an increase in the left ventricle cavity volume. However, *Mlp*$^{-/-}$ shows more pronounced dilation and a lower ejection fraction than AngII-*Ttn*$^{mut/+}$ (EF: 34% in *Mlp*$^{-/-}$ vs ~50% in AngII-*Ttn*$^{mut/+}$) while the latter shows substantially more fibrosis (~3-4% in *Mlp*$^{-/-}$ vs. ~10-20% in AngII-*Ttn*$^{mut/+}$) (Gramlich et al., 2009; Omens et al., 2002; Yamamoto et al., 2007; Zhou et al., 2017) and (Elbeck et al., 2022)

Fibrosis is associated with the disease severity in DCM. Although it may initially represent a reparative mechanism, excessive fibrosis leads to stiffening of the heart walls, diastolic dysfunction, and eventually heart failure (Eijgenraam et al., 2020). Moreover, as the titin protein, its isoforms, and its post translational modifications are the major determinants of cardiomyocytes stiffening (Herwig et al., 2020), stiffening is further impacted in AngII-*Ttn*$^{mut/+}$ by the presence of a shorter isoform of titin (skipping of exon 236). Heart stiffness greatly impacts cardiac preload and/or afterload, and therefore increases energy demand and ROS generation. Altogether, these observations indicate that the two mouse models are substantially

different in the DCM sub-phenotype, which may explain their different response to miR-208b-3p knockdown.

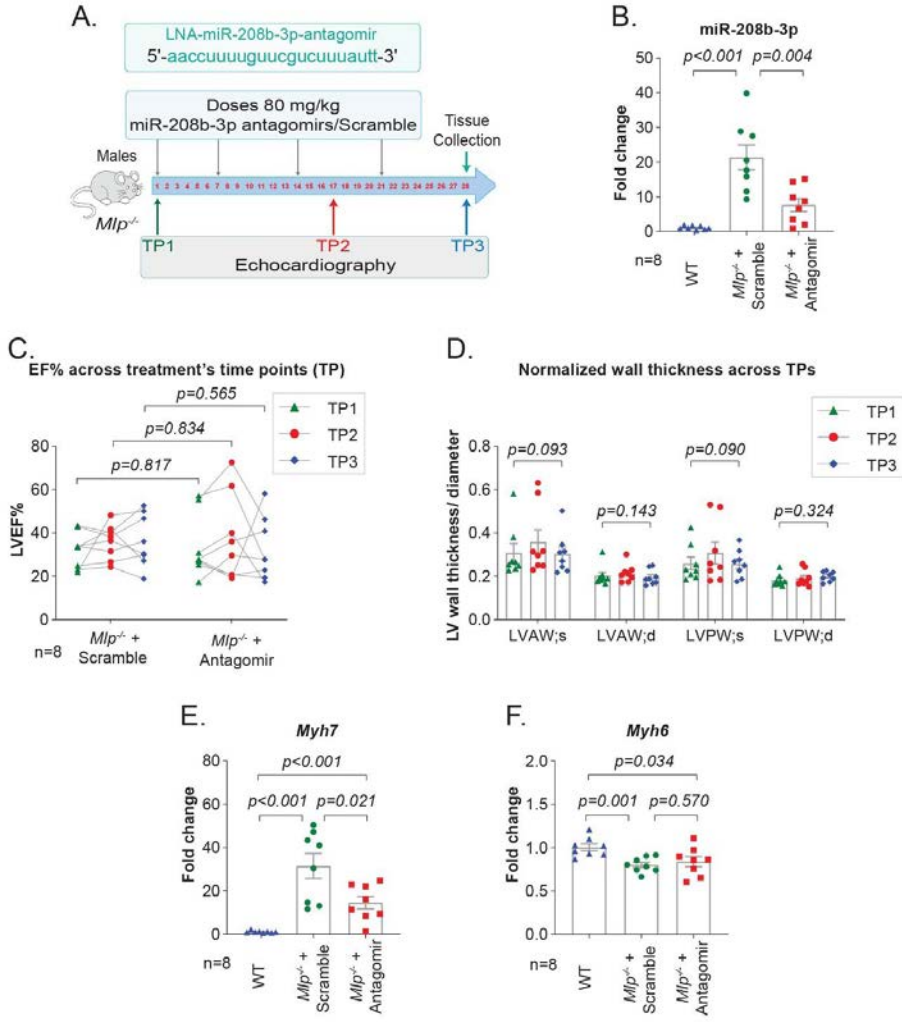

Figure II-4: Treatment of *Mlp*$^{-/-}$ with miR-208b-3p antagomirs

A. A scheme for the experimental settings of in-vivo treatment of *Mlp*$^{-/-}$ with LNA modified antagomirs targeting miR-208-3p. The age of the animals at the study start was 8 weeks. **B.** qPCR analysis of miR-208b-3p expression in LV myocardium of *Mlp*$^{-/-}$ mice treated with miR-208b-3p antagomirs. The fold change was normalized to the levels in untreated WT littermate controls. Bars are the mean values ±SEM with unpaired two-tailed *t*-test. **C.** Changes over time of EF% for individual animals treated with miR-208b-3p antagomirs or scramble control. **D.** Changes over time of LV anterior (LVAW) or posterior (LVPW) wall thickness, normalized to LV diameter, in *Mlp*$^{-/-}$ mice treated with miR-208b-3p antagomirs in systole (s) or diastole (d). The values in **C** and **D** are the mean values ±SEM with paired two-tailed *t*-test. **E and F.** qPCR analysis of *Myh7* and *Myh6* expressions in LV myocardium of *Mlp*$^{-/-}$ mice treated with miR-208b-3p antagomirs or scramble control. The fold change was normalized to the levels in untreated WT littermate controls. Bars are the mean values ±SEM with unpaired two-tailed *t*-test. The echocardiography was performed by Humam Siga and Mohammad Bakhtiar Hossain (ICMC). The data of echocardiography was analyzed by Humam Siga (ICMC).

Another explanation to the observed discrepancy in the response of *Mlp*$^{-/-}$ and AngII-*Ttn*$^{mut/+}$ to miR-208b-3p knockdown could be attributed to the different initial levels of miR-208b-3p between the two models. At the time of starting with miR-208b-3p antagomir administration, *Mlp*$^{-/-}$ had a ~ 20-fold elevation in miR-208b-3p levels (**Figure II-2B**), meanwhile, AngII-*Ttn*$^{mut/+}$ had only ~5-fold increase in mir208b-3p levels upon one week of AngII infusion (Figure 1E in (Zhou et al., 2017)). We could achieve a higher ratio of miR-208b-3p knockdown than Zhou *et al.* (~70% vs ~50%, respectively) through refining the administration route (subcutaneous vs. intraperitoneal, respectively) and the number of doses (4 doses over 4 weeks vs. 2 doses over two weeks, respectively). However, despite this, the residual levels of miR-208b-3p after a 70% knocking-down in *Mlp*$^{-/-}$ was probably still substantially higher than that of AngII-*Ttn*$^{mut/+}$ after 50% knock-down. Therefore, it appears as if more knockdown of miR-208b-3p was required in *Mlp*$^{-/-}$ to observe an effect on the cardiac phenotype. However, achieving substantially higher knockdown than 70% in the heart *in vivo* is currently very challenging, and would probably require an inducible knockout model for miR-208b-3p.

In conclusion, data and conclusion presented by Zhou *et al.*, 2017 regarding the deleterious effect of miR-208b-3p appears to be specific to their AngII-*Ttn*$^{mut/+}$mouse model. Therefore, the very high levels of miR208b-3p in the myocardium of *Mlp*$^{-/-}$, accompanied by a substantially lower fibrosis than that in AngII-*Ttn*$^{mut/+}$, and the fact that *Mlp*$^{-/-}$ still undergo a reverse cardiac remodeling associated with improved cardiac function (Elbeck et al 2022), suggest that miR208b-3p is less likely to trigger the development of fibrosis, and rather has a beneficial role in the heart.

5.2.4 Targets of miR-208b-3p in the heart

The very high level of miR-208b-3p in the *Mlp*$^{-/-}$ model, makes it an interesting model to explore potential target genes for miR-208b-3p. MiR-208b-3p has been reported to target *Myh7*'s transcriptional repressors *Sox6*, *Purβ*, *HP-1β* (*Cbx1*), *Sp3* and *Thrap1* (*Med13*) (van Rooij et al., 2009). Interestingly, RNA sequencing revealed that despite the marked downregulation of *Myh7* expression in anti-miR-208b-3p-treated animals, the treatment did not upregulate any known transcriptional repressor of *Myh7*, such as *Sox6*, *Purβ*, *HP-1β* (*Cbx1*), *Sp3* and *Thrap1* (*Med13*) (**Figure II-5**) (van Rooij et al., 2009). In addition, none of these genes were even initially significantly downregulated in the myocardium of untreated *Mlp*$^{-/-}$mouse despite the strong upregulation of miR-208b-3p and *Myh7* in these hearts. However, some of these repressors showed a small downregulation in the human patients with DCM (**Figure II-5**).

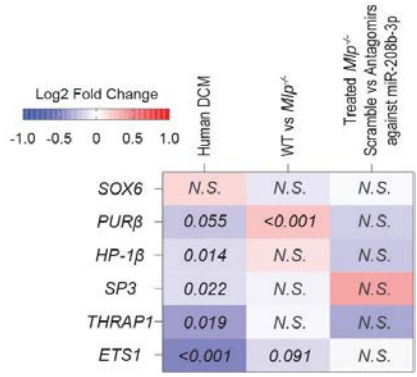

Figure II-5: The expression of miR-208b-3p targeted genes in heart failure

Expression of *Myh7* 's transcriptional repressors genes and *ETS1* gene in the myocardium of patients with DCM and in the myocardium of *Mlp*$^{-/-}$ mouse model estimated by RNA sequencing. The patient data is a published transcriptomic data from 64 samples of cardiac tissue from patients with DCM left ventricle (van Heesch et al., 2019). Transcriptomic data of *Mlp*$^{-/-}$ is obtained from (Elbeck et al., 2022). Numbers in italic inside the boxes indicate *p*-values.

Additionally, Itoh et al reported miR208b-3p to target *Ets1* in preosteoblasts (Itoh et al., 2010). This gene seemed to be slightly downregulated in *Mlp*$^{-/-}$ and in the DCM patients, but its level did not increase upon knocking down miR-208b-3p in *Mlp*$^{-/-}$ (**Figure II-5**).

Apart from the studies mentioned above, there are few other experimentally validated targets for miR-208b-3p that have been recently reported in the heart, such as Kcnj5, a gene that encodes for a potassium channel protein (Hupfeld et al., 2021). However, *Kcnj5* did not seem to be significantly downregulated in *Mlp*$^{-/-}$. Neither did its levels show significant recovery upon knocking down miR-208b-3p in *Mlp*$^{-/-}$, nor was it significantly downregulated in the myocardial samples of patients with DCM. Moreover, Zhou et al reported that they found several other predicted targets for miR-208b-3p to be downregulated in HL-1 cells overexpressing miR-208b-3p (Zhou et al., 2017). However, the observed downregulation does not necessarily imply that these genes were targeted by miR-208b-3p, as such a high overexpression of miR-208b-3p may indirectly affect the expression of these genes through occupying the AGO complexes and impacting the biogenesis of other endogenous miRNAs. Therefore, in conclusion, direct targets of mature miR-208b-3p in the heart remain elusive.

Primary miR-208b (pri-miR-208b) was found to modulate the transcription of α and β myosin heavy chain directly by binding to the chromatin and interacting with the epigenetic regulators Ezh2 in a mouse heart failure model of transverse aortic constriction (Mathiyalagan et al., 2014). However, the high induction of the mature miR-208b-3p in heart failure, and not only the pri-miR-208b, indicates that the mature miR208b-3p itself plays a crucial role in the cardiomyocytes, which still needs to be elucidated.

In conclusion, none of the previously few identified targets of miR-208b-3p were found to be affected by the high expression of miR208b-3p in the myocardium of *Mlp*$^{-/-}$. This might be explained by possible silencing of the targeted mRNAs through translational repression rather than through mRNA decay, which would require protein profiling to unveil. It might also be explained by the need for a cooperative repression induced by miRNA clusters, and not only by miR-208b-3p alone, in order to obtain a more marked repressive effect. However, the high expression of miR-208b-3p only (>20-fold increase), but not other members of the MyomiR family in *Mlp*$^{-/-}$, indicates that the real direct targets of miR-208b-3p may not have been discovered yet.

5.2.5 The role of miR-208b-3p in antioxidative response

Massive elevation of miR-208b-3p (<~2000-fold) were detected in the circulation of heart failure patients after acute myocardial infarction (Corsten et al., 2010; Gidlof et al., 2011), where there is also a rise in oxidative stress and its responses (Grieve et al., 2004; Hori and Nishida, 2009). This may suggest a possible link between miR-208b-3p induction and oxidative stress in heart failure.

Intriguingly, we observed that reducing miR-208b-3p levels induced higher elevation in the levels of *Hmox1* and *Nqo1* in the myocardium of *Mlp*$^{-/-}$. It also induced elevation in *Osgin1* gene expression (**Figure II-6**), indicating a possible upstream repressor effect of miR-208b-3p on these antioxidative genes. OSGIN1 is an oxidative stress response protein that mediates apoptosis by inducing the release of cytochrome c from mitochondria (Brennan et al., 2017). This would indicate that miR-208b-3p orchestrates an antioxidative response under acute and chronic oxidative stress conditions in heart failure, to enable effective defense, while avoiding ROS-induced cell death or overwhelming the cell with antioxidant equivalents. However, further evidence is needed through measuring the antioxidative capacity of the myocardium of *Mlp*$^{-/-}$ treated with antagomirs against miR-208b-3p.

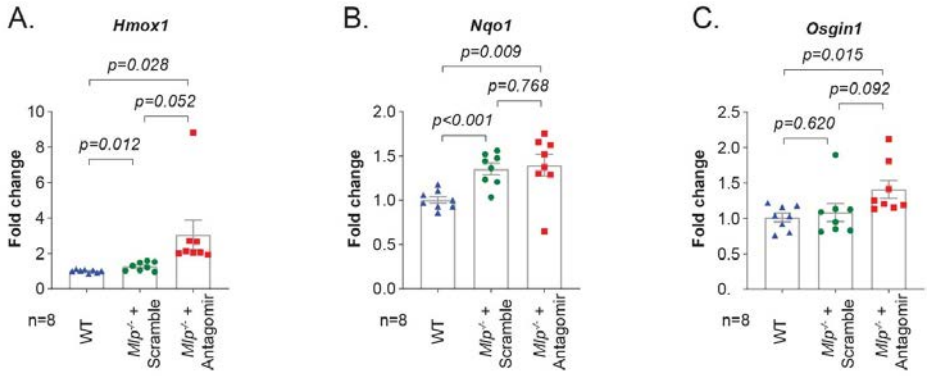

Figure II-6: The role of miR208b-3p in antioxidative response

A-C. qPCR analysis of *Hmox1, Nqo1* & *Osgin1* expression in the myocardium of *Mlp*$^{-/-}$ treated with antagomirs against miR-208b-3p or scramble control. The fold change was normalized to the levels in untreated WT littermate controls. Bars are the mean values ±SEM with unpaired two-tailed *t*-test.

5.2.5.1 Does Mir208b-3p target Idh2?

The coincidence of extreme upregulation of miR-208b-3p in the myocardium of *Mlp*$^{-/-}$ and in patients with eccentric DCM, accompanied by a simultaneous downregulation of *IDH2* led us to think about a possible link between miR-208b-3p and the post transcriptional regulation of *IDH2*.

In silico prediction for miR-208b-3p targets did not indicate a strong complementarity of its canonical seed sequence to any potential target sites on the 3´UTR of *IDH2* mRNA. However, *IDH2* is a predicted target for the 5p arm of pre-miR-208b, *i.e.*, miR-208b-5p, but its relatively low levels in the myocardium of *Mlp*$^{-/-}$ suggested that miR-208b-5p does not have another functional role beyond being a passenger strand for miR-208b-3p (**Figure II-3**).

However, the lack of canonical seed-matching binding sites of miR-208-3p and *IDH2* do not rule out the presence of other non-canonical binding sites, similar to what has been identified for other miRNAs with minimal seed-pairing (Gebert and MacRae, 2019). Moreover, knocking down miR-208b-3p with antagomir in the myocardium of *Mlp*$^{-/-}$ induced a slight recovery in Idh2 levels, although it was statistically insignificant (**Figure II-7A**). To determine whether this recovery of *Idh2* expression was directly linked to the reduction of miR-208b-3p levels, I overexpressed miR-208b-3p in HEK393 cells and checked the expression of *IDH2*. Overexpressing miR-208b-3p nevertheless did not induce *IDH2* downregulation (**Figure II-7B and C**), ruling out potential direct targeting of *IDH2* mRNA by miR-208b-3p.

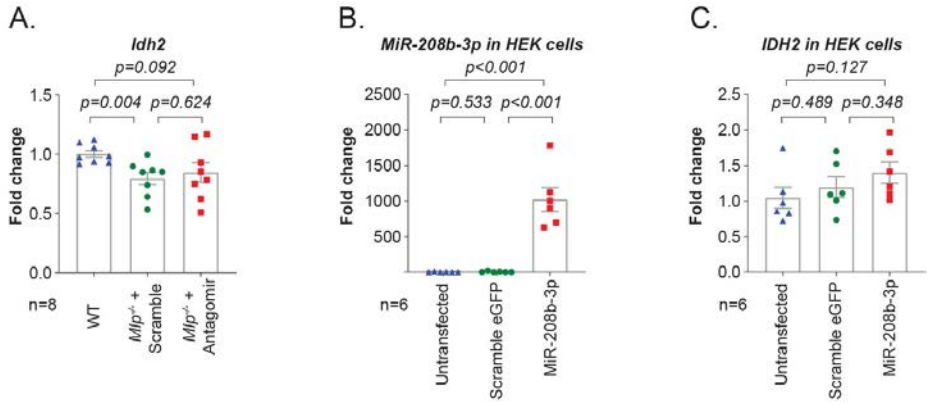

Figure II-7: The role of miR208b-3p in regulating IDH2 expression

A. qPCR analysis of *IDH2* expression in the myocardium of *Mlp*$^{-/-}$ treated with antagomirs against miR-208b-3p or scramble control. **B** and **C.** the expression of miR208b-3p and *IDH2* in HEK cells overexpressing miR-208b-3p. The fold change was normalized to the levels in untreated WT littermate controls in **A**, or untransduced HEK cells in **B** and **C**. Bars are the mean values ±SEM with unpaired two-tailed *t*-test.

However, the lack of a direct targeting of miR-208b-3p to *IDH2* does not rule out a potential indirect effect of miR208b-3p on *IDH2* expression. In our previous work (Elbeck et al., 2022) we highlighted *IDH2* as a key regulator of the antioxidative defense in cardiomyocytes. Owing to the potential regulatory role of miR-208b-3p in orchestrating the antioxidative defense that we identified in this study, a potential network involving both IDH2 and miR-208b-3p might play a key role in regulating the antioxidative response in cardiomyocytes. Moreover, the very high induction of miR208b-3p (~ 20-fold increase) and the ambiguity regarding its direct targets [4] makes it an interesting and important topic for future research, especially in the field of antioxidative defense.

[4] I add in this footnote some personal notes regarding the extremely negative impact of scientific misconduct on the discoveries and advances in the field of miRNA, and non-coding RNA in general. The field of non-coding RNA has expanded tremendously over the recent years, and ambiguities regarding their functions and targets seem to have made them an appealing victim of fraudster research paper-mills, with hundreds of papers being reported and retracted every year in the recent few years (further information can be found on microbiomedigest.com and forbetterscience.com). As one should always base one's own work on previously published work, it is extremely damaging when one cannot trust almost anything. MiR-208b is the best example of this, in which I was tricked by and struggled with several published fake papers, before discovering that they were completely fabricated (not even falsified) and reporting them, I got few retracted now, but many more to come, and this only a single miRNA, so one can just imagine what else is out there!

Acknowledgements in this project: *I would like to acknowledge Humam Siga and Mohammad Bakhtiar Hussain for their substantial efforts in echocardiography and data analysis. Xidan Li for the analysis of the small RNA sequencing data. Christer Betsholtz group (Jianping Liu, Sonja Gustafsson and Byambajav Buyandelger) for their help in preparing and sequencing the RNA of the miR-208b-3p antagomir study. David Brodin (BEA facility, KI) for analyzing the RNA sequencing data.*

5.3 STUDY III: NOVEL ISOFORMS OF MLP AND THEIR ROLE IN THE REMODELING OF HEART FAILURE

5.3.1 Background

Cardiomyopathies, and especially genetic cardiomyopathies are usually associated with different type of mutations in genes encoding sarcomeres, cytoskeleton, ion channel proteins or other genes in cardiomyocytes (Richard et al., 2006). Deletions, insertions, or point-mutations (missense or nonsense) in genes may result in the translation of truncated or misfolded proteins. Some of these truncated proteins may share part of the sequence with their respective full-length proteins, containing some of their functional domains. Harboring these domains would enable them to compete with their respective full-length proteins for binding with legends, and therefore act as poison peptides in heterozygote patients with dominant mutations. However, as some proteins are multifunctional, i.e., mediating multiple functions (Singh and Bhalla, 2020), truncated peptides harboring functional domains might confer some beneficial effects in heterozygote patients with haploinsufficiency or in homozygote patients.

Muscle LIM protein (MLP, also known as cysteine and glycine rich protein 3, CSRP3) is a small protein composed of 194 amino acids in both human and mice (Uniprot ID P50461 and P50462 respectively). The protein is encoded by an mRNA composed of 6 exons with a full length of 1283 nt in humans and 899 nt in mouse (Ensembl ID ENST00000265968.9 and ENSMUST00000167786.4, respectively). MLP protein is 100% conserved across human and mice, despite having some differences in their mRNA sequences (91% similarity). MLP is enriched in striated muscle cells, and it consists of two LIM domains followed by a glycine rich region (**figure III-1A**) (Arber, 1994). MLP localizes to the actin-based cytoskeleton including sarcomeres, where it interacts with α-actinin and with the titin-binding protein telethonin (T-cap), and acts as mechanical stretch sensor. It also localizes to the nucleus where it interacts with transcription factors (Arber, 1994; Boateng et al., 2007; Hoshijima, 2006). Knocking out *Mlp* in a mouse model results in dilated cardiomyopathy (Arber et al., 1997).

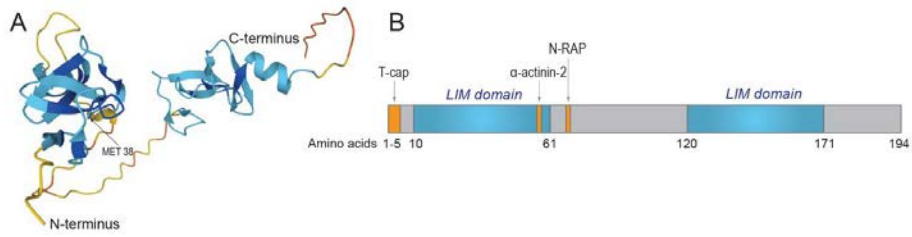

Figure III-1: The structure of MLP: A cartoon visualizes the 3D structure of MLP (UniProt, 2023). B: the position of main functional domains and sites of interacting proteins harbored by MLP.

Mlp$^{-/-}$ mice were generated by deleting exon 2 of *Mlp* locus that harbors the start codon, preventing the translation of Mlp protein (Arber et al., 1997). *Mlp*$^{-/-}$ was for long believed to be a complete knockout of all Mlp isoforms, as the only other reported MLP isoform in human is MLP-b, which is also initiated from the start codon located in exon 2 while skipping exons 3 and 4 and therefore changing the reading frame for successive exons 4 and 6 (Vafiadaki et al., 2014). However, our recent data described in this monograph indicate the presence of another novel isoform of Mlp, which is initiated from an noncanonical start codon located in exon 3 (MET 38, **figure III-1A**) and has the same reading frame as the full length Mlp.

5.3.2 The discovery of Mlp/Csrp3 novel isoform

Serendipity and curiosity led us to discover new isoforms of Mlp, initiated by me trying to resolve inconstancy between different methods of bioinformatic analysis, and followed by a lot of skepticisms about the presence of these novel isoforms, and ended up with direct experimental evidence proving their presence.

5.3.2.1 In silico predication for the presence of a novel isoform of Mlp:

Two independent bioinformatic analyses of the same transcriptomic data on left ventricle myocardium of *Mlp*$^{-/-}$ mice gave slightly different results. The interesting part was in the difference of the regulation trend of *Mlp* mRNA, which was the gene knocked-out in this murine model. In the first analysis, in which PCR duplicates were excluded from the analysis, *Mlp* appeared to be downregulated. Meanwhile, in the second analysis, in which PCR duplicates were kept, *Mlp* appeared to be upregulated (**Figure III-2**).

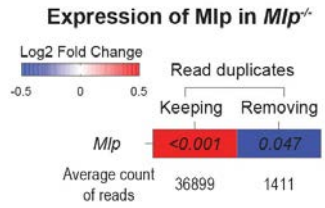

Figure III-2: Inconstancy in the expression trend of *Mlp* between different analysis of same data set:
Expression of Mlp in *Mlp*$^{-/-}$ estimated by RNA seq. Data was analysed with a method that keep all duplicated reads of sequencing (left panel), and a method that remove all duplicated ones (right panel). Numbers in *italic* inside the boxes indicate *p*-values, while numbers below the boxes indicate the average count of reads that were aligned to *Mlp* locus.

Sequencing libraries were prepared with the True seq total RNA library preparation kit (Illumina 20020598). This kit uses a thermal fragmentation approach for the mRNA after depleting the ribosomal RNA. As mentioned above, murine *Mlp* mRNA consist of 899 nt, and therefore, mathematically, a maximum number of 899 unique reads can be generated for *Mlp*

in the WT from each side, and a smaller number can be generated in *Mlp*$^{-/-}$ lacking exon 2. This mathematically estimated number is close to the number observed in the bioinformatic approach that removes duplicated reads (**Figure III-2**). Moreover, as *Mlp* is highly expressed in the heart, a high percentage of identical reads may be expected naturally in addition to duplicated reads generated by PCR amplification of the sequencing libraries. Therefore, keeping duplicated reads appeared the more appropriate approach here. To validate it experimentally, I performed a qPCR analysis on RNA extracted from LV myocardium of *Mlp*$^{-/-}$ with primers that target exon 2, exon 3 and exon 6 of *Mlp*. The results confirmed the upregulation of *Mlp* mRNA in the *Mlp*$^{-/-}$ (**Figure** III-3).

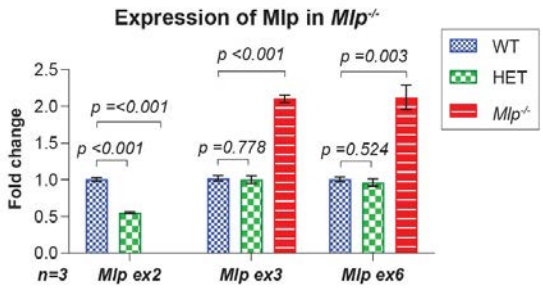

Figure III-3: Expression of exons of *Mlp* in *Mlp*$^{-/-}$

QPCR analysis of exons 2, 3 and 6 of *Mlp* in the myocardium of *Mlp*$^{-/-}$, in which exon 2 was knocked out. The animals were.18 weeks-old males. Bars are the mean values ±SEM with unpaired two-tailed *t*-test.

In addition to the 2-fold increase of *Mlp* in the myocardium of *Mlp*$^{-/-}$, a consistent level of transcription of *Mlp* among different *Mlp*$^{-/-}$ animals can be inferred from the relatively small variation in expression of exons 3 and 6 among different biological replicates (**Figure** III-3). This observation made me consider that there might be a negative feedback-loop that controls the expression of *Mlp-Δexon2* mRNA and keeps it at a constant level. This loop appears to be mediated through a putative protein translated from the *Mlp-Δexon2* mRNA. However, the 2-fold increase in *Mlp-Δexon2* expression in *Mlp*$^{-/-}$ indicated that if a putative protein would be translated from this mRNA, it would be happening at a low level.

To first identify all full-length transcripts of mRNA transcribed from the *Mlp* locus, we performed a 3rd generation long-read sequencing using Oxford-Nanopore technology on RNA extracted from the myocardium of WT and *Mlp*$^{-/-}$. We utilized both a targeted approach, using enriched *Mlp* cDNA, and another unbiased approach using direct RNA sequencing without converting it to cDNA. Results of the long-read sequencing revealed that there were no novel transcripts of *Mlp* with alternative splicing or intron inclusion in neither WT nor *Mlp*$^{-/-}$ (**Figure III-4**).

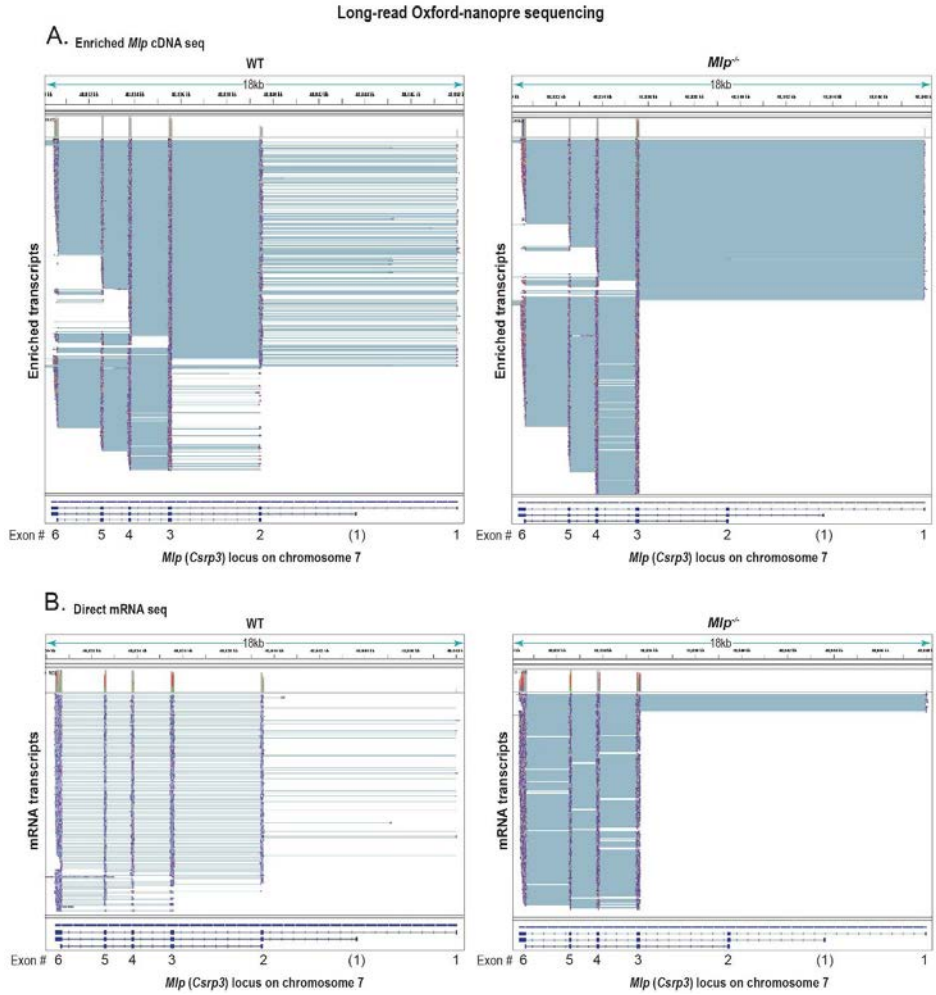

Figure III-4: Oxford-Nanopore long read sequencing on *Mlp* transcripts in the myocardium of WT and *Mlp*$^{-/-}$

A. Unknown cDNAs of all putative *Mlp* mRNA isoforms that share exon 6 were amplified by using a single primer targeting the 3′ end of exon 6, and another universal custom-made primer targeting the Template Switching Oligo at the 5′ end, which was ligated during the cDNA synthesis (for more details, see the method part). The libraries were prepared using 1D^2 sequencing of genomic DNA (SQK-LSK308) kit. **B.** mRNA was enriched from total RNA, and then processed with the Direct RNA Sequencing Kit (SQK-RNA001). All animals were 12-weeks-old males (n=1 per group). The experiments were jointly performed with Dominique Koppenhöfer (ICMC, KI), and the raw data was analyzed by Humam Siga (ICMC, KI). To visualize all transcripts in each sequencing, multiple screenshots were taken from the Integrative Genomic Viewer and then fused together in Adobe Illustrator.

Later, I performed in silico prediction of translatable open reading frames (ORF) from the *Mlp-Δexon2* mRNA using the ATGpr tool (Salamov et al., 1998)). An ORF encoding for a 7kDa C-terminal isoform of Mlp with the same reading frame as the full-length Mlp protein had a good score (**Figure III-5**).

A.

Reference Mlp sequence

```
1   MPNWGGGAKC GACEKTVYHA EEIQCNGRSF HKTCFHCMAC RKALDSTTVA
51  AHESEIYCKV CYGRRYGPKG IGFGQGAGCL STDTGEHLGL QFQQSPKPAR
101 AATTSNPSKF SAKFGESEKC PRCGKSVYAA EKVMGGGKPW HKTCFRCAIC
151 GKSLESTNVT DKDGELYCKV CYAKNFGPTG IGFGGLTQQV EKKE
```

B.

No.of ATG from 5'end	Reliability	Frame	Identity to Kozak rule A/GXXATGG	Start (bp)	Finish (bp)	ORF Length (aa)	Stop codon found?	Sequence
5	0.14	2	GXXATGG	344	526	61	Yes	MGGGKPWHKTCFRCAICGKSLESTNVTDKD GELYCKVCYAKNFGPTGIGFGGLTQQVEKKE

Figure III-5: In silico prediction of translatable ORF from *Mlp-Δexon2* mRNA using ATGpr tool

A. Reference sequence of Mlp, **B.** Predicted translatable ORF with high scores from *Mlp-Δexon2* mRNA.

5.3.2.2 Experimental evidence for the presence of a novel 17 KDa isoform of Mlp

To detect a band corresponding to the predicted protein described above in Western blotting, some optimization and modification was needed to the protocol to enable the detection of relatively low amounts of a relatively small protein. I therefore increased the amounts of total protein lysate loaded on the gel to > 60 µg, and then used a PDVF membrane for the transferring step, as it enables chemical crosslinking to the membrane after fixating it with 0.4 % formalin (Lee and Kamitani, 2011). Furthermore, I increased the primary antibody concentration, and the incubation time to 4°C to increase specificity and sensitivity of binding. These adjustments enabled me to detect a band at ~ 17 kDa corresponding to a putative isoform of Mlp (**Figure III-6**, band (1)). However, further experimental evidence was still needed as this detected band might be an unspecific binding of the primary antibody utilized. Additional bands were also detected at ~ 7 and 50 kDa, but I decided to focus subsequent experiments on the most prominent band (*i.e.*, 17 kDa). I termed this putative 17 kDa isoform as Mlp-C to distinguish it from the previously reported isoform MLP-b (Vafiadaki et al., 2014).

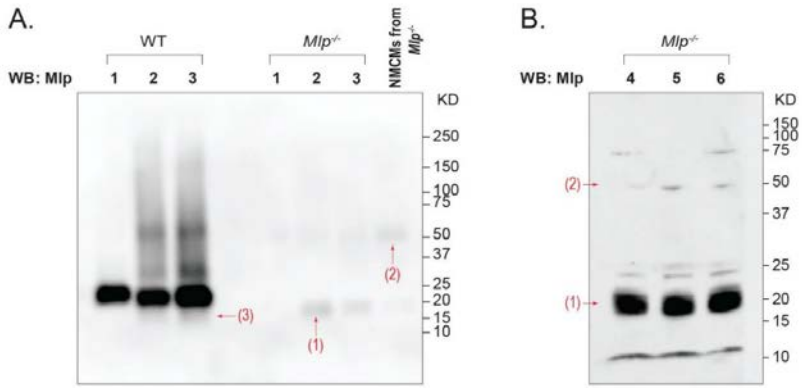

Figure III-6: Optimized Western blotting for detection of the Mlp-C isoform

A. Western blotting of Mlp in protein lysate of myocardium of WT and *Mlp*$^{-/-}$ **B.** Another Western blotting of Mlp in protein lysate of myocardium of *Mlp*$^{-/-}$ with longer exposure time. The utilized antibody (ab155538) recognizes a peptide located at the C-terminus of Mlp.

I was later able to detect a signal for Mlp localized to the sarcomeres using immunofluorescence in neonatal murine cardiomyocytes isolated from *Mlp*$^{-/-}$ pups at the age of 1-3 days (**Figures III-7 and 8**). The immunofluorescence results gave further evidence for the presence of a putative Mlp isoform in *Mlp*$^{-/-}$, but the evidence was still inconclusive, due to the possibility of unspecific binding of the primary antibody.

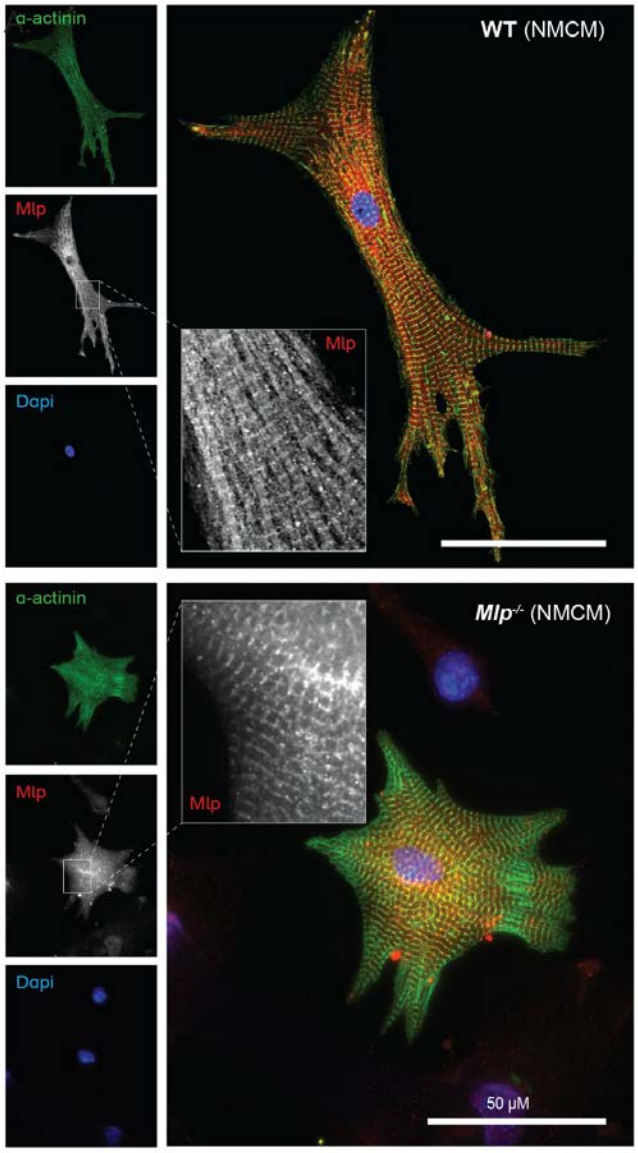

Figure III-7: Immunofluorescence analysis of Mlp in neonatal murine cardiomyocytes (NMCMs)
The images were captured utilizing confocal Zeiss microscope with Airyscan for the WT cells, and a bright field Zeiss microscope for the cells from *Mlp*$^{-/-}$.

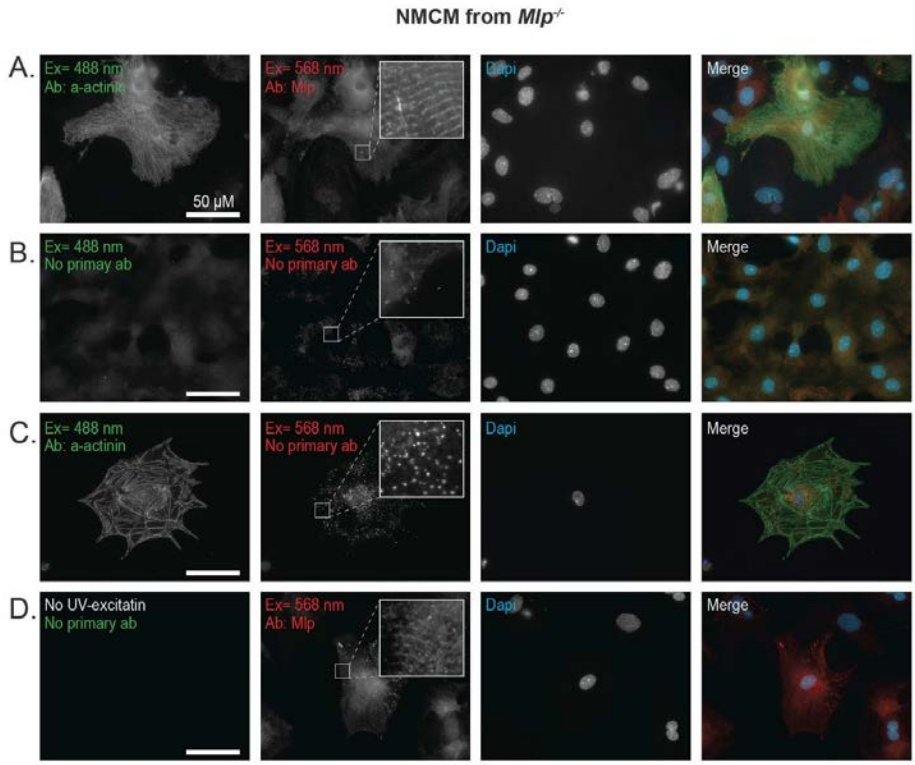

Figure III-8: Positive and negative controls for immunofluorescence analysis of Mlp in NMCMs

A. NMCMs were stained with primary antibodies against α-actinin and Mlp. **B.** NMCMs were not stained with any primary antibody as negative controls. **C.** Cells were only stained with primary antibodies against α-actinin, but not Mlp. **D.** Cells were only stained with primary antibodies against Mlp, but not α-actinin. Cells in figures **A-D** were incubated with the secondary antibodies Alexa Fluor Donkey anti mouse 488 (ab150105) and Alexa Fluor Donkey anti rabbit 568 (ab175470). All images were acquired using a bright field Zeiss microscope with sequential imaging. The striations observed in the magnified images in figures **A** and **D** show that the putative Mlp isoforms localize to the sarcomeres. A comparison between images shown in figures **C** and in **D** indicates that there are no observable artifacts of spectral bleed-through of the Alexa Fluor 488 into the red channel. Images shown in **B** indicate that there are no observable artifacts of autofluorescence in the red channel. These observations indicate that the signal observed in the red channel in figures **A** and **D** is specific for the primary antibody against Mlp.

To finally provide more concrete evidence, I immunoprecipitated Mlp from protein lysates of myocardium of *Mlp*$^{-/-}$. After separating the precipitated proteins by electrophoresis, and staining the gel with Coomassie Blue, I could excise the gel corresponding to the 17 kDa band and send it for a mass spec analysis. Protein finger printing by mass spectrometric analysis of these bands indicated the presence of multiple peptides of Mlp in the band of 17 kDa (**Figure III-9**). These results confirmed that a novel isoform of Mlp is translated from the *Δexon-2* mRNA of *Mlp*.

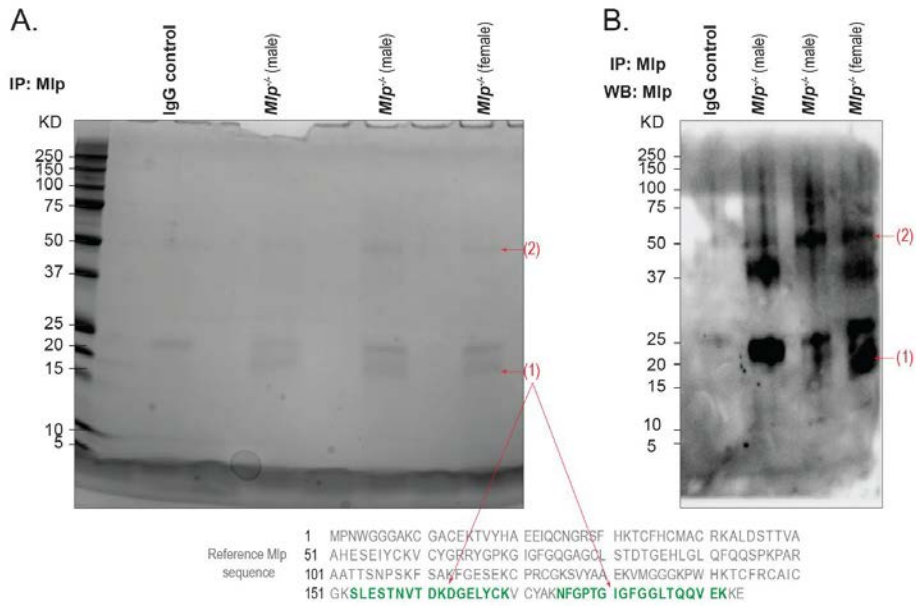

Figure III-9: Immunoprecipitation and protein fingerprinting by mass spec of Mlp-C isoform

Mlp were precipitated with primary antibodies against Mlp cross-linked to a Dynabeads™ Protein G. Precipitated proteins were electrophorized and the gel was then stained with Coomassie blue (**A**) for mass spectrometric analysis. A small fraction (~10%) of the precipitated proteins was electrophorized and blotted with the same primary antibodies against Mlp that were used in the immunoprecipitation (**B**). Mass spectrometric analysis was performed by Akos Vegvari.

In a follow-up work together with the master thesis student Dominique Koppenhöfer, whom I supervised, we demonstrated that the 17 kDa isoform of Mlp (Mlp-C) is most likely translated from a non-canonical start codon located in exon 3 (Methionine 38, **Figure III-1**), through utilizing *in vitro* overexpression of multiple cDNA constructs of *Mlp* in HEK cells (**Figure III-10**). In construct #2, we overexpressed a cDNA of *Δexon-2 Mlp* that we observed with nanopore sequencing (**Figure III-4**), this cDNA lacked both exons 1 and 2, but had 4 nucleotides (gcag) extension at the 5`-end. The overexpression of this construct gave a 17 kDa isoform of Mlp (Mlp-C). In constructs #3 and #4, we tested the alternative usage of the two different sequences of exon 1 (201 and 202) present in the *Mlp* locus. The usage of exon 1-202 resulted in a marked higher expression of Mlp-C than that of exon 1-201. In fact, cardiomyocytes seem to utilize only exon 1-202, as can be observed from the Nanopore sequencing data (**Figure III-4**). In construct 5, we removed the second stop codon in exon 6 that is needed for the translation of an alternative reading frame of Mlp (we termed it Arf-Mlp), and fused it instead with a cDNA encoding for green florescence protein (eGFP). The purpose of fusing eGFP was both to increase the molecular weight of any putative Arf-Mlp, and to enable the utilization of antibodies against GFP to detect them. A ~ 20 kDa protein seemed to

be expressed from this construct, but at an extremely low level. We also confirmed the presence of the 17 kDa isoform of Mlp (Mlp-C) in *Mlp*$^{-/-}$ by a new immunoprecipitation experiment followed by mass spectrometric analysis (**Figure III-11**).

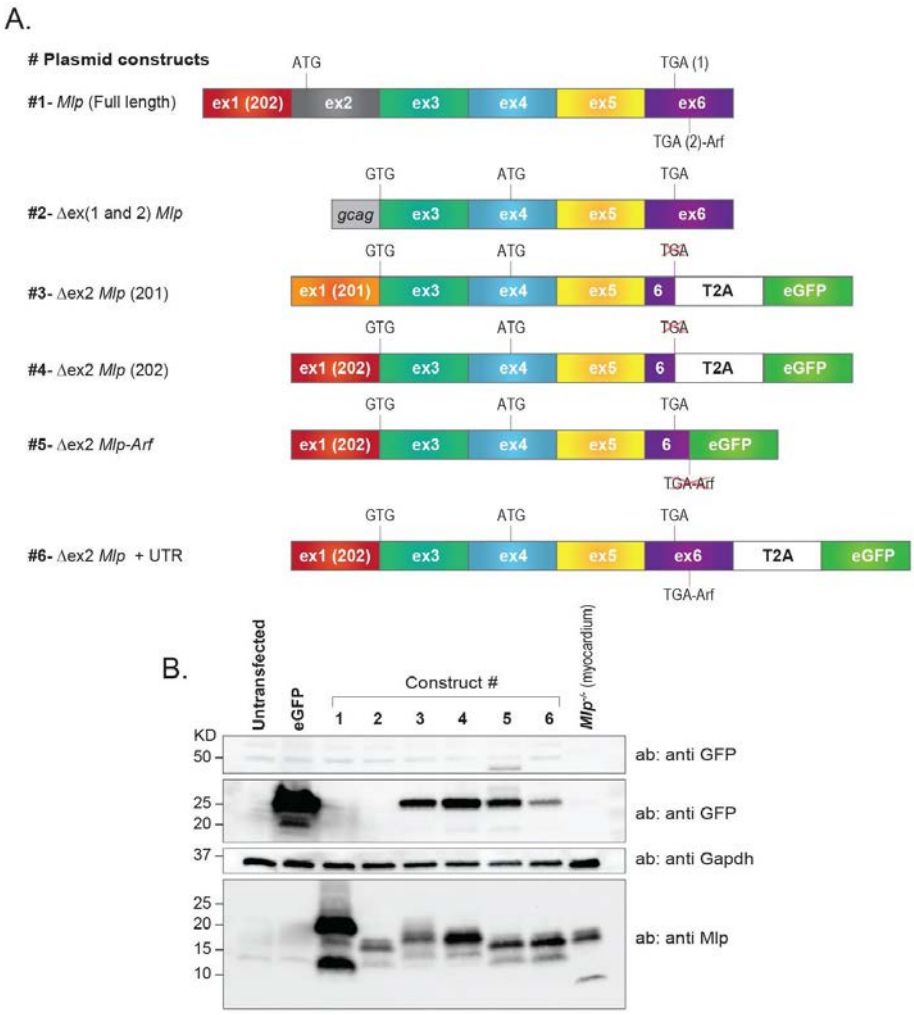

Figure III-10: Transfecting HEK cells with different constructs of Mlp cDNA

HEK cells were transfected with different cDNA constructs encompassing different possible mRNAs encoding for Mlp-C, or for an alternative reading frame of Mlp (Mlp-Arf). T2A is a 2A self-cleaving peptide. The experiment and the plasmid constructs were jointly designed and performed with Dominique Koppenhöfer.

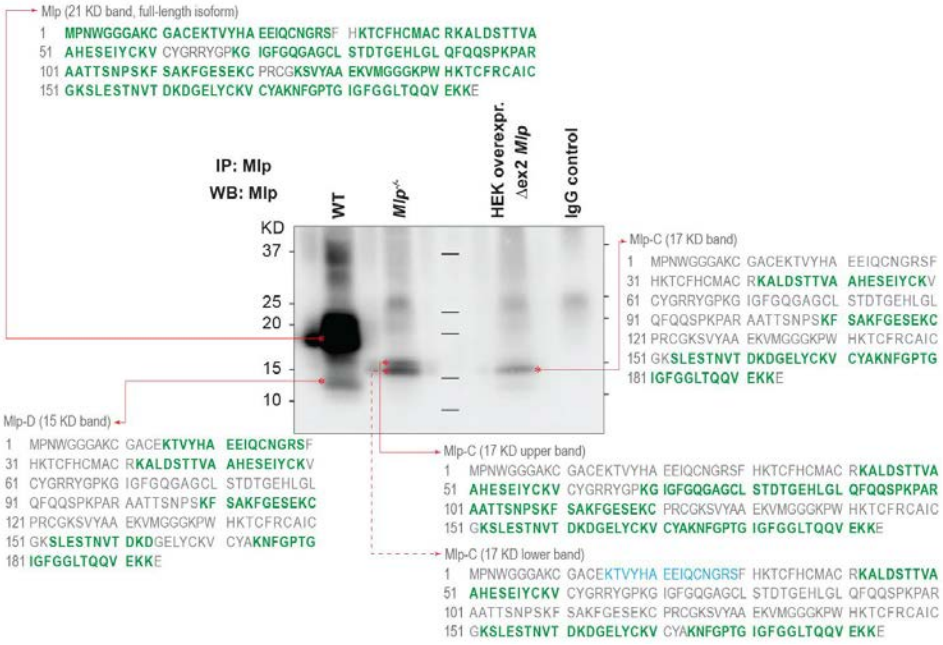

Figure III-11: Immunoprecipitation and protein fingerprinting by mass spec of Mlp-C isoform

Mlp from protein lysates of WT, *Mlp*$^{-/-}$ and HEK cells overexpressing *Δexon2-Mlp* (construct #4 in figure III-10) was precipitated with primary antibodies against Mlp cross-linked to Dynabeads™ Protein G. Precipitated proteins were electrophorized and the gel was then stained with silver staining for mass spectrometric analysis. A small fraction (~10%) of the precipitated proteins was electrophorized and blotted with the same primary antibodies against Mlp that were utilized in the immunoprecipitation. The peptides labelled in green were those detected with low error rate, while the one labelled in blue was detected with high error rate (indicating a possible cross contamination from the nearby band of the full-length Mlp in the WT lane). The experiment and the plasmid constructs were jointly designed and performed with Dominique Koppenhöfer. The mass spectrometric analysis was performed by Akos Vegvari. The analysis of the mass spectrometric data was performed by Dominique Koppenhöfer.

5.3.3 Molecular role of Mlp-C

The identified 17 kDa isoform of Mlp has one LIM domain, probably enabling it to mediate part of Mlp functions, such as interactions with α-actinin-2 (Geier et al., 2003), and nebulin-related anchoring protein (Gehmlich et al., 2004). However, lacking the N-terminus of the full length Mlp isoform may make this shorter isoform incapable of mediating all of the Mlp functions, such as interacting with Tcap (Knoll et al., 2002), and therefore, it may act as a poison peptide, through competing with the full length Mlp and occupying some of its legends.

Immunofluorescence images in NMCMs from *Mlp*$^{-/-}$ shows that Mlp-C localizes to the sarcomeres, but probably not to the actin filaments, indicating a possible distinct localization to that of its full-length isoform (**Figure III-12**). However, no conclusive exact localization of Mlp can be drawn from the presented images, as they were acquired with different technologies. Nevertheless, the clear localization of Mlp-C to the sarcomeres may indicate that

it is not a misfolded protein at least, and it is therefore most likely a functional protein.

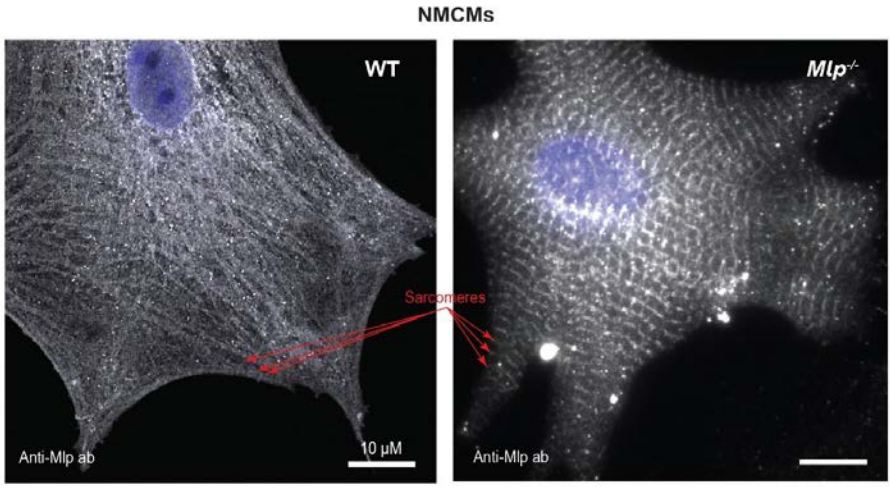

Figure III-12: A comparison of different localizations of Mlp isoforms between WT and *Mlp*$^{-/-}$
Immunofluorescence analysis of Mlp in neonatal murine cardiomyocytes (NMCMs). The images were captured utilizing confocal Zeiss microscope with Airyscan for the WT cells, and a bright field Zeiss microscope for the *Mlp*$^{-/-}$ cells.

5.3.3.1 Is Mlp-C expressed in the myocardium of WT animals?

Mlp-C isoform might also exist in the myocardium of WT mice, as it can be technically translated from the full-length mRNA of *Mlp*. In fact, a faint band corresponding to a 17 kDa protein appeared in the western blotting of Mlp in the myocardium of WT animals (band 3 in **Figure III-6**). Moreover, a band corresponding to a 17 kDa protein appeared also in the western blotting of HEK cells overexpressing the full-length of Mlp cDNA (Lane of construct 1 in **Figure III-10**). However, experimentally validating the presence of Mlp-C in the myocardium of WT animals through mass spectrometric protein finger printing is technically not feasible, due its very low translation levels in comparison to its full-length isoform, and its close molecular weight to it (band 3 in **Figure III-6**). These features make it difficult to excise this band from the gel without any cross-contamination from the full-length isoform of Mlp. Two-dimensional electrophoresis utilizing a prior isoelectric focusing step did not work as both isoforms have very close isoelectric points.

Moreover, both experiments of overexpressing the full-length cDNA of *Mlp* (**Figure III-10**), and the immunoprecipitation of Mlp from protein lysates of WT (**Figure III-11**) indicated the presence of another short C-terminal isoform of Mlp (~15 kDa). Protein fingerprinting could detect multiple peptides of Mlp in this 15 kDa band, indicating that it is probably another novel isoform of Mlp. We termed this new isoform as Mlp-D.

Notably, both Mlp-C and Mlp-D are distinct isoforms from the one reported by Vafiadaki *et. al*. (MLP-b), as both Mlp-C and Mlp-D was detected by antibodies raised against the c-terminal peptide of MLP, which does not exist in MLP-b, which has a different reading-frame in its C-terminus (Vafiadaki et al., 2014). Mlp-D might also be translated from the *Δexon-2 Mlp* mRNA in *Mlp*$^{-/-}$, albeit at a very low level. A faint band, corresponding to a 15 kDa, can be observed by overexpressing *Δexon-2 Mlp* cDNA in HEK cells (constructs 2-6 in **Figure III-10**).

Mlp$^{-/-}$ mice were extensively utilized as negative controls for studies unravelling molecular functions and interacting partners of Mlp. However, our data that indicates a presence of novel isoforms of Mlp in *Mlp*$^{-/-}$ may impact the outcome of some of these studies and open up opportunities for new discoveries. However, subsequent experiments to unveil the cellular localizations and the distinct molecular functions of the novel isoforms of Mlp are definitely needed. Such experiments could utilize co-immunoprecipitation of Mlp to identify interacting proteins. Moreover, these novel isoforms might have clinical importance, especially with patients that suffer from mutations in *MLP*. However, the latter is dependent first on whether novel isoforms of Mlp that we identified in this work in mice could also be translated in humans.

Moreover, *edgetic* perturbation effect (edge-specific genetic perturbation) of knocking out Mlp should also be considered as a potential reason for the translation of novel isoforms of Mlp observed in *Mlp*$^{-/-}$, but not in WT animals. This concept implies that certain proteins or metabolites that are linked together through biochemical or physical interactions form an interactome. Perturbations such as truncating mutations that preserve some of the functional domains of the protein my induce the translation of partially functional gene products (Zhong et al., 2009).

5.3.3.2 Do novel isoforms of Mlp play a role in left ventricle reversed remodeling?

MLP is reported to be downregulated at the protein level, but not at the mRNA level in LV myocardium of chronic heart failure patients with dilated or ischemic cardiomyopathy compared with non-failing donors (Zolk et al., 2000). However, our analysis of publicly available transcriptomic data on the LV myocardium of patients with DCM revealed that *MLP* was also significantly downregulated on the mRNA levels in multiple DCMs (**Figure III-13**).

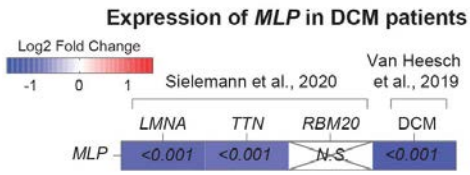

Figure III-13: Expression of *MLP* in the myocardium of DCM patients -

The expression of MLP in DCM patients were assessed by analyzing published transcriptomic data from left ventricular (LV) myocardium of patients with end-stage heart failure (Sielemann et al., 2020; van Heesch et al., 2019).

The observed downregulation of MLP in DCM patients is a consequence of cardiac remodeling associated with DCM, and it would therefore be expected also in the murine models of DCM. However, this condition is not applicable in the case of *Mlp*$^{-/-}$ mice, as the DCM phenotype in this model is the consequence of knocking out this protein. Instead, *Mlp*$^{-/-}$ exhibit upregulation in *Mlp Δexon2* mRNA as a result of a negative feedback loop proposed above. However, *Mlp Δexon2* seemed to be substantially upregulated in male *Mlp*$^{-/-}$ mice, but not much in females, with almost 2-fold-increase in male *Mlp*$^{-/-}$ compared to female (**Figure III-14**). This observation was interesting, as we had previously observed that females *Mlp*$^{-/-}$ have a better cardiac function than the males (**Figure 5** in Elbeck *et al*., 2022). This observation raised the questions whether Mlp-C is involved in the reverse cardiac remodeling, either as a protective role promoting the males to express more, or as a deleterious role making the females expressing less.

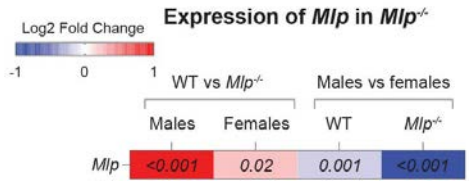

Figure III-14: Expression of *Mlp* in the myocardium of male and female *Mlp*$^{-/-}$

The expression of MLP in the LV myocardium of both male and female *Mlp*$^{-/-}$ were assessed from the analysis of transcriptomic data of *Mlp*$^{-/-}$ presented in Elbeck *et. al.,* 2022.

To determine whether the novel short isoforms of Mlp have poison or beneficial effects, we generated a complete knockout mouse of the whole *Mlp* locus on chromosome 7 (*Mlp*$^{-/-(complete)}$) in collaboration with Taconic Biosciences. Like *Mlp*$^{-/-}$, *Mlp*$^{-/-(complete)}$ also developed a DCM phenotype (**Figure III-15**), which was slightly more severe at younger ages than those of *Mlp*$^{-/-}$, suggesting a possible beneficial role for Mlp-C. However, initial observations indicated that female mice of *Mlp*$^{-/-(complete)}$ exhibited LV reverse remolding associated with improved cardiac function as they grow older, similar to what we observed in *Mlp*$^{-/-}$ (Elbeck *et. al.*, 2022).

However, a higher number of animals, and simultaneous comparisons between *Mlp*$^{-/-}$ and *Mlp*$^{-/-(complete)}$ at different ages would be needed to draw more conclusive conclusions, and to determine to what extent Mlp-C mediates beneficial roles in cardiomyocytes.

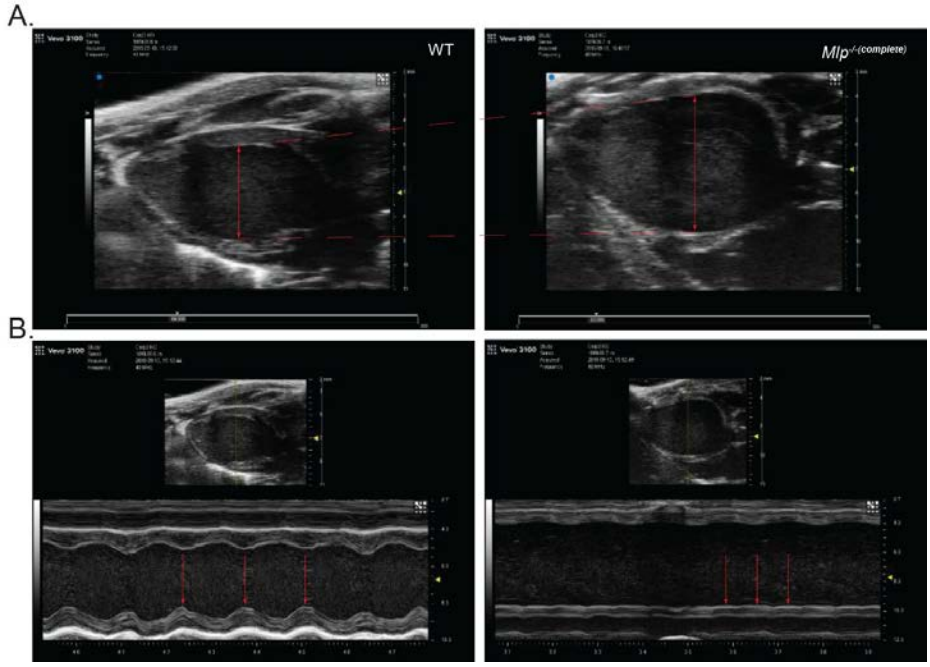

Figure III-15: Echocardiography in *Mlp*$^{-/-(complete)}$

A. A screen shot of the B-mode echocardiography analysis showing severe enlargement of the left ventricle chamber in *Mlp*$^{-/-(complete)}$ comparing to the WT control. **B.** A screen shot of the B-mode showing severe impairment of cardiac contractility in *Mlp*$^{-/-(complete)}$. Echocardiography was performed by Humam Siga.

MLP is an interesting protein, and despite the extensive research that has been carried out to reveal its functions, we still do not know much about it, and especially its role in the nucleus, or other cellular or tissues localizations. MLP was also reported to play important roles in other organs beyond the heart, such as its role in promoting axon regeneration in the central nervous system (Levin et al., 2019). Therefore, it would be important to characterize the functions of the new isoforms of Mlp identified in this work. Moreover, knowledge about the existence of shorter novel isoforms with distinct functions and localizations of Mlp can be applicable to all other proteins. It just requires some motivation to explore beyond the boundaries, with some curiosity, dedication, and commitment to discover them.

Acknowledgements in this project:

I would like to acknowledge Dominique Koppenhöfer for her substantial efforts in the in vitro overexpression, immunoprecipitation and Nanopore sequencing. Humam Siga for his efforts in echocardiography and in analysing the data of Nanopore sequencing. Akos Vegvari for his efforts in performing mass spectrometric analysis. Xidan Li and Mike Firth for their efforts in the initial analysis of the next generation RNA seq data.

6 CONCLUSIONS AND FUTURE PERSPECTIVE

In this monograph, I aimed to highlight redox biology from a different perspective than the common one, through utilizing basic principles of redox chemistry, and biological evidence from our recent work, as well as from published literature.

Oxidative species are a divergent group of cellular metabolites, with a wide variety of functions. Together with reductants, they form the redox system that controls and regulates a vast range of cellular functions. Redox species mediate intracellular communication and crosstalk through acting as cellular signaling molecules. Redox system also controls numerous biological reactions, either by providing the optimum redox milieu, or by regulating the folding of proteins and their redox-posttranslational modifications, through which, redox indirectly regulates all associated biological functions that involve these proteins.

Diversions or disruptions of mechanisms involving redox elements might result in redox stress, among which oxidative stress represents a common mechanism associated with numerous diseases. However, cells, and especially cardiomyocytes, are equipped with potent antioxidative mechanisms to fight this stress. One should note here, though, that shifts in the homeostasis of oxidative species are not the main causes of diseases, but rather secondary consequences of diseases, that may in some circumstances further propagate the pathogenic cues and progression of the diseases. Apart from mutations in enzymes that directly regulate redox homeostasis, potentially excessive ROS production would be the consequences of initial aberration of any other molecular mechanisms.

Henceforth, antioxidative defense represents only a small function for the reductive system, which, as stated above, controls several cellular functions. Therefore, nonspecific exogenous antioxidative treatments with a broad spectrum of downstream targets would negatively interfere with multiple other functions of the reductive system.

In this regard, in our recent work(Elbeck et al., 2022), we unveiled that mitochondrial IDH2 governs an extensive regulatory mechanism in cardiac mitochondria. We showed that IDH2 coordinates other antioxidative elements such as NRF2 through a feedforward cycle involving 2OG and L2HG. We also showed that this redox cycle regulates gene expression through unconventional mechanism involving intronic DNA hydroxy methylation. We next explored the possible implications of these findings for the treatment of patients with heart failure, taking into consideration previously failed clinical trials that aimed to ameliorate oxidative stress associated with heart failure. We first demonstrated that there are differences in the antioxidative defense between males and females, with females having more robust

antioxidative system. A phenomenon that was even reflected on the phenotype of heart failure, with female having less severe DCM than males. We next employed this sex difference to test our hypothesis, through utilizing a novel molecule (AZ925) to activate NRF2 pathway. We concluded that boosting antioxidative capacity – only when endogenous one is deteriorated - improves cardiac function, thus highlighting new utilities in precision medicine.

I want to emphasize here that I am not implying that heart failure is associated with normal redox homeostasis, but rather with remodeled redox homeostasis associated with overall adequate endogenous antioxidative capacity, which counteracts increased oxidative stress. Therefore, potentially successful antioxidative treatments should rely on a personalized approach, in which not only a certain subgroup or subtype of patients is treated, but also a specific edged (not nodal) element of the redox mechanism affected by heart failure is directly and precisely targeted. Recent advances in gene therapy, such as antisense oligonucleotides and siRNA have enabled such precise targeted approaches to be achieved. However, more knowledge in basic molecular mechanisms that regulate antioxidative capacity is needed before this precise and personalized approach of the antioxidative therapy can achieve clinical success.

However, I am probably overall against the current view of oxidative species as molecular *explosive materials* that damage everything they touch or reach. Instead, I rather perceive them as functional metabolites like any other metabolites when present at physiologically adequate concentrations. Moreover, I am also against the general belief that antioxidative supplements are always beneficials, as we have provided experimental evidence indicating that the presence of excessive reductants induces cardiomyocytes death and interferes with the broad functions of the reductive system. Decades of research and numerous clinical trials have failed in providing concrete evidence for any benefits of such therapies, therefore a radical change in the way we understand this field would be needed to advance such treatment strategies.

Emerging technical advances have dramatically changed our way of discovering and perceiving biology. I am still at an early stage of my scientific career, but I clearly remember when I was first introduced to genomic DNA outside of the coding regions as ‘junk DNA’ (one will still find it on the internet). However, emerging RNA sequencing has changed this view radically, with a rapidly developing field of functional small and long noncoding RNAs, which ultimately imply that very little, if any, DNA is “junk”, but rather carry distinct and important genetic information. The same concept was until recently also associated with DNA methylation. A few years before I start my PhD work, DNA methylation was considered a ¨random¨ process mostly associated with cellular linage imprinting or associated with an

inhibitory mechanism when present in promoters. This view has now also changed dramatically, and it is acceptable to say that each single nucleotide (Cytosine or Adenine) methylation (5mC, 5hmC, 5fC, 5caC) in any genomic region have distinct regulatory functions on numerous molecular mechanisms. The field of posttranslational modifications of proteins and alternative spliced isoforms have also recently surged with multiple technical advances in methodologies.

“Omics” of single cells also represents a greatly promising approach, especially in highly specialized organs such as the heart. The heart is not only composed of different cell types, but it is conceivable that every single cell of every cell type would have unique feature, as they all carry unique spatial position, and therefore, would be subjected to a unique combination of molecular stimuli and mechanical forces.

Therefore, technical advances in the recent few years have enabled the exploration of complex mechanisms beyond traditional boundaries, by utilizing multiple types of omics. Epigenetics is one of these fields that require complex approaches of omics on multilayers to unveil functions. Epigenetics is not only a question of DNA methylation, but also of histone modifications, both of which orchestrate the regulation of gene expression. Therefore, manipulating DNA methylation alone is not always enough to render a change in gene expression.

Moreover, histone demethylases are also regulated by the cofactors 2OG, L2HG, D2HG and other mitochondrial metabolites, which emphasis the importance of multilayer omics to unveil mitochondria-nucleus crosstalk, even much more complex that the approach we utilized in our studies. However, posttranslational modifications of histones are extremely complex to explore, as they include several moieties such as methylation, phosphorylation, acetylation, ubiquitylation, sumoylation and others, each of them would have distinct impact on chromatin structure and the recruitment of transcriptional factors.

Noncoding RNAs also add another layer to this complexity, as they are not only themselves regulated by DNA methylation and histone posttranslational modifications, but they themselves also regulate gene expression through regulating the previous factors.

Therefore, technical advances, such as third generation sequencing, that would be applicable also for proteins, would aid the exploration of novel mechanisms controlling all cellular functions, and especially within the field of redox biology and the endogenous antioxidative capacity. This would ultimately aid in developing novel targets for personalized medicine, and even for rare diseases.

7 ACKNOWLEDGEMENTS

My PhD is ending in extreme triumph, meaning that I have had a wonderful journey full of hard work, excitement, but also many difficult moments. Reaching this stage was not an easy task but it definitely feels extremely rejoicing, after 9 years of day and night work and struggles. A hard struggle that I did not choose for myself, but I found myself forced into it, and decided to never let anyone take away my dreams, values, morals, and ethics without a fight. A long fight to protect scientific integrity, particularly in medical science, where there are millions of patients or their families awaiting any small news that can alleviate their suffering. I am very happy to be able to make significant scientific contribution, but I am even more proud that I got the opportunity to support scientific integrity.

I definitely did not achieve this alone, not even a fraction of it, and without the help of many wonderful people, I would have for sure ended up without a PhD. Being right is not always enough, but it requires a supportive environment, guidance, and regulations. I was lucky enough to do my PhD in Sweden, a country that has many people who highly values scientific integrity, and even more lucky to be at a prestigious university such as Karolinska Institutet and at the department of medicine in Huddinge with all its supportive system and wonderful colleagues. I am grateful to everyone who supported me, even with only a kind word or just a smile, particularly during the dark times and moments. I would not be able to acknowledge you all, but please accept my gratitude.

With the utmost respect and gratitude, I would like to begin my acknowledgments by recognizing two individuals to whom I owe an immense debt. My current main Supervisor **Christer Betsholtz**, who I cannot find proper words to acknowledge everything you did for me, and how honored I feel to finish my PhD under your guidance. I owe you not only my future and career but also my life, without your heroic intervention, I would have ended up in uncharted waters. Your wisdom, kindness and calmness, unlimited support, brilliant guidance, and belief in my potential have been instrumental in shaping not just my academic journey but also my character. It's evident that extending a helping hand is in your nature, as I am not the first to have benefited from your remarkable generosity. You are not only one of the best and most known vascular scientists globally, but also the most ethical and moral individual I've had the privilege of knowing. You have been more than just a supervisor; you've been a genuine mentor and role model, and despite the relatively short period that I have worked with you, I have learned a lot; to act with integrity and transparency and then fear nothing. I do feel sorry for the trouble that my situation may have caused you, but if there might have been any positive outcome emerged of these troubles, then it's the opportunity it afforded me to work with you—a true blessing in my life and career. I eagerly anticipate the future adventures and meaningful research that await under your guidance. Once again, thank you from the bottom of my heart.

The second person I would like to acknowledge is our PhD study director, **Mattias Svensson**. You played a pivotal role in my academic journey by adopting me and providing a protective shield during one of the most challenging periods of my life. I was completely hopeless and

filled with distrust before I reached out to you, but you were able to rebuild this trust within a very short period through your kindness, wisdom, and expertise. You were not only the study director but my true supervisor, who did not hesitate to provide any help that was needed, even during weekends and vacations, despite your very busy schedule. I want to express my gratitude for our frequent and lengthy meetings, for the trust you've placed in me, for your unwavering belief in my potential, and for your relentless efforts to support me in recovering and achieving my dreams. Your guidance, advice, and unwavering support have been invaluable, and I am deeply appreciative.

My co-supervisor **Ákos Végvári**, I would like to express how grateful I am for everything you have done for me, for all the support, and for all the mass spec analyses. Your skillful knowledge makes nothing difficult for you, and together we solved hurdles that others have struggled with for years. Without your critical efforts, none of my work would have come to light. Thank you for believing in my potential, and for all the work you have done to help me, particularly during evenings and weekends. I am looking forward to all future mass spec work and meaningful adventures.

My co-supervisor **Lars Lund**, having an expert in cardiology and molecular cardiology like you has filled me with a profound sense of assurance in this project; for that, I am sincerely appreciative. You have consistently been approachable, supportive, resourceful, and eager to share your extensive knowledge and insights. I extend my gratitude for your support and all the valuable feedback and motivation.

My previous co-supervisor, colleague, and best friend **Mohammad Bakhtiar Hossain**, thank you for all your support. Your decision to join our group was one of the crucial catalysts that initiated all these positive changes. Your calm nature and easy-going personality make it a pleasure to work with you, and your great spirit and friendly attitude have been truly uplifting. I am grateful for all your hard work and contributions, and I eagerly anticipate all the future adventures we'll embark on together.

My mentor, **Emil Hansson**, thank you for your unwavering support, guidance, our lengthy discussions, valuable feedback, and insightful suggestions. Your composed nature and expertise were indispensable in helping me navigate the challenges during my PhD journey.

Tomas Ekström and **Maria Falkenberg**, I extend my heartfelt gratitude to both of you for diligently reviewing my monograph and providing me with fruitful suggestions and feedback. Tomas, I also want to thank you for your kind feedback and support during my halftime review, alongside **Urban Lendahl** and **Anna Wredenberg**. Your guidance and insights were invaluable and marked the beginning of the end of the challenging phase of my PhD journey. Urban and **Johan Björkegren**, I appreciate your generosity in offering me the opportunity to use your offices and for all of your kind support. Your collective support and encouragement have greatly contributed to the successful completion of my PhD journey.

Our department head, **Petter Höglund**, I extend my heartfelt gratitude for your unwavering support, especially during challenging times. Your support has been invaluable to me. I would also like to extend my thanks to all the MedH admin staff for their assistance and support throughout these years, with a special mention to **Annamaj Stolt**, **Klas Karlsson, Jenna Almosawi**, **Ulrika Markne**, and **Christina Johansson**. Your efforts have been greatly appreciated.

Our incredible group members at NEO, **Eike-Benjamin Braune**, **Francesca Del Gaudio**, **Marie Jeansson**, and **Lars Muhl**, I extend my heartfelt gratitude to each of you for your unwavering assistance, your willingness to share your vast knowledge and experience, and for generously providing access to your valuable reagents and instruments. Becoming a part of your lab was one of the most rewarding experiences after my transition to NEO, as it made me feel like a genuine member of your group. I've had the privilege of learning an incredible amount from all of you; your expertise in the field is so extensive that it seems boundless. Furthermore, I deeply appreciate the strong ethical values you uphold and all the stimulating discussions we've had. Eike, I want to express my gratitude for chairing my PhD defense; it's a tremendous honor for me. Marie, thank you for your unwavering encouragement and support, as well as for the delicious cakes you've shared, which have added a delightful touch to our lab environment. All your contributions have made a significant impact on my PhD journey. **Yuyang Miao**, I want to thank you for enjoyable company in the lab during evenings and weekends, as well as for sharing the cell culture room with me. **Katrine Dahl Bjørnholm**, I want to express my gratitude for sharing your bench and desk with me. **Martin Uhrbom**, I deeply appreciate our shared commitment to scientific integrity and ethical values. It has been my pleasure to get to know you. Thank you for your support and collaboration. **Elisabeth Raschperger**, **Sonja Gustafsson**, **Jianping Liu**, I want to express my heartfelt gratitude for the immense help and support you provided during my time at ICMC and at NEO. Your contributions have been invaluable to me, and I am deeply appreciative. Thank you Jianping for being my reference for job applications when many others refused to help. Your help meant a lot to me.

Our fellow group members at Uppsala University, **Elisa Vazquez**, I extend my heartfelt gratitude for your assistance with image analysis and for helping me get acquainted with the lab. **Malavika Bimal Desai** and **Weihan Li**, your support in setting up experiments, teaching me new techniques, and introducing me to the lab were invaluable. I also want to thank **Maarja Andaloussi Mäe**, **Konstantin Gängel**, **Liqun He**, **Riikka Pietilä**, **Michael Vanlandewijck**, **Michael Orlich**, **Hélène Leksell**, **Jana Chmielniakova**, **Veronica Sundell**, **Amanda Norrén** and all the other members of the Betsholtz' lab for their camaraderie and support. I eagerly anticipate the future adventures and meaningful research that awaits, and I am grateful for the warm and welcoming environment you provided.

Christoph Maack, having the opportunity to work with a scientist of your calibre, globally renowned in the field of molecular cardiology and redox biology, has been an immense blessing in my academic journey. I am profoundly grateful for your generous support and the invaluable

feedback you've provided throughout my PhD. I also want to take this moment to sincerely apologize for any inconvenience my situation may have caused you. Your kindness in hosting me in your lab in the beautiful city of Würzburg and providing unwavering support for my PhD project has meant the world to me. I am deeply thankful for your understanding and assistance. Furthermore, I'd like to extend my heartfelt thanks to all the members of your research group and your collaborators, particularly **Alexander Nickel**, **Michael Kohlhaas**, and **Anja Sauer**, as well as, **Katrin Streckfuß-Bömeke**, and **Jan Dudek**.

My esteemed overseas collaborators, **Cristobal dos Remedios** and **Amy Li**, I want to extend my heartfelt thanks for all the kind support, especially during the most challenging moments. Your assistance was invaluable, particularly when it was needed the most. Cris, your heroic help will never be forgotten.

Nikolay Oskolkov and **Oscar Franzén**, I want to express my sincere gratitude for your invaluable contributions and efforts in overcoming the challenges of epigenomic data analysis. Working with both of you has been a pleasure, and I appreciate your expertise and collaborative spirit.

I would like to acknowledge AstraZeneca for their generous funding and support throughout my research journey. I am especially grateful to **Kenny Hansson**, the Head of Bioscience Cardiovascular at AstraZeneca, for his incredible support. Your assistance was crucial in helping me complete my PhD, and I apologize for any trouble my PhD may have caused you. I also want to extend my thanks to all my collaborators at AstraZeneca, particularly **Fedir Kiskin**, **Susanna Eketjäll**, **Malin Palmér**, **Daniela Später** and **Qing-Dong Wang**, for their invaluable help and support throughout my research. I want to extend my heartfelt gratitude to all my co-authors from AstraZeneca, **Fredrik K.**, **Julia L.**, **Anna W.**, **Rebecca J.**, **Roland B.**, **Tanguy J.**, **Elske F.**, **Mike F.**, **Andrea D.**, **Claus B.** and **Robert I. M** for all your kind efforts and support.

I want to acknowledge and deeply thank my former and current colleagues and friends at Karolinska Institutet and **ICMC**, where I spend the majority of my PhD journey:

Humam Siga, witnessing your growth as a diligent and brilliant scientist has brought me immense joy. I want to extend my heartfelt gratitude to you for your invaluable contributions to my research. Additionally, I am grateful for the friendship we've shared and the adventures we've embarked on, both within and beyond the walls of ICMC. **Dominique Koppenhöfer** I want to express my sincere appreciation for the wealth of knowledge I've gained from you. Meeting a scientist as skilled and precise as you have been an honor, and I am truly grateful for the chance to collaborate with you. I deeply acknowledge your crucial contributions and hard work on the novel isoforms of the MLP project. **Sven Sagasser,** working with you has been an absolute blast, and I'll always remember our encounters with your single-celled creatures. Thank you for your unwavering support, your guidance in single-cell RNA sequencing, and for being there during the challenging times in the lab. Your expertise and camaraderie have

meant a great deal to me. **Lwaki Ebaras**, I extend my heartfelt thanks to you for your wisdom, valuable advice, and the wonderful company you provided during those late nights in the lab. Your presence made the hard work much more enjoyable. **Christina Savva**, or C. Western as we fondly call you, our best lab neighbor, I want to express my gratitude for all your assistance and the enjoyable discussions we've had. Your presence added a lot of value to my time in the lab. **Nina Gennebäck**, **Charlotte Webster, Sara Fernandez Leon, Phoebe K.T. Uhl, Annika Kerstin Wunsch, Raquel Firnkes**, I want to extend my gratitude for your invaluable assistance and support throughout my research journey. Thank you for your unwavering commitment to scientific excellence.

Erwin De Genst, **Jesper Sohlmér**, **Gizem Korkut**, **Eduarde Rohner**, **Omid Faridani**, **Stefanos Leptidis**, **Alan Kavsek**, **Alejandro Hidalgo-Gonzalez**, **Bing He**, **Sonia Zambrano Sevilla**, **Patricia Rodrigues**, **Rami Richi**, **Anton Gisterå**, I want to express my heartfelt gratitude for your friendship, help and camaraderie, and I am truly happy to have met you during my time at ICMC and KI. I also want to extend my thanks to all my friends and colleagues at ICMC, including, **Georgia P**, **Mimmi M**, **Aldo M**, **Nelly R**, **Emmanuelle C**, **Ilke S**, **Jerôme S**, **Kristine B**, **Katja M-H**, **Byambajav B**, **Xidan L**, **Giuseppe M**, and many others. I also want to express my gratitude to all the administrators at ICMC, including **Steven Applequist**, **Malin Engberg**, **Tove Berg**, and **Bora Baskaner**, as well as the former director of ICMC, **Bo Anglin**, and the principal investigator **Christian Riedel**. All of your unwavering support and invaluable contributions have played a crucial role in my journey, and I deeply appreciate all that you've done.

I want also to acknowledge and deeply thank my colleagues and friends at **NEO**, and particularly:

Elena Rodriguez-Vieitez and **Mukesh Varshney**, I want to extend my gratitude for the friendly chats we've had during lunch and for all the help and support you've provided. To my dear friends, **Loca Love**, **Marjan Abbasi**, **Sumonto Mitra**, **Aphrodite Demetriou**, **Debabrata Ghosh** and many others, thank you for your camaraderie and support. I also want to acknowledge the administrative support team at NEO, including **Johan Dethlefsen**, **Nantor**, and **Petri Köttö**, for their invaluable assistance. Your contributions have made my academic journey smoother, and I am truly grateful.

I also want to express my gratitude to the core facilities at NEO, with special mention to the LCI facility and its incredible members: **Sylvie Le Guyader**, **Gabriela Imreh**, and **Gisele Miranda**. Your immense help and support have been invaluable. Sylvie, I appreciate our friendly chats during lunch and all your help and support. I would also like to acknowledge the BEA facility, represented by **Fredrik Fagerström-Billai** and **David Brodin**, for their kind support. Additionally, I want to extend my thanks to all the members of the pre-clinical facility over the years, including **Moustapha Hassan**, **Mikael Zmarzlak**, **Kristian Königsson**, and **Sandra Oerther**. Your contributions have been greatly appreciated.

Navigating through the challenging phases and successfully completing my journey towards obtaining my PhD, along with all the accomplishments achieved along the way, would not have been possible without the unwavering support system at Karolinska Institutet. I want to start by expressing my heartfelt gratitude to **Belinda Pannagel**, your friendly and approachable demeanor encouraged me to speak out and seek help when I needed it the most. It all began with you, and I wish to acknowledge **Åsa Samuelsson Ökmengil**, the Doctoral Students' Ombudsperson at Medicinska Föreningen, who warmly welcomed me and provided invaluable assistance and support. Thank you for the countless lengthy meetings, for your guidance in both academic and personal matters, for motivating me to make necessary changes in my situation, for your invaluable help with initiating my halftime seminar, and for connecting me with Mattias. I also want to extend my appreciation to **Ninna Oom** from Medicinska Föreningen for her kind support and valuable advice. Additionally, I would like to express my gratitude to **Claes Frostell**, **Torkel Falkenberg**, and **Venus Azhary** for their unwavering assistance and for being instrumental in helping me overcome the challenging moments in my journey. Lastly, I want to convey my deepest thanks to the career service at KI, and in particular, **Ayla De Paepe**, for your unwavering kindness and invaluable assistance when I needed it the most. I am also thankful for the support and assistance provided by the dissertation department at KI, represented by **Gunilla Hovén Malinowski**. Your guidance and support have been instrumental in completing my journey, and I am truly appreciative.

And friends:

Abdel Rahman Ismail, to whom I owe a tremendous debt of gratitude. You may have endured some malicious practices even more than I did, yet you made the unwavering decision never to yield to pressure. You wanted me to succeed and not fall into the same exhausting path. Thank you very much for your kind advice, your comforting words, our lengthy conversations to calm down, and your visionary perspective for the future.

Ayman Alhamdow, **Rami Kallah**, **Hazem Akad**, and **Ahmad Ramzy**, you are not just friends, but dear brothers! I am profoundly thankful for your unwavering help and support, our enlightening discussions, memorable trips and adventures, your warm invitations, unforgettable evenings at Espresso House, and so much more. Additionally, I want to express my gratitude to **Mokhles Hafez**, **Hani Mobarak**, **Hatem Elmongy**, **Yaser Megali**, **Mohamed Elsayed**, **Ahmed Waraky**, **Basem Alhassan, Badreddin Radwan**, **Ahmed Aido, Mufti Mahmud Rakib**, **Osama Hallak**, **Hadi Brais** and many others for all the wonderful moments, chats, and events we've shared together and for your help and support.

Oscar Rino Granström, my bror and best friend, I want to express my sincere appreciation for sharing the room with me. Your fun-loving nature, easy-going personality, great spirit, and friendly attitude have been truly uplifting. I have never met such an innovative person like you. Thank you for being a constant source of inspiration. I also want to extend my gratitude to **Qian Lu** and **Wenjie Shen** for the wonderful moments, chats, and events we've shared together.

To Rodineliussen family, **Rasmus**, **Valentina**, **Lili** and **Leo**. You are my real family in Sweden, and I want to express my heartfelt gratitude for inviting me to your Christmas dinners and for all the wonderful moments and events we have shared together. It has been a blessing to have this friendship over all these years, and I look forward to many more to come.

To my family

To my beloved mother, **Ghalia**, you experienced every detail of this PhD journey, rejoiced in every successful experiment, and shared my sadness for every failure and every challenge I faced. I vividly remember accompanying you to your clinic when I was a child, and your deep appreciation for science and ethical values served as the inspiration that guided me into the field of biology. A word of thanks, gratitude, or any derivative thereof can never truly convey my deep appreciation for you. This thesis stands as a testament to your sacrifices for me. You held back nothing precious for our sake, and you continue to do so. I hope that through this humble work, I have brought pride and happiness to your heart. Your contentment and joy remain my ultimate aspirations in this world. I also want to pay tribute to the memory of my father, who instilled in me the values of morality, respect for humanity, and the importance of never yielding to difficulties. His legacy continues to inspire me.

To my beloved niece **Sara**, and my sister **Fatemh Zahra** and my brother-in-law **Ahmed**, A simple 'thank you' or words of gratitude, no matter how heartfelt, can never fully capture the depth of my appreciation for you. Thank you for your unwavering support and for tolerating me throughout this challenging journey. Your presence was the guiding light that led me through it. My thanks also to my extended family in Aleppo and all over the world. I hope to meet you all soon.

For those who did and continue to do their best to undermine science with their malicious practices and actions, I would like to highlight that you only made me stronger. Obtaining my PhD marks the end of one chapter, but my commitment and striving for scientific integrity will persist, whether against you or others. It is regrettable that there are no legal consequences for such actions, but I implore you to reflect on the impact your actions have had on the countless patients whose hopes you betrayed, and the precious funds wasted on personal matters and the promotion of a fictitious career. Someday, everyone will face illness or witness the suffering of loved ones, and at that time, the burden of responsibility will rest squarely upon your shoulders.

I'd like to conclude this acknowledgment with personal reflection and a message for anyone who might find themselves in a similar situation. It's crucial to remember that even in the darkest of times, there's always a glimmer of hope. Just three years ago, I couldn't see any light at the end of the tunnel. Six years of an arduous and unjust battle had drained me of all my strength. However, I remained resolute in my commitment to never compromise my values or yield to pressure. In truth, my situation couldn't worsen any further, and I had nothing left to lose. It was this realization, coupled with the unwavering support of true friends, that bolstered my courage to speak out and seek help. Through this journey, I discovered that kind-hearted

colleagues and coworkers often surround us, even if they may not be privy to all the intricate details of our struggles. I also learned that oppressors are often weaker than they appear, akin to fragile spiderwebs that collapse with the gentlest touch. Being in Sweden and at Karolinska Institutet, with their supportive regulations and systems, undeniably played a pivotal role in my case. However, it's essential to recognize that even the most well-intentioned regulations may still harbour loopholes. Therefore, it's not sufficient to be in the right; your morality must be fortified by power—indisputable evidence. After all, few will rally behind a cause without the undeniable weight of proof.

My PhD journey is drawing to a close, and it's concluding in the best possible scenario—one I wouldn't have dared to dream of. It has brought me achievements that I might not have accomplished even after a long and exhausting postdoc. However, **the most significant reward of this tough journey has been the remarkable individuals it introduced me to**—people I would have never crossed paths with otherwise. These are individuals who uphold values such as integrity, morality, and ethics, which lie at the core of our existence and the legacy we aim to leave behind. If I could turn back time, I wouldn't change a thing. I'd walk the same path, even making the same mistakes and undoubtedly committing new ones along the way. And I'd do it all without an ounce of regret, eternally proud of the choices I've made.

8 REFERENCES

Abate, C., Patel, L., Rauscher, F.J., 3rd, and Curran, T. (1990). Redox regulation of fos and jun DNA-binding activity in vitro. Science *249*, 1157-1161.

Akbay, E.A., Moslehi, J., Christensen, C.L., Saha, S., Tchaicha, J.H., Ramkissoon, S.H., Stewart, K.M., Carretero, J., Kikuchi, E., Zhang, H., et al. (2014). D-2-hydroxyglutarate produced by mutant IDH2 causes cardiomyopathy and neurodegeneration in mice. Genes & development *28*, 479-490.

Ambardekar, A.V., and Buttrick, P.M. (2011). Reverse remodeling with left ventricular assist devices: a review of clinical, cellular, and molecular effects. Circ Heart Fail *4*, 224-233.

Arber, S. (1994). Muscle LIM protein, a novel essential regulator of myogenesis, promotes myogenic differentiation. Cell *79*, 221-231.

Arber, S., Hunter, J.J., Ross, J., Hongo, M., Sansig, G., Borg, J., Perriard, J.-C., Chien, K.R., and Caroni, P. (1997). MLP-Deficient Mice Exhibit a Disruption of Cardiac Cytoarchitectural Organization, Dilated Cardiomyopathy, and Heart Failure. Cell *88*, 393-403.

Auclair, J.R., Brodkin, H.R., D'Aquino, J.A., Petsko, G.A., Ringe, D., and Agar, J.N. (2013). Structural consequences of cysteinylation of Cu/Zn-superoxide dismutase. Biochemistry *52*, 6145-6150.

Baker, M. (2015). Reproducibility crisis: Blame it on the antibodies. Nature *521*, 274-276.

Balaban, R.S., Nemoto, S., and Finkel, T. (2005). Mitochondria, oxidants, and aging. Cell *120*, 483-495.

Balligand, J.L., Kobzik, L., Han, X., Kaye, D.M., Belhassen, L., O'Hara, D.S., Kelly, R.A., Smith, T.W., and Michel, T. (1995). Nitric oxide-dependent parasympathetic signaling is due to activation of constitutive endothelial (type III) nitric oxide synthase in cardiac myocytes. The Journal of biological chemistry *270*, 14582-14586.

Balligand, J.L., Ungureanu-Longrois, D., Simmons, W.W., Pimental, D., Malinski, T.A., Kapturczak, M., Taha, Z., Lowenstein, C.J., Davidoff, A.J., and Kelly, R.A. (1994). Cytokine-inducible nitric oxide synthase (iNOS) expression in cardiac myocytes. Characterization and regulation of iNOS expression and detection of iNOS activity in single cardiac myocytes in vitro. Journal of Biological Chemistry *269*, 27580-27588.

Baumer, A.T., Flesch, M., Wang, X., Shen, Q., Feuerstein, G.Z., and Bohm, M. (2000). Antioxidative enzymes in human hearts with idiopathic dilated cardiomyopathy. Journal of Molecular and Cellular Cardiology *32*, 121-130.

Benderdour, M., Charron, G., Comte, B., Ayoub, R., Beaudry, D., Foisy, S., Deblois, D., and Des Rosiers, C. (2004). Decreased cardiac mitochondrial NADP+-isocitrate dehydrogenase activity and expression: a marker of oxidative stress in hypertrophy development. American journal of physiology. Heart and circulatory physiology *287*, H2122-2131.

Bertero, E., and Maack, C. (2018). Metabolic remodelling in heart failure. Nature Reviews Cardiology *15*, 457-470.

Blaskovic, S., Blanc, M., and van der Goot, F.G. (2013). What does S-palmitoylation do to membrane proteins? FEBS J *280*, 2766-2774.

Boateng, S.Y., Belin, R.J., Geenen, D.L., Margulies, K.B., Martin, J.L., Hoshijima, M., de Tombe, P.P., and Russell, B. (2007). Cardiac dysfunction and heart failure are associated

with abnormalities in the subcellular distribution and amounts of oligomeric muscle LIM protein. American journal of physiology. Heart and circulatory physiology *292*, H259-269.

Bortolotti, M., Polito, L., Battelli, M.G., and Bolognesi, A. (2021). Xanthine oxidoreductase: One enzyme for multiple physiological tasks. Redox biology *41*, 101882.

Brennan, M.S., Matos, M.F., Richter, K.E., Li, B., and Scannevin, R.H. (2017). The NRF2 transcriptional target, OSGIN1, contributes to monomethyl fumarate-mediated cytoprotection in human astrocytes. Scientific reports *7*, 42054.

Broughton, J.P., Lovci, M.T., Huang, J.L., Yeo, G.W., and Pasquinelli, A.E. (2016). Pairing beyond the Seed Supports MicroRNA Targeting Specificity. Molecular cell *64*, 320-333.

Brown, K.K., and Hampton, M.B. (2011). Biological targets of isothiocyanates. Biochimica et biophysica acta *1810*, 888-894.

Bunik, V.I., and Degtyarev, D. (2008). Structure-function relationships in the 2-oxo acid dehydrogenase family: substrate-specific signatures and functional predictions for the 2-oxoglutarate dehydrogenase-like proteins. Proteins *71*, 874-890.

Burkhoff, D., Topkara, V.K., Sayer, G., and Uriel, N. (2021). Reverse Remodeling With Left Ventricular Assist Devices. Circulation research *128*, 1594-1612.

Cairns, R.A., and Mak, T.W. (2013). Oncogenic isocitrate dehydrogenase mutations: mechanisms, models, and clinical opportunities. Cancer discovery *3*, 730-741.

Canning, P., and Bullock, A.N. (2014). New strategies to inhibit KEAP1 and the Cul3-based E3 ubiquitin ligases. Biochem Soc Trans *42*, 103-107.

Charron, G., Li, M.M., MacDonald, M.R., and Hang, H.C. (2013). Prenylome profiling reveals S-farnesylation is crucial for membrane targeting and antiviral activity of ZAP long-isoform. Proceedings of the National Academy of Sciences of the United States of America *110*, 11085-11090.

Chen, H., Denton, T.T., Xu, H., Calingasan, N., Beal, M.F., and Gibson, G.E. (2016). Reductions in the mitochondrial enzyme alpha-ketoglutarate dehydrogenase complex in neurodegenerative disease - beneficial or detrimental? Journal of neurochemistry *139*, 823-838.

Cheng, X., Ku, C.H., and Siow, R.C. (2013). Regulation of the Nrf2 antioxidant pathway by microRNAs: New players in micromanaging redox homeostasis. Free radical biology & medicine *64*, 4-11.

Chung, H.S., Wang, S.B., Venkatraman, V., Murray, C.I., and Van Eyk, J.E. (2013). Cysteine oxidative posttranslational modifications: emerging regulation in the cardiovascular system. Circulation research *112*, 382-392.

Comte, B., Vincent, G., Bouchard, B., Benderdour, M., and Des Rosiers, C. (2002). Reverse flux through cardiac NADP(+)-isocitrate dehydrogenase under normoxia and ischemia. American journal of physiology. Heart and circulatory physiology *283*, H1505-1514.

Corsten, M.F., Dennert, R., Jochems, S., Kuznetsova, T., Devaux, Y., Hofstra, L., Wagner, D.R., Staessen, J.A., Heymans, S., and Schroen, B. (2010). Circulating MicroRNA-208b and MicroRNA-499 reflect myocardial damage in cardiovascular disease. Circ Cardiovasc Genet *3*, 499-506.

Cullinan, S.B., Zhang, D., Hannink, M., Arvisais, E., Kaufman, R.J., and Diehl, J.A. (2003). Nrf2 is a direct PERK substrate and effector of PERK-dependent cell survival. Mol Cell Biol *23*, 7198-7209.

Cunnington, C., Van Assche, T., Shirodaria, C., Kylintireas, I., Lindsay, A.C., Lee, J.M., Antoniades, C., Margaritis, M., Lee, R., Cerrato, R., et al. (2012). Systemic and vascular oxidation limits the efficacy of oral tetrahydrobiopterin treatment in patients with coronary artery disease. Circulation *125*, 1356-1366.

Dai, W., Xu, L., Yu, X., Zhang, G., Guo, H., Liu, H., Song, G., Weng, S., Dong, L., Zhu, J., et al. (2020). OGDHL silencing promotes hepatocellular carcinoma by reprogramming glutamine metabolism. J Hepatol *72*, 909-923.

Dass, S., Holloway, C.J., Cochlin, L.E., Rider, O.J., Mahmod, M., Robson, M., Sever, E., Clarke, K., Watkins, H., Ashrafian, H., et al. (2015). No Evidence of Myocardial Oxygen Deprivation in Nonischemic Heart Failure. Circ Heart Fail *8*, 1088-1093.

de Zeeuw, D., Akizawa, T., Audhya, P., Bakris, G.L., Chin, M., Christ-Schmidt, H., Goldsberry, A., Houser, M., Krauth, M., Lambers Heerspink, H.J., et al. (2013). Bardoxolone methyl in type 2 diabetes and stage 4 chronic kidney disease. New England Journal of Medicine *369*, 2492-2503.

Dinkova-Kostova, A.T., Holtzclaw, W.D., Cole, R.N., Itoh, K., Wakabayashi, N., Katoh, Y., Yamamoto, M., and Talalay, P. (2002). Direct evidence that sulfhydryl groups of Keap1 are the sensors regulating induction of phase 2 enzymes that protect against carcinogens and oxidants. Proceedings of the National Academy of Sciences of the United States of America *99*, 11908-11913.

Doenst, T., Nguyen, T.D., and Abel, E.D. (2013). Cardiac metabolism in heart failure: implications beyond ATP production. Circulation research *113*, 709-724.

Eijgenraam, T.R., Sillje, H.H.W., and de Boer, R.A. (2020). Current understanding of fibrosis in genetic cardiomyopathies. Trends Cardiovasc Med *30*, 353-361.

Elbeck, Z., Hossain, M.B., Siga, H., Oskolkov, N., Karlsson, F., Lindgren, J., Walentinsson, A., Remedios, C.D., Koppenhöfer, D., Jarvis, R., et al. (2022). Epigenetic modulators link mitochondrial redox homeostasis to cardiac function. BioRxiv.

EMBL-EBI (2019). Isocitrate/isopropylmalate dehydrogenase. (European Molecular Biology Laboratory).

Espinosa-Diez, C., Miguel, V., Mennerich, D., Kietzmann, T., Sanchez-Perez, P., Cadenas, S., and Lamas, S. (2015). Antioxidant responses and cellular adjustments to oxidative stress. Redox biology *6*, 183-197.

Esterbauer, H., Wag, G., and Puhl, H. (1993). Lipid peroxidation and its role in atherosclerosis. Br Med Bull *49*, 566-576.

Fan, J., Teng, X., Liu, L., Mattaini, K.R., Looper, R.E., Vander Heiden, M.G., and Rabinowitz, J.D. (2015). Human phosphoglycerate dehydrogenase produces the oncometabolite D-2-hydroxyglutarate. ACS Chem Biol *10*, 510-516.

Fierro-Fernandez, M., Miguel, V., and Lamas, S. (2016). Role of redoximiRs in fibrogenesis. Redox biology *7*, 58-67.

Frizzell, N., Lima, M., and Baynes, J.W. (2011). Succination of proteins in diabetes. Free Radic Res *45*, 101-109.

Fu, X., Huang, X., Li, P., Chen, W., and Xia, M. (2014). 7-Ketocholesterol inhibits isocitrate dehydrogenase 2 expression and impairs endothelial function via microRNA-144. Free radical biology & medicine *71*, 1-15.

Gaasch, W.H., and Zile, M.R. (2011). Left ventricular structural remodeling in health and disease: with special emphasis on volume, mass, and geometry. Journal of the American College of Cardiology *58*, 1733-1740.

Gebert, L.F.R., and MacRae, I.J. (2019). Regulation of microRNA function in animals. Nat Rev Mol Cell Biol *20*, 21-37.

Gehmlich, K., Geier, C., Osterziel, K.J., Van der Ven, P.F., and Furst, D.O. (2004). Decreased interactions of mutant muscle LIM protein (MLP) with N-RAP and alpha-actinin and their implication for hypertrophic cardiomyopathy. Cell Tissue Res *317*, 129-136.

Geier, C., Perrot, A., Ozcelik, C., Binner, P., Counsell, D., Hoffmann, K., Pilz, B., Martiniak, Y., Gehmlich, K., van der Ven, P.F., et al. (2003). Mutations in the human muscle LIM protein gene in families with hypertrophic cardiomyopathy. Circulation *107*, 1390-1395.

Gidlof, O., Andersson, P., van der Pals, J., Gotberg, M., and Erlinge, D. (2011). Cardiospecific microRNA plasma levels correlate with troponin and cardiac function in patients with ST elevation myocardial infarction, are selectively dependent on renal elimination, and can be detected in urine samples. Cardiology *118*, 217-226.

Gilsbach, R., Preissl, S., Gruning, B.A., Schnick, T., Burger, L., Benes, V., Wurch, A., Bonisch, U., Gunther, S., Backofen, R., et al. (2014). Dynamic DNA methylation orchestrates cardiomyocyte development, maturation and disease. Nature communications *5*, 5288.

Gilsbach, R., Schwaderer, M., Preissl, S., Gruning, B.A., Kranzhofer, D., Schneider, P., Nuhrenberg, T.G., Mulero-Navarro, S., Weichenhan, D., Braun, C., et al. (2018). Distinct epigenetic programs regulate cardiac myocyte development and disease in the human heart in vivo. Nature communications *9*, 391.

Gramlich, M., Michely, B., Krohne, C., Heuser, A., Erdmann, B., Klaassen, S., Hudson, B., Magarin, M., Kirchner, F., Todiras, M., et al. (2009). Stress-induced dilated cardiomyopathy in a knock-in mouse model mimicking human titin-based disease. J Mol Cell Cardiol *47*, 352-358.

Greco, C.M., Kunderfranco, P., Rubino, M., Larcher, V., Carullo, P., Anselmo, A., Kurz, K., Carell, T., Angius, A., Latronico, M.V., et al. (2016). DNA hydroxymethylation controls cardiomyocyte gene expression in development and hypertrophy. Nature communications *7*, 12418.

Grieve, D.J., Byrne, J.A., Cave, A.C., and Shah, A.M. (2004). Role of oxidative stress in cardiac remodelling after myocardial infarction. Heart Lung Circ *13*, 132-138.

Groenewegen, A., Rutten, F.H., Mosterd, A., and Hoes, A.W. (2020). Epidemiology of heart failure. Eur J Heart Fail *22*, 1342-1356.

Hage, C., Michaelsson, E., Linde, C., Donal, E., Daubert, J.C., Gan, L.M., and Lund, L.H. (2017). Inflammatory Biomarkers Predict Heart Failure Severity and Prognosis in Patients With Heart Failure With Preserved Ejection Fraction: A Holistic Proteomic Approach. Circ Cardiovasc Genet *10*.

Herwig, M., Kolijn, D., Lodi, M., Holper, S., Kovacs, A., Papp, Z., Jaquet, K., Haldenwang, P., Dos Remedios, C., Reusch, P.H., et al. (2020). Modulation of Titin-Based Stiffness in Hypertrophic Cardiomyopathy via Protein Kinase D. Front Physiol *11*, 240.

Hofseth, L.J. (2018). Getting rigorous with scientific rigor. Carcinogenesis *39*, 21-25.

Hori, M., and Nishida, K. (2009). Oxidative stress and left ventricular remodelling after myocardial infarction. Cardiovascular research *81*, 457-464.

Hoshijima, M. (2006). Mechanical stress-strain sensors embedded in cardiac cytoskeleton: Z disk, titin, and associated structures. American journal of physiology. Heart and circulatory physiology *290*, H1313-1325.

Huang, H.C., Nguyen, T., and Pickett, C.B. (2002). Phosphorylation of Nrf2 at Ser-40 by protein kinase C regulates antioxidant response element-mediated transcription. The Journal of biological chemistry *277*, 42769-42774.

Hupfeld, J., Ernst, M., Knyrim, M., Binas, S., Kloeckner, U., Rabe, S., Quarch, K., Misiak, D., Fuszard, M., Grossmann, C., et al. (2021). miR-208b Reduces the Expression of Kcnj5 in a Cardiomyocyte Cell Line. Biomedicines *9*.

Intlekofer, A.M., Dematteo, R.G., Venneti, S., Finley, L.W., Lu, C., Judkins, A.R., Rustenburg, A.S., Grinaway, P.B., Chodera, J.D., Cross, J.R., et al. (2015). Hypoxia Induces Production of L-2-Hydroxyglutarate. Cell metabolism *22*, 304-311.

Intlekofer, A.M., Wang, B., Liu, H., Shah, H., Carmona-Fontaine, C., Rustenburg, A.S., Salah, S., Gunner, M.R., Chodera, J.D., Cross, J.R., et al. (2017). L-2-Hydroxyglutarate production arises from noncanonical enzyme function at acidic pH. Nature chemical biology *13*, 494-500.

Islam, M.S., Leissing, T.M., Chowdhury, R., Hopkinson, R.J., and Schofield, C.J. (2018). 2-Oxoglutarate-Dependent Oxygenases. Annual Review of Biochemistry *87*, 585-620.

Itoh, T., Takeda, S., and Akao, Y. (2010). MicroRNA-208 modulates BMP-2-stimulated mouse preosteoblast differentiation by directly targeting V-ets erythroblastosis virus E26 oncogene homolog 1. The Journal of biological chemistry *285*, 27745-27752.

Janssen, M., Koster, J.F., Bos, E., and de Jong, J.W. (1993). Malondialdehyde and glutathione production in isolated perfused human and rat hearts. Circulation research *73*, 681-688.

Janssen, Y.M., Matalon, S., and Mossman, B.T. (1997). Differential induction of c-fos, c-jun, and apoptosis in lung epithelial cells exposed to ROS or RNS. Am J Physiol *273*, L789-796.

Jefferies, J.L., and Towbin, J.A.J.T.L. (2010). Dilated cardiomyopathy. *375*, 752-762.

Karlstaedt, A., Zhang, X., Vitrac, H., Harmancey, R., Vasquez, H., Wang, J.H., Goodell, M.A., and Taegtmeyer, H. (2016). Oncometabolite d-2-hydroxyglutarate impairs alpha-ketoglutarate dehydrogenase and contractile function in rodent heart. Proceedings of the National Academy of Sciences *113*, 10436-10441.

Kaufman, E.E., Nelson, T., Fales, H.M., and Levin, D.M. (1988). Isolation and characterization of a hydroxyacid-oxoacid transhydrogenase from rat kidney mitochondria. The Journal of biological chemistry *263*, 16872-16879.

Kil, I.S., and Park, J.W. (2005). Regulation of mitochondrial NADP+-dependent isocitrate dehydrogenase activity by glutathionylation. The Journal of biological chemistry *280*, 10846-10854.

Knoll, R., Hoshijima, M., Hoffman, H.M., Person, V., Lorenzen-Schmidt, I., Bang, M.L., Hayashi, T., Shiga, N., Yasukawa, H., Schaper, W., et al. (2002). The cardiac mechanical stretch sensor machinery involves a Z disc complex that is defective in a subset of human dilated cardiomyopathy. Cell *111*, 943-955.

Knowles, R.G., and Moncada, S. (1994). Nitric oxide synthases in mammals. Biochem J *298 (Pt 2)*, 249-258.

Koivunen, P., and Laukka, T. (2018). The TET enzymes. Cellular and molecular life sciences : CMLS *75*, 1339-1348.

Koju, N., Qin, Z.H., and Sheng, R. (2022). Reduced nicotinamide adenine dinucleotide phosphate in redox balance and diseases: a friend or foe? Acta Pharmacol Sin.

Kranendijk, M., Struys, E.A., Salomons, G.S., Van der Knaap, M.S., and Jakobs, C. (2012). Progress in understanding 2-hydroxyglutaric acidurias. J Inherit Metab Dis *35*, 571-587.

Ku, H.J., Ahn, Y., Lee, J.H., Park, K.M., and Park, J.W. (2015). IDH2 deficiency promotes mitochondrial dysfunction and cardiac hypertrophy in mice. Free radical biology & medicine *80*, 84-92.

Lee, B.R., and Kamitani, T. (2011). Improved immunodetection of endogenous alpha-synuclein. PloS one *6*, e23939.

Lee, D.F., Kuo, H.P., Liu, M., Chou, C.K., Xia, W., Du, Y., Shen, J., Chen, C.T., Huo, L., Hsu, M.C., et al. (2009). KEAP1 E3 ligase-mediated downregulation of NF-kappaB signaling by targeting IKKbeta. Molecular cell *36*, 131-140.

Levin, E., Leibinger, M., Gobrecht, P., Hilla, A., Andreadaki, A., and Fischer, D. (2019). Muscle LIM Protein Is Expressed in the Injured Adult CNS and Promotes Axon Regeneration. Cell reports *26*, 1021-1032 e1026.

Liao, J., Li, Q., Hu, Z., Yu, W., Zhang, K., Ma, F., Han, Q., Zhang, H., Guo, J., Hu, L., et al. (2022). Mitochondrial miR-1285 regulates copper-induced mitochondrial dysfunction and mitophagy by impairing IDH2 in pig jejunal epithelial cells. J Hazard Mater *422*, 126899.

Lim, G., Venetucci, L., Eisner, D.A., and Casadei, B. (2008). Does nitric oxide modulate cardiac ryanodine receptor function? Implications for excitation-contraction coupling. Cardiovascular research *77*, 256-264.

Lin, A.P., Abbas, S., Kim, S.W., Ortega, M., Bouamar, H., Escobedo, Y., Varadarajan, P., Qin, Y., Sudderth, J., Schulz, E., et al. (2015). D2HGDH regulates alpha-ketoglutarate levels and dioxygenase function by modulating IDH2. Nature communications *6*, 7768.

Lingappan, K. (2018). NF-kappaB in Oxidative Stress. Curr Opin Toxicol *7*, 81-86.

Lu, S.C. (2013). Glutathione synthesis. Biochimica et biophysica acta *1830*, 3143-3153.

Lucas, D.T., and Szweda, L.I. (1999). Declines in mitochondrial respiration during cardiac reperfusion: age-dependent inactivation of alpha-ketoglutarate dehydrogenase. Proceedings of the National Academy of Sciences of the United States of America *96*, 6689-6693.

Ma, S., Sun, R., Jiang, B., Gao, J., Deng, W., Liu, P., He, R., Cui, J., Ji, M., Yi, W., et al. (2017). L2hgdh Deficiency Accumulates l-2-Hydroxyglutarate with Progressive Leukoencephalopathy and Neurodegeneration. Mol Cell Biol *37*.

Maas, E., and Bisswanger, H. (1990). Localization of the α-oxoacid dehydrogenase multienzyme complexes within the mitochondrion. FEBS Letters *277*, 189-190.

Mailloux, R.J., Gardiner, D., and O'Brien, M. (2016). 2-Oxoglutarate dehydrogenase is a more significant source of O2(.-)/H2O2 than pyruvate dehydrogenase in cardiac and liver tissue. Free radical biology & medicine *97*, 501-512.

Mathiyalagan, P., Okabe, J., Chang, L., Su, Y., Du, X.J., and El-Osta, A. (2014). The primary microRNA-208b interacts with Polycomb-group protein, Ezh2, to regulate gene expression in the heart. Nucleic Acids Res *42*, 790-803.

McKenna, W.J., Maron, B.J., and Thiene, G. (2017). Classification, Epidemiology, and Global Burden of Cardiomyopathies. Circulation research *121*, 722-730.

Meister, A. (1988). Glutathione metabolism and its selective modification. Journal of Biological Chemistry *263*, 17205-17208.

Meng, Y., and Li, L.J.a.p.a. (2021). Cysteine post-translational modifications: ten years from chemical proteomics to bioinformatics.

Merlo, M., Caiffa, T., Gobbo, M., Adamo, L., and Sinagra, G. (2018). Reverse remodeling in Dilated Cardiomyopathy: Insights and future perspectives. Int J Cardiol Heart Vasc *18*, 52-57.

Milo, R., and Phillips, R. (2015). Cell biology by the numbers. (Garland Science).

Minamino, T., and Kitakaze, M. (2010). ER stress in cardiovascular disease. J Mol Cell Cardiol *48*, 1105-1110.

Moini, H., Packer, L., and Saris, N.E. (2002). Antioxidant and prooxidant activities of alpha-lipoic acid and dihydrolipoic acid. Toxicol Appl Pharmacol *182*, 84-90.

Moore, M.J., Scheel, T.K., Luna, J.M., Park, C.Y., Fak, J.J., Nishiuchi, E., Rice, C.M., and Darnell, R.B. (2015). miRNA-target chimeras reveal miRNA 3'-end pairing as a major determinant of Argonaute target specificity. Nature communications *6*, 8864.

Moreno-Loshuertos, R., Acin-Perez, R., Fernandez-Silva, P., Movilla, N., Perez-Martos, A., Rodriguez de Cordoba, S., Gallardo, M.E., and Enriquez, J.A. (2006). Differences in reactive oxygen species production explain the phenotypes associated with common mouse mitochondrial DNA variants. Nat Genet *38*, 1261-1268.

Munro, D., and Treberg, J.R. (2017). A radical shift in perspective: mitochondria as regulators of reactive oxygen species. J Exp Biol *220*, 1170-1180.

Munzel, T., Camici, G.G., Maack, C., Bonetti, N.R., Fuster, V., and Kovacic, J.C. (2017). Impact of Oxidative Stress on the Heart and Vasculature: Part 2 of a 3-Part Series. Journal of the American College of Cardiology *70*, 212-229.

Murphy, M.P. (2009). How mitochondria produce reactive oxygen species. Biochem J *417*, 1-13.

Nauta, J.F., Hummel, Y.M., Tromp, J., Ouwerkerk, W., Van Der Meer, P., Jin, X., Lam, C.S.P., Bax, J.J., Metra, M., Samani, N.J., et al. (2019). Concentric vs. eccentric remodelling in heart failure with reduced ejection fraction: clinical characteristics, pathophysiology and response to treatment. European Journal of Heart Failure.

NCBI (2019a). IDH2 isocitrate dehydrogenase (NADP(+)) 2 [Homo sapiens (human)]. In NCBI, Protein Atlas.

NCBI (2019b). IDH3A isocitrate dehydrogenase (NAD(+)) 3 catalytic subunit alpha [Homo sapiens (human)]. In NCBI. Protein Atlas.

Nickel, A.G., von Hardenberg, A., Hohl, M., Loffler, J.R., Kohlhaas, M., Becker, J., Reil, J.C., Kazakov, A., Bonnekoh, J., Stadelmaier, M., et al. (2015). Reversal of Mitochondrial Transhydrogenase Causes Oxidative Stress in Heart Failure. Cell metabolism *22*, 472-484.

Nordberg, J., and Arnér, E.S.J. (2001). Reactive oxygen species, antioxidants, and the mammalian thioredoxin system1 1This review is based on the licentiate thesis “Thioredoxin reductase—interactions with the redox active compounds 1-chloro-2,4-dinitrobenzene and lipoic acid” by Jonas Nordberg, 2001, Karolinska Institute, Stockholm, ISBN 91-631-1064-4. Free Radical Biology and Medicine *31*, 1287-1312.

Oldford, C., Kuksal, N., Gill, R., Young, A., and Mailloux, R.J. (2019). Estimation of the hydrogen peroxide producing capacities of liver and cardiac mitochondria isolated from C57BL/6N and C57BL/6J mice. Free radical biology & medicine *135*, 15-27.

Oldham, W.M., Clish, C.B., Yang, Y., and Loscalzo, J. (2015). Hypoxia-Mediated Increases in L-2-hydroxyglutarate Coordinate the Metabolic Response to Reductive Stress. Cell metabolism *22*, 291-303.

Omens, J.H., Usyk, T.P., Li, Z., and McCulloch, A.D. (2002). Muscle LIM protein deficiency leads to alterations in passive ventricular mechanics. American journal of physiology. Heart and circulatory physiology *282*, H680-687.

Palmer, B.M. (2005). Thick filament proteins and performance in human heart failure. Heart failure reviews *10*, 187-197.

Palmer, J.W., Tandler, B., and Hoppel, C.L. (1977). Biochemical properties of subsarcolemmal and interfibrillar mitochondria isolated from rat cardiac muscle. The Journal of biological chemistry *252*, 8731-8739.

Pepin, M.E., Drakos, S., Ha, C.M., Tristani-Firouzi, M., Selzman, C.H., Fang, J.C., Wende, A.R., and Wever-Pinzon, O. (2019a). DNA methylation reprograms cardiac metabolic gene expression in end-stage human heart failure. American journal of physiology. Heart and circulatory physiology *317*, H674-H684.

Pepin, M.E., Ha, C.M., Crossman, D.K., Litovsky, S.H., Varambally, S., Barchue, J.P., Pamboukian, S.V., Diakos, N.A., Drakos, S.G., Pogwizd, S.M., et al. (2019b). Genome-wide DNA methylation encodes cardiac transcriptional reprogramming in human ischemic heart failure. Laboratory investigation; a journal of technical methods and pathology *99*, 371-386.

Picelli, S., Faridani, O.R., Bjorklund, A.K., Winberg, G., Sagasser, S., and Sandberg, R. (2014). Full-length RNA-seq from single cells using Smart-seq2. Nature Protocols *9*, 171-181.

Ponnaluri, V.K., Ehrlich, K.C., Zhang, G., Lacey, M., Johnston, D., Pradhan, S., and Ehrlich, M. (2017). Association of 5-hydroxymethylation and 5-methylation of DNA cytosine with tissue-specific gene expression. Epigenetics *12*, 123-138.

Prosser, B.L., Ward, C.W., and Lederer, W.J. (2011). X-ROS signaling: rapid mechano-chemo transduction in heart. Science *333*, 1440-1445.

Richard, P., Villard, E., Charron, P., and Isnard, R. (2006). The Genetic Bases of Cardiomyopathies. Journal of the American College of Cardiology *48*, A79-A89.

Ross, D., and Siegel, D. (2004). NAD(P)H:quinone oxidoreductase 1 (NQO1, DT-diaphorase), functions and pharmacogenetics. Methods Enzymol *382*, 115-144.

Sack, M.N., Fyhrquist, F.Y., Saijonmaa, O.J., Fuster, V., and Kovacic, J.C. (2017). Basic Biology of Oxidative Stress and the Cardiovascular System: Part 1 of a 3-Part Series. Journal of the American College of Cardiology *70*, 196-211.

Salamov, A.A., Nishikawa, T., and Swindells, M.B. (1998). Assessing protein coding region integrity in cDNA sequencing projects. Bioinformatics *14*, 384-390.

Sanchez, G., Pedrozo, Z., Domenech, R.J., Hidalgo, C., and Donoso, P. (2005). Tachycardia increases NADPH oxidase activity and RyR2 S-glutathionylation in ventricular muscle. J Mol Cell Cardiol *39*, 982-991.

Santos, C.X., Anilkumar, N., Zhang, M., Brewer, A.C., Shah, A.M.J.F.R.B., and Medicine (2011). Redox signaling in cardiac myocytes. Free Radical Biology and Medicine *50*, 777-793.

Sarhene, M., Wang, Y., Wei, J., Huang, Y., Li, M., Li, L., Acheampong, E., Zhengcan, Z., Xiaoyan, Q., Yunsheng, X., et al. (2019). Biomarkers in heart failure: the past, current and future. Heart failure reviews *24*, 867-903.

Satoh, M., Minami, Y., Takahashi, Y., Tabuchi, T., and Nakamura, M. (2010). Expression of microRNA-208 is associated with adverse clinical outcomes in human dilated cardiomyopathy. J Card Fail *16*, 404-410.

Schwertner, H.A., and Vitek, L. (2008). Gilbert syndrome, UGT1A1*28 allele, and cardiovascular disease risk: possible protective effects and therapeutic applications of bilirubin. Atherosclerosis *198*, 1-11.

Sen, T., Sen, N., Noordhuis, M.G., Ravi, R., Wu, T.C., Ha, P.K., Sidransky, D., and Hoque, M.O. (2012). OGDHL is a modifier of AKT-dependent signaling and NF-kappaB function. PloS one *7*, e48770.

Shelar, S., Shim, E.H., Brinkley, G.J., Kundu, A., Carobbio, F., Poston, T., Tan, J., Parekh, V., Benson, D., Crossman, D.K., et al. (2018). Biochemical and Epigenetic Insights into L-2-Hydroxyglutarate, a Potential Therapeutic Target in Renal Cancer. Clin Cancer Res *24*, 6433-6446.

Sielemann, K., Elbeck, Z., Gartner, A., Brodehl, A., Stanasiuk, C., Fox, H., Paluszkiewicz, L., Tiesmeier, J., Wlost, S., Gummert, J., et al. (2020). Distinct Myocardial Transcriptomic Profiles of Cardiomyopathies Stratified by the Mutant Genes. Genes (Basel) *11*.

Singh, N., and Bhalla, N. (2020). Moonlighting Proteins. Annu Rev Genet *54*, 265-285.

Smith, A.J., Clutton, R.E., Lilley, E., Hansen, K.E.A., and Brattelid, T. (2018). PREPARE: guidelines for planning animal research and testing. Lab Animal *52*, 135-141.

Song, M., Chen, Y., Gong, G., Murphy, E., Rabinovitch, P.S., and Dorn, G.W., 2nd (2014). Super-suppression of mitochondrial reactive oxygen species signaling impairs compensatory autophagy in primary mitophagic cardiomyopathy. Circulation research *115*, 348-353.

Sozen, E., Karademir, B., and Ozer, N.K. (2015). Basic mechanisms in endoplasmic reticulum stress and relation to cardiovascular diseases. Free radical biology & medicine *78*, 30-41.

Spruijt, C.G., Gnerlich, F., Smits, A.H., Pfaffeneder, T., Jansen, P.W., Bauer, C., Munzel, M., Wagner, M., Muller, M., Khan, F., et al. (2013). Dynamic readers for 5-(hydroxy)methylcytosine and its oxidized derivatives. Cell *152*, 1146-1159.

Starkov, A.A. (2013). An update on the role of mitochondrial alpha-ketoglutarate dehydrogenase in oxidative stress. Molecular and cellular neurosciences *55*, 13-16.

Starkov, A.A., Fiskum, G., Chinopoulos, C., Lorenzo, B.J., Browne, S.E., Patel, M.S., and Beal, M.F. (2004). Mitochondrial alpha-ketoglutarate dehydrogenase complex generates

reactive oxygen species. The Journal of neuroscience : the official journal of the Society for Neuroscience *24*, 7779-7788.

Steenweg, M.E., Jakobs, C., Errami, A., van Dooren, S.J., Adeva Bartolome, M.T., Aerssens, P., Augoustides-Savvapoulou, P., Baric, I., Baumann, M., Bonafe, L., et al. (2010). An overview of L-2-hydroxyglutarate dehydrogenase gene (L2HGDH) variants: a genotype-phenotype study. Hum Mutat *31*, 380-390.

Strong, E. (2021). The Cardiac Action Potential. YouTube.

Struys, E.A., Salomons, G.S., Achouri, Y., Van Schaftingen, E., Grosso, S., Craigen, W.J., Verhoeven, N.M., and Jakobs, C. (2005). Mutations in the D-2-hydroxyglutarate dehydrogenase gene cause D-2-hydroxyglutaric aciduria. Am J Hum Genet *76*, 358-360.

Sucharov, C.C., Kao, D.P., Port, J.D., Karimpour-Fard, A., Quaife, R.A., Minobe, W., Nunley, K., Lowes, B.D., Gilbert, E.M., and Bristow, M.R. (2017). Myocardial microRNAs associated with reverse remodeling in human heart failure. JCI Insight *2*, e89169.

Sun, J., Druhan, L.J., and Zweier, J.L. (2010). Reactive oxygen and nitrogen species regulate inducible nitric oxide synthase function shifting the balance of nitric oxide and superoxide production. Arch Biochem Biophys *494*, 130-137.

Suzuki, T., and Yamamoto, M. (2015). Molecular basis of the Keap1-Nrf2 system. Free radical biology & medicine *88*, 93-100.

Tanaka, H., Sasayama, T., Tanaka, K., Nakamizo, S., Nishihara, M., Mizukawa, K., Kohta, M., Koyama, J., Miyake, S., Taniguchi, M., et al. (2013). MicroRNA-183 upregulates HIF-1alpha by targeting isocitrate dehydrogenase 2 (IDH2) in glioma cells. J Neurooncol *111*, 273-283.

Thienpont, B., Steinbacher, J., Zhao, H., D'Anna, F., Kuchnio, A., Ploumakis, A., Ghesquiere, B., Van Dyck, L., Boeckx, B., Schoonjans, L., et al. (2016). Tumour hypoxia causes DNA hypermethylation by reducing TET activity. Nature *537*, 63-68.

Thoenes, M., Forstermann, U., Tracey, W.R., Bleese, N.M., Nussler, A.K., Scholz, H., and Stein, B. (1996). Expression of inducible nitric oxide synthase in failing and non-failing human heart. J Mol Cell Cardiol *28*, 165-169.

Triposkiadis, F., Butler, J., Abboud, F.M., Armstrong, P.W., Adamopoulos, S., Atherton, J.J., Backs, J., Bauersachs, J., Burkhoff, D., Bonow, R.O., et al. (2019). The continuous heart failure spectrum: moving beyond an ejection fraction classification. Eur Heart J *40*, 2155-2163.

UniProt, C. (2023). UniProt: the Universal Protein Knowledgebase in 2023. Nucleic Acids Res *51*, D523-D531.

Vafiadaki, E., Arvanitis, D.A., Papalouka, V., Terzis, G., Roumeliotis, T.I., Spengos, K., Garbis, S.D., Manta, P., Kranias, E.G., and Sanoudou, D. (2014). Muscle lim protein isoform negatively regulates striated muscle actin dynamics and differentiation. FEBS J *281*, 3261-3279.

van der Pol, A., van Gilst, W.H., Voors, A.A., and van der Meer, P. (2019). Treating oxidative stress in heart failure: past, present and future. European Journal of Heart Failure *21*, 425-435.

van Heesch, S., Witte, F., Schneider-Lunitz, V., Schulz, J.F., Adami, E., Faber, A.B., Kirchner, M., Maatz, H., Blachut, S., Sandmann, C.L., et al. (2019). The Translational Landscape of the Human Heart. Cell *178*, 242-260 e229.

van Rooij, E., Quiat, D., Johnson, B.A., Sutherland, L.B., Qi, X., Richardson, J.A., Kelm, R.J., Jr., and Olson, E.N. (2009). A family of microRNAs encoded by myosin genes governs myosin expression and muscle performance. Dev Cell *17*, 662-673.

Vasquez-Vivar, J., Martasek, P., Whitsett, J., Joseph, J., and Kalyanaraman, B. (2002). The ratio between tetrahydrobiopterin and oxidized tetrahydrobiopterin analogues controls superoxide release from endothelial nitric oxide synthase: an EPR spin trapping study. Biochem J *362*, 733-739.

Vieira, H.L., Queiroga, C.S., and Alves, P.M. (2008). Pre-conditioning induced by carbon monoxide provides neuronal protection against apoptosis. Journal of neurochemistry *107*, 375-384.

Wagner, M., Bertero, E., Nickel, A., Kohlhaas, M., Gibson, G.E., Heggermont, W., Heymans, S., and Maack, C. (2020). Selective NADH communication from alpha-ketoglutarate dehydrogenase to mitochondrial transhydrogenase prevents reactive oxygen species formation under reducing conditions in the heart. Basic Research in Cardiology *115*, 53.

Wakabayashi, N., Itoh, K., Wakabayashi, J., Motohashi, H., Noda, S., Takahashi, S., Imakado, S., Kotsuji, T., Otsuka, F., Roop, D.R., et al. (2003). Keap1-null mutation leads to postnatal lethality due to constitutive Nrf2 activation. Nat Genet *35*, 238-245.

Wang, Y., and Hekimi, S. (2016). Understanding Ubiquinone. Trends in cell biology *26*, 367-378.

Weissman, D., and Maack, C. (2021). Redox signaling in heart failure and therapeutic implications. Free radical biology & medicine *171*, 345-364.

WHO (2019). Cardiovascular Diseases. (World Health Organization).

Winterbourn, C.C. (2016). Revisiting the reactions of superoxide with glutathione and other thiols. Arch Biochem Biophys *595*, 68-71.

Wise, D.R., Ward, P.S., Shay, J.E., Cross, J.R., Gruber, J.J., Sachdeva, U.M., Platt, J.M., DeMatteo, R.G., Simon, M.C., and Thompson, C.B. (2011). Hypoxia promotes isocitrate dehydrogenase-dependent carboxylation of α-ketoglutarate to citrate to support cell growth and viability. Proceedings of the National Academy of Sciences *108*, 19611-19616.

Xiong, Y., Uys, J.D., Tew, K.D., and Townsend, D.M. (2011). S-glutathionylation: from molecular mechanisms to health outcomes. Antioxidants & redox signaling *15*, 233-270.

Xu, W., Yang, H., Liu, Y., Yang, Y., Wang, P., Kim, S.H., Ito, S., Yang, C., Wang, P., Xiao, M.T., et al. (2011). Oncometabolite 2-hydroxyglutarate is a competitive inhibitor of alpha-ketoglutarate-dependent dioxygenases. Cancer cell *19*, 17-30.

Yamamoto, R., Akazawa, H., Ito, K., Toko, H., Sano, M., Yasuda, N., Qin, Y., Kudo, Y., Sugaya, T., Chien, K.R., et al. (2007). Angiotensin II type 1a receptor signals are involved in the progression of heart failure in MLP-deficient mice. Circ J *71*, 1958-1964.

Yang, X., Han, H., De Carvalho, D.D., Lay, F.D., Jones, P.A., and Liang, G. (2014). Gene body methylation can alter gene expression and is a therapeutic target in cancer. Cancer cell *26*, 577-590.

Yi-Dan, H., Ying-Xin, Z., Shi-Wei, Y., and Yu-Jie, Z. (2021). High-Energy Phosphates and Ischemic Heart Disease: From Bench to Bedside. Front Cardiovasc Med *8*, 675608.

Yu, W., Dittenhafer-Reed, K.E., and Denu, J.M. (2012). SIRT3 protein deacetylates isocitrate dehydrogenase 2 (IDH2) and regulates mitochondrial redox status. Journal of Biological Chemistry *287*, 14078-14086.

Zhong, Q., Simonis, N., Li, Q.R., Charloteaux, B., Heuze, F., Klitgord, N., Tam, S., Yu, H., Venkatesan, K., Mou, D., et al. (2009). Edgetic perturbation models of human inherited disorders. Mol Syst Biol *5*, 321.

Zhou, B., and Tian, R. (2018). Mitochondrial dysfunction in pathophysiology of heart failure. Journal of Clinical Investigation *128*, 3716-3726.

Zhou, L., Wang, F., Sun, R., Chen, X., Zhang, M., Xu, Q., Wang, Y., Wang, S., Xiong, Y., Guan, K.L., et al. (2016). SIRT5 promotes IDH2 desuccinylation and G6PD deglutarylation to enhance cellular antioxidant defense. EMBO reports *17*, 811-822.

Zhou, Q., Schotterl, S., Backes, D., Brunner, E., Hahn, J.K., Ionesi, E., Aidery, P., Sticht, C., Labeit, S., Kandolf, R., et al. (2017). Inhibition of miR-208b improves cardiac function in titin-based dilated cardiomyopathy. International journal of cardiology *230*, 634-641.

Zolk, O., Caroni, P., and Bohm, M. (2000). Decreased expression of the cardiac LIM domain protein MLP in chronic human heart failure. Circulation *101*, 2674-2677.